

The Role of Gtl2 in Hepatocarcinogenesis

Dissertation

der Mathematisch-Naturwissenschaftlichen Fakultät

der Eberhard Karls Universität Tübingen

zur Erlangung des Grades eines

Doktors der Naturwissenschaften

(Dr. rer. nat.)

vorgelegt von

Eva Christina Zeller

aus Göppingen

Tübingen

2014

Gedruckt mit Genehmigung der Mathematisch-Naturwissenschaftlichen Fakultät der
Eberhard Karls Universität Tübingen.

Tag der mündlichen Prüfung: 15.04.2015

Dekan: Prof. Dr. Wolfgang Rosenstiel

1. Berichterstatter: Prof. Dr. Michael Schwarz

2. Berichterstatter: Prof. Dr. Klaus Schulze-Osthoff

The presented thesis was prepared at the Institute of Experimental and Clinical Pharmacology and Toxicology, Department of Toxicology, at the Eberhard Karls Universität Tübingen between June 2011 and December 2014 under the supervision of Prof. Dr. Michael Schwarz.

During this time, I took over the supervision of one diploma student and two bachelor students who worked on different aspects of my thesis.

Viktoria Kramer-Potapenja created the Gtl2 expression vector pCMV4-Gtl2, Ute Köber established the switchable Gtl2 expressing cell line and Natalie Agarwala studied the effect of adenoviral overexpression of Gtl2 *in vitro* and to some extent *in vivo*.

Part of this work has been done in cooperation with external partners.

The Affymetrix microarray analysis was carried out at the Microarray Facility at the University of Tübingen, statistical analysis on it was done by Michael Römer, Department of Computer Science, Cognitive Systems, Tübingen. Bart van den Berg, NMI, Protein Analytic, Reutlingen, performed the in-gel digestion and adjacent mass spectrometry to detect RNA-protein interactions. Michael McMahon, University of Dundee, Scotland, created the adenoviral Gtl2 construct. Gtl2 *in situ* hybridization was conducted at the Novartis Institutes for Biomedical Research in Basel, Switzerland. Andreas Schmid performed the PET and MRI analysis on the glutamine synthetase (GS) reporter mice while Prof Dr. Bence Sipos and Dr. Ursula Kohlhofer helped with the section and evaluation of two GS reporter mice to create a glutamine synthetase gene expression mouse atlas.

Für meine Eltern

Data presented in this work have been published:

Zeller E, Mock K, Horn M, Colnot S, Schwarz M, Braeuning A: Dual-specificity phosphatases are targets of the Wnt/ β -catenin pathway and candidate mediators of β -catenin/ Ras signaling interactions. **Biological Chemistry 2012**

Zeller E, Hammer K, Kirschnick M, Braeuning A: Mechanisms of RAS/ β -catenin interactions. **Archives of Toxicology 2013**

Zeller E, Unterberger E, Agarwala N, Köber U, Braeuning A, Schwarz M: Long non-coding RNA Gtl2/ MEG3 and its role in hepatocarcinogenesis. **(in preparation spring 2015)**

Zeller E, Braeuning A, Schwarz M: Monitoring selective poisoning of *Ctnnb1* mutated hepatoma cells in a multi-reporter mouse model **(in preparation summer 2015)**

Parts of this work have been presented:

Zeller E, Kramer-Potapenja V, Unterberger E, Braeuning A, Schwarz M: Long non-coding RNA Gtl2/ Meg3 and its role in hepatic cancer. 79th meeting of the German Society of Pharmacology and Toxicology, Halle (Saale), Germany, 2013 **(poster presentation)**

Zeller E, Kramer-Potapenja V, Unterberger E, Braeuning A, Schwarz M: Long non-coding RNA Gtl2/ Meg3 and its role in hepatic cancer. AEK Symposium, Heidelberg, Germany, 2013 **(poster presentation)**

Zeller E, Köber U, Braeuning A, Schwarz M: Gtl2/ Meg3 – a reliable marker for hepatocarcinogenesis? 80th meeting of the German Society of Pharmacology and Toxicology, Hannover, Germany, 2014 **(poster presentation)**

Zeller E, Agarwala N, Braeuning A, Schwarz M: Gtl2/ Meg3 – a marker for hepatocarcinogenesis? 2nd meeting of Pharmacology and Toxicology in Baden-Württemberg, Heidelberg, Germany, 2014 **(poster presentation)**

Acknowledgements

At first, I would like to express my deep gratitude to Prof. Dr. Michael Schwarz, my research supervisor, for his patient guidance, enthusiastic encouragement and useful critiques of this research work.

Also I want to thank my colleagues for the pleasant working atmosphere and their support in getting through all the difficulties.

Many thanks go to Viktoria, Ute and Natalie, the diploma and bachelor students I supervised from 2012 - 2014, for their hard work.

I wish to thank various external partners for their contribution to this project and the IMI MARCAR consortium for financial support.

I would like to warmly thank Andreas for his understanding and for always being there.

Finally, my loving thanks go to my parents and my brother for their trust and support in every possible way and encouragement throughout my study.

Table of contents

Acknowledgements.....	VI
Table of contents	VII
Abbreviations	XII
1. Introduction.....	1
1.1 The Dlk1-Dio3 Imprinted Gene Cluster.....	2
1.2 Constitutive Androstane Receptor	4
1.3 Canonical Wnt Signaling Pathway	6
1.4 Chemical Carcinogenesis	8
1.4.1 Hepatocellular Malignancies	9
1.4.2 Induced Hepatocarcinogenesis in Mice.....	10
1.5 Zonated Gene Expression in the Liver	11
1.6 Aims and Objectives	12
2. Material	13
2.1 Laboratory Equipment.....	13
2.2 Expandable Items and Small Devices	14
2.3 Chemicals and Biochemicals.....	15
2.4 Buffers and Solutions.....	19
2.4.1 Eukaryotic Cell Culture	19
2.4.2 Cell Treatment	20
2.4.3 Perfusion.....	21
2.4.4 Prokaryotic Cell Culture	22
2.4.5 Reporter Gene Analysis	23
2.4.6 Gel Electrophoresis.....	24
2.4.7 Immunohistochemistry.....	25
2.4.8 Western Blot.....	29
2.4.9 RNA-Protein-Pulldown.....	30
2.4.10 Cell Fractionation.....	31

2.5	Primers.....	32
2.5.1	Genotyping.....	32
2.5.2	Mutation analysis and sequencing	32
2.5.3	Gtl2-T3 PCR	32
2.5.4	Gtl2 upstream region PCR.....	32
2.5.5	Sequencing.....	33
2.5.6	LightCycler PCR	33
2.6	Antibodies	34
2.7	Vectors.....	35
2.8	Cell lines.....	38
2.9	Rodent strains.....	38
2.10	Kits.....	38
2.11	Tissue Samples.....	39
2.12	Software.....	39
3.	Methods.....	40
3.1	Animals.....	40
3.1.1	Animal Housing.....	40
3.1.2	Breeding of the GS Reporter Mouse.....	40
3.1.3	Genotyping.....	41
3.1.4	Organ Harvesting	42
3.1.5	Preliminary Reporter Testing in the GS Reporter Mouse	42
3.1.6	Section of the GS Reporter Mouse	42
3.1.7	Induction of <i>Cttnb1</i> mutated Liver Tumors in the GS Reporter Mouse.....	43
3.1.8	Mutation Analysis	43
3.1.9	Adenoviral Gene Transfer into C3H Mice	44
3.2	Cell Culture.....	45
3.2.1	General Remarks.....	45
3.2.2	Medium Change and Cell Passaging	45
3.2.3	Thawing and Freezing of Cells.....	45
3.2.4	Transfection	46

3.2.5	Tet-On Advanced Inducible System.....	46
3.2.6	Transduction.....	47
3.2.7	Treatment.....	47
3.3	Isolation and Cultivation of Primary Cells from Mouse Liver.....	48
3.3.1	Preparation of Collagen-Coated Culture Dishes.....	48
3.3.2	Isolation of Primary Hepatocytes.....	48
3.4	Quantitative Real-time PCR.....	48
3.4.1	Isolation of RNA from Frozen Liver.....	48
3.4.2	Isolation of RNA from Cell Culture.....	49
3.4.3	Reverse Transcription.....	49
3.4.4	LightCycler PCR.....	50
3.5	Global Gene Expression Analysis.....	50
3.6	Electrophoresis.....	51
3.6.1	Agarose Gel Electrophoresis.....	51
3.6.2	Acrylamide Gel Electrophoresis.....	51
3.7	Plasmid Preparation.....	52
3.7.1	Amplification of Gtl2-T3.....	52
3.7.2	Amplification of Gtl2 upstream regions.....	53
3.7.3	Cloning Strategy.....	54
3.7.4	Plasmid Progeny and Isolation.....	54
3.7.5	DNA Quantification.....	55
3.8	Luciferase Assays.....	55
3.8.1	Firefly Luciferase Measurement in Homogenate of GS mice.....	55
3.8.2	Duale Luciferase Reporter System.....	55
3.9	Immunohistochemistry and <i>in situ</i> Hybridization.....	56
3.9.1	Frozen Liver Sections.....	56
3.9.2	Carnoy Fixation.....	56
3.9.3	Formalin Fixation.....	56
3.9.4	Preparation.....	56
3.9.5	X-Gal Staining.....	57

3.9.6	Glucose-6-phosphatase Staining	57
3.9.7	HE Staining	57
3.9.8	Staining of Cyps and GS	57
3.9.9	Meg3/ Gtl2 <i>in situ</i> Hybridization.....	58
3.10	Digitonin Based Cell Fractionation.....	58
3.11	Western Blot	59
3.12	RNA protein pulldown	60
3.12.1	<i>In vitro</i> Transcription.....	60
3.12.2	RNA Protein Pulldown.....	61
3.13	PET Imaging.....	62
3.14	MRI Imaging	63
3.15	Statistic data processing	63
4.	Results.....	64
4.1	Gtl2 Expression in Different Tumor Tissues.....	64
4.1.1	Expression of Gtl2 Transcript Variant 3 in Murine Liver.....	64
4.1.2	Induction of Gtl2/ MEG3 Expression in Human, Mouse and Rat Liver.....	65
4.1.3	Gtl2 Expression in Murine Primary Hepatocytes.....	73
4.1.4	Gtl2/ MEG3 Expression in Hepatoma Cell Lines	74
4.1.5	CAR Regulation of Gtl2 Upstream Regions	76
4.1.6	Role of Gtl2 in β -Catenin Signaling Regulation	77
4.2	Generation and Characterization of Engineered Gtl2 Expressing Cell Lines	78
4.3	Adenoviral Overexpression of Gtl2 <i>in vivo</i>	83
4.3.1	Determination of Gtl2 Expression after Adenoviral Transduction <i>in vivo</i>	83
4.3.2	Phenotype of Gtl2 Transduced Murine Liver.....	86
4.3.3	Quantification of Dlk1-Dio3 Cluster Genes.....	87
4.3.4	Effects of Gtl2 Overexpression on Proliferation	88
4.4	GS Reporter Mouse.....	89
4.4.1	Preliminary Testing of Reporter Genes in GS Mice.....	90
4.4.2	Glutamine Synthetase Gene Expression “Atlas” in Murine Organs.....	94
4.4.3	Monitoring Tumor Formation in GS Reporter Mice	96

5.	Discussion	101
5.1	The Role of the Imprinted Dlk1-Dio3 Cluster in Liver.....	101
5.2	The GS Reporter Mouse as a Model to Determine GS Expression.....	113
6.	Summary (english).....	119
7.	Zusammenfassung (deutsch).....	120
8.	Curriculum vitae	121
9.	Supplementary data	122
10.	Literature	130

Abbreviations

AAF	2-acetylaminofluorene
AhR	aryl hydrocarbon receptor
AMV-RT	avian myeloblastosis virus reverse transcriptase
APC	adenomatous polyposis coli
APS	ammonium persulfate
bp	base pairs
BSA	bovine serum albumin
bwt	body weight
CAR	constitutive androstane receptor
CCRP	cytoplasmic CAR retention protein
CF	clofibrate
CK1	casein kinase 1
Ctnnb1	β -catenin
Cyp	cytochrome P450
Cypro	cyproconazole
del	deleted
DEN	diethylnitrosamine
Dio3	type 3 iodothyronine deiodinase
Dlk1	delta-like 1 homolog
DMEM/ F12	dulbecco's modified eagle medium
DMR	differentially methylated region
DNA	deoxyribonucleic acid
FHBG	9-(4-18F-fluoro-3-[hydroxymethyl]butyl)guanine
GAPDH	glyceraldehyde 3-phosphate dehydrogenase
GC	genotoxic carcinogen
Gls2	glutaminase 2
GSK3 β	glycogen synthase kinase 3 β
GTP	guanosine-5'-triphosphate
Ha-ras	harvey rat sarcoma
HB	hepatoblastoma
HCC	hepatocellular carcinoma
HRP	horseradish peroxidase
Hsp90	heatshock protein 90
IG-DMR	intergenic differentially methylated region

lncRNA	long non-coding RNA
MAPK	mitogen-activated protein kinase
MDM2	mouse double minute 2
Meg3/ Gtl2	maternally expressed 3 / gene-trap locus 2
Mirg	miRNA containing gene
miRNA	micro ribonucleic acid
MOI	multiplicity of infection
mRNA	messenger ribonucleic acid
NGC	non-genotoxic carcinogen
NMM	nitrosomorpholine
Nr4a2	nuclear receptor subfamily 4 group A member 2
snRNA	small nuclear ribonucleic acid
snoRNA	small nucleolar ribonucleic acid
Olfir	olfactory receptor
PB	phenobarbital
PBS	phosphate buffered saline
PP2A	protein phosphatase 2A
Procl	prochloraz
Ras	rat sarcoma
Raf	rapidly accelerated fibrosarcoma
Rb	retinoblastoma
Rian	RNA imprinted and accumulated in nucleus
Rtl1	retrotransposon-like 1
Sds	serine dehydratase
TCF/ LEF	t-cell factor / lymphoid enhancer-binding factor 1
TEMED	tetramethylethylenediamine
Wnt	consists of wingless and int-1
wt	wild type

1. Introduction

After cardiovascular diseases, cancer is the second most frequent cause of death in Germany (Becker and Holzmeier 2014). Despite the considerable efforts, cancer remains largely lethal. The malignant tumors are not just one disease, but have several things in common: among these are uncontrolled cell growth, the ability of cells to migrate and their invasiveness into normal tissue which may ultimately result in the formation of metastases. These processes are triggered by a combination of genetic and epigenetic changes, denoting phenotypic alterations. A number of chemicals are known cancer risk factors. Classic genotoxic carcinogens (GC) are electrophilic chemicals capable of producing cancer by directly altering the genetic material of target cells. Mechanisms of non-genotoxic carcinogens (NGC) are caused by events other than changes in the underlying DNA sequence; perturbations in DNA methylation and histone modification are examples.

The main tool in identifying carcinogens is the experimental long-term chemical carcinogenesis bioassay in rodents, mainly mice and rats. This is time consuming and needs a large number of animals (Benigni *et al.* 2013). As the liver represents the main target organ for metabolism and toxification, searching for an early biomarker of NGC action to help to generate a tool reducing the requirement for long-term biological testing is desirable. NGC could then be deselected before non-clinical trials. The establishment of early biomarkers for NGC to reliably and robustly predict cancer development is one of the aims of the EU project MARCAR. The MARCAR consortium consists of industrial and academic partners, who are working in close collaboration. Funded under the Innovative Medicines Initiative Joint Undertaking, MARCAR is a 5 year project (MARCAR 2010). The present thesis arose during MARCAR research from 2011 up to and including 2014.

1.1 The Dlk1-Dio3 Imprinted Gene Cluster

Recently, MARCAR partners identified Dlk1-Dio3 imprinted gene cluster non-coding RNAs as novel biomarker candidates for liver tumor promotion in rodents (Lempiainen *et al.* 2013). The Dlk1-Dio3 cluster located on mouse distal chromosome 12 and human chromosome 14q32, respectively, is the largest imprinted gene cluster, meaning mono allelic gene expression in a parent-of-origin dependent manner (Schuster-Gossler *et al.* 1998, Miyoshi *et al.* 2000). Imprinted genes differentiate their parent-of-origin by parent characteristic epigenetic marks like methylations in CpG islands (Hore *et al.* 2007). The Dlk1-Dio3 cluster is under the control of an imprinted control region (ICR), located several kilobases upstream of the lncRNA promoter (Benetatos *et al.* 2011). It contains two differentially methylated regions (DMR) which are the germline derived intergenic DMR (IG-DMR) and the postfertilization derived MEG3-DMR. The Dlk1-Dio3 cluster (figure 1) consists of three paternally expressed protein coding genes including Dlk1 (delta like 1), Rtl1 (retrotransposon like 1) and Dio3 (type 3 iodothyronine deiodinase) as well as several maternally expressed large and small non-coding RNAs. Beside Rian (RNA imprinted and accumulated in nucleus, snoRNAs) and Mirg (micro RNA containing gene), containing 53 miRNAs, Meg3/ Gtl2 (maternally expressed 3/ gene trap locus 2) represents a large non-coding RNA on the maternal allele (Miyoshi *et al.* 2000, Zhou *et al.* 2012). Within MARCAR, Meg3/ Gtl2 was identified as one candidate early biomarker of rodent hepatocarcinogenesis.

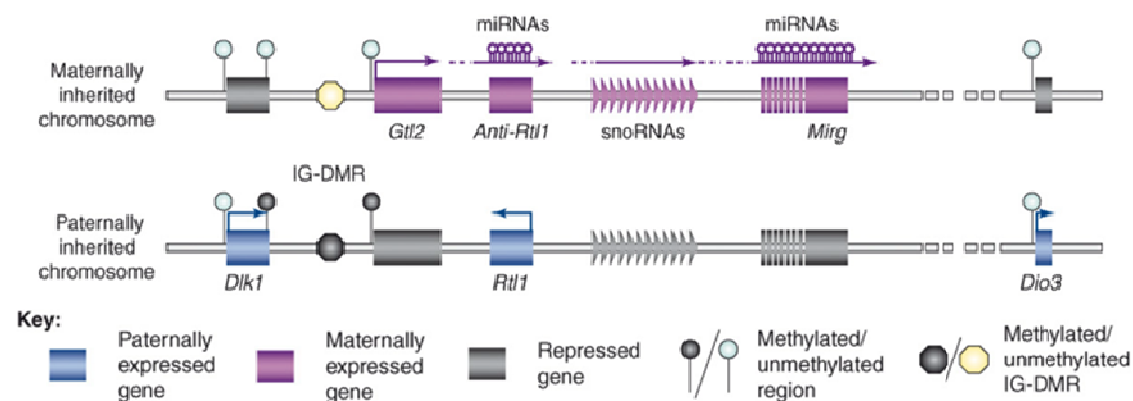


Figure 1: Structure of the Dlk1-Dio3 imprinted gene cluster (modified from da Rocha *et al.* 2008). It consists of three known protein genes named Dlk1, Rtl1 and Dio3 on the paternal allele and several non-coding RNAs, snoRNAs and miRNAs on the maternal inherited allele, among Gtl2, Rian (snoRNAs) and Mirg. Arrows indicate the expression status. The IG-DMR is methylated on the paternal allele.

Multiple RNA isoforms transcribed from murine Gtl2 have been reported (Schuster-Gossler et al. 1998). The physiological and pathological functions of Gtl2 are largely unknown. Gtl2 bears antiproliferative functions by suppressing mouse double minute 2 (MDM2) expression and stimulation of tumor suppressor p53, a known target gene in human cancer cells (Zhou et al. 2007). Gtl2 is also able to directly regulate retinoblastoma protein (Rb) phosphorylation thereby suppressing cell proliferation by the inhibition of M phase to G1 transition, too. Also an indirect way exists, which controls Rb via p16INK4a activation (Zhang et al. 2010, Zhang et al. 2010). Studies in Gtl2 knockout embryos of mice uncovered a relation between Gtl2 and angiogenesis, as these embryos were shown to express increased amounts of vascular endothelial growth factor (Gordon et al. 2010). Some long non-coding RNAs have been shown to regulate transcription of neighboring genes lying on the same chromosome in a *cis* acting mechanism (Royo and Cavaille 2008). Gtl2 has been reported to act as a cofactor of the polycomb repressor complex 2 (PRC2) by directing the chromatin modifying complex to Dlk1, thereby regulating Dlk1 gene expression (Zhao et al. 2010). Physiologically, Gtl2 is expressed in many tissues. It is highly expressed in normal adrenal cortex, pituitary gland and ovary compared to other human tissues (Assie et al. 2014). Loss of Gtl2 expression has been found in all cancer cell lines investigated so far, derived from bladder, colon, breast, lung and liver (Braconi et al. 2011, Benetatos et al. 2011, Zhou et al. 2012). Through reexpression of Gtl2 in cancer cell lines, cell proliferation could be obstructed (Zhou et al. 2012). Expression of MEG3 (MEG3 is the human orthologue of mouse Gtl2) is also lost in 82 % of hepatocellular cancers (Braconi et al. 2011) as well as in pituitary tumors, lung cancer and neuroblastoma, just to mention a few (Zhao et al. 2005, Hu et al. 2009, Astuti et al. 2005). Thus, Gtl2 is believed to be a tumor suppressor (Zhou et al. 2012) having a central role in carcinogenesis.

Two Gtl2 knockout mouse models have been reported in literature. Takahashi *et al.* 2009 created a Gtl2^{KO} (knockout) mouse harboring a 10 kb deletion in exons 1-5. Mice carrying a maternal deletion have a milder phenotype and are able to survive 4 weeks, whereas mice with a paternal deletion suffer perinatal lethality, indicating that Gtl2 plays an important role in embryonic development. Due to their short lifetime, these animals are unsuitable for tumor promotion experiments. Only homozygous mutants

survive. Another mouse model exists with locus specific defects in miRNA expression (Cavaillé, unpublished), but is not available for further investigations. Hence, one aim of the present doctoral thesis was to create a mouse system with altered Gtl2 expression in their hepatocytes to study Gtl2 dependent effects *in vivo*.

Recent work of the MARCAR partners supported the carcinogenic relevance of Dlk1-Dio3 cluster genes by their genetic dependence on CAR and β -catenin signaling, two pathways essential for phenobarbital (PB) dependent liver tumor promotion (figure 2) (Lempiainen *et al.* 2013).

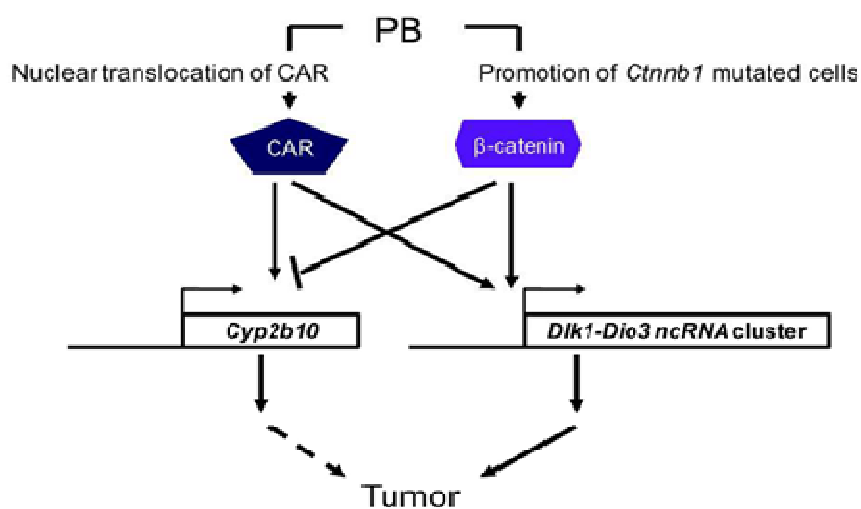


Figure 2: Schematic illustration of the phenobarbital (PB) induced perturbations in *Cyp2b10* and *Dlk1-Dio3* cluster genes (modified after Lempiainen *et al.* 2013). PB activates CAR thus inducing *Cyp2b10*, the classic CAR target gene, and *Dlk1-Dio3* cluster genes. On the other hand, β -catenin inhibits *Cyp2b10* expression but upregulates *Dlk1-Dio3* cluster genes. Aberrant β -catenin signaling has to do with tumor formation.

1.2 Constitutive Androstane Receptor

The orphan nuclear constitutive androstane receptor (CAR) plays a crucial role in the induction of drug metabolism and transporter as well as secretion of both xenobiotics and endobiotics. Thus, CAR upregulates a set of genes that encode cytochrome P450 2B, CYP2C, CYP3A, NADPH-cytochrome P450 reductase, sulfotransferases, glucuronosyltransferases and glutathione S-transferases (Ueda *et al.* 2002). Since the discovery of phenobarbital's Cyp inducing potential (Remmer and Merker 1963), this anticonvulsant serves as a prototype for structurally diverse chemicals that induce CYP2B. Due to the fact that many pharmaceuticals can activate CAR, it forms a central

defense mechanism against their toxicity (Yamamoto *et al.* 2003). The ligand PB does not bind directly to cytoplasmic CAR, rather ligand exposure activates CAR signaling by dissociation of the co-chaperons cytoplasmic CAR retention protein (CCRP) and Hsp90 leading to nuclear CAR translocation. This translocation is presumably dependent on receptor dephosphorylation by protein phosphatase PP2A. In the nucleus, CAR forms a heterodimer with RXR and binds to phenobarbital responsive enhancer elements like PBREM and DR4, where it activates transcription of known target genes (figure 3) (Kodama and Negishi 2006).

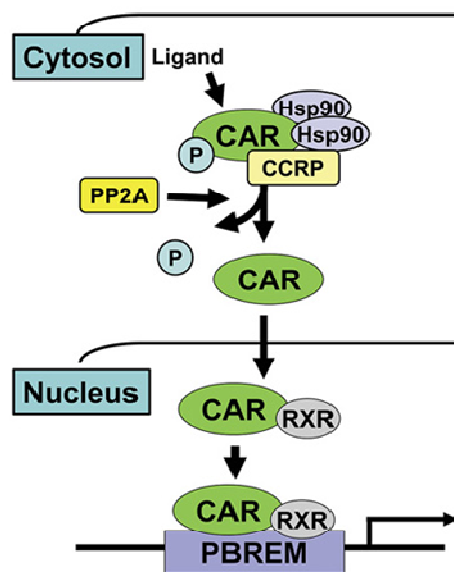


Figure 3: Schematic illustration of CAR signaling pathway (Kakizaki *et al.* 2011). After activation of the cytosolic receptor CAR upon ligand exposure, the co-chaperons CCRP and Hsp90 dissociate and CAR translocates to the nucleus. This translocation is presumably dependent on receptor dephosphorylation by protein phosphatase PP2A. In the nucleus, CAR forms a heterodimer with RXR and binds to the PBREM, where it activates transcription of known target genes. Abbreviations: CAR constitutive androstane receptor; Hsp90 heatshock protein 90; PP2A protein phosphatase 2A; p phosphorylation; RXR retinoid X receptor; PBREM Phenobarbital responsive enhancer module.

PB is no human carcinogen although it was used in humans a long time to treat epilepsy (Lamminpaa *et al.* 2002). Human hepatocytes are resistant to the ability of PB in increasing cell proliferation (Parzefall *et al.* 1991). In contrast, rodents chronically exposed to PB develop hepatocellular carcinoma (Peraino *et al.* 1971) since PB is the prototype of a non-genotoxic carcinogen that causes tumors without inducing DNA mutation. For more information on the use of PB in murine hepatocarcinogenesis, please refer to 1.4.2. No PB mediated induction of Gtl2 was observed in CAR^{KO} mice, indicating that CAR is necessary for PB dependent activation of the Dlk1-Dio3 cluster gene expression (Lempiainen *et al.* 2013).

1.3 Canonical Wnt Signaling Pathway

As already mentioned above, not only CAR, but also β -catenin is crucial for Dlk1-Dio3 cluster expression. Basal Gtl2 expression levels are reduced and PB mediated induction is extinct in *Cttnb1*^{KO} (*Cttnb1* encodes β -catenin) mice revealing the requirement of β -catenin for both basal and PB induced Gtl2 expression (Lempiainen *et al.* 2013).

β -Catenin plays two major roles in the cell regulating cell adhesion as an integral component of the classic cadherin complex (Vestweber and Kemler 1984) and gene transcription via the Wnt/ β -catenin signaling pathway (Reya and Clevers 2005).

Int-1, the first Wnt gene, was identified long time ago as a proto-oncogene after infection of mice with mouse mammary tumor virus. The name Wnt is a composition of the *Drosophila* segment polarity gene wingless (Wg) and integration-1 (Int-1) (Nusse and Varmus 1982, Rijsewijk *et al.* 1987). The canonical Wnt/ β -catenin signaling pathway (figure 4) is physiologically activated by Wnt glycoproteins which bind to the seven transmembrane receptor Frizzled/ low density lipoprotein receptor-related protein 5 or 6 (LRP5/6) complex at the cell surface. Aberrantly, genetic or epigenetic alterations affecting key players of the pathway are able to activate β -catenin signaling. In the absence of Wnt molecules β -catenin is phosphorylated in a cytosolic protein complex, called destruction complex, containing the proteins APC (adenomatous polyposis coli), Axin, GSK3 β (glycogen synthase kinase 3 β) and CK1 (casein kinase 1) and primed for proteasomal degradation by phosphorylation and ubiquitinylation. With a Wnt ligand binding to its receptors, the destruction complex gets destabilized while GSK3 β is phosphorylated. Thus β -catenin is stabilized, accumulates in the cytoplasm and translocates to the nucleus where it interacts with DNA-bound T cell factor (TCF)/ lymphoid enhancer factor (LEF) transcription factors (Reya and Clevers 2005), thereby activating known target genes required for proliferation and differentiation such as c-myc, Cyclin D1, MMP7 (matrix metalloprotease 7) and glutamine synthetase (GS) (Morin 1999, Cadoret *et al.* 2001, Sansom *et al.* 2005).

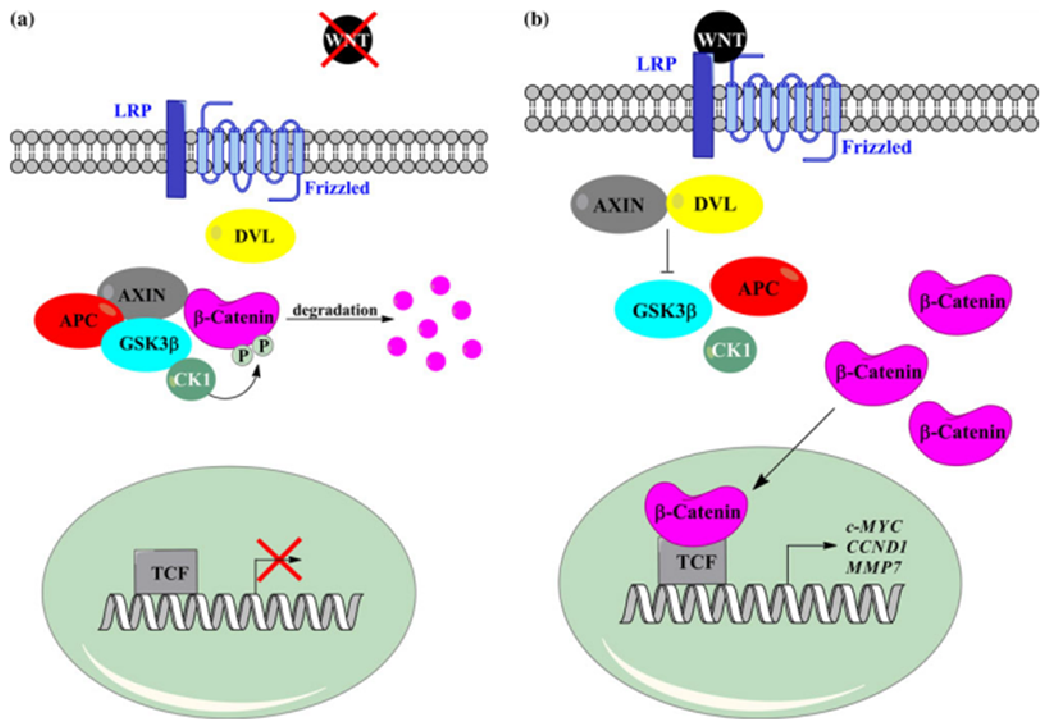


Figure 4: Simplified schematic overview of the canonical Wnt/ β -catenin signaling pathway (Zeller *et al.* 2013). **(a)** In the absence of Wnt molecules, β -catenin is phosphorylated in a cytosolic protein complex containing the proteins APC, Axin, GSK3 β and CK1, and primed for proteasomal degradation. **(b)** When the Wnt ligand binds to the FZD receptor, β -catenin gets phosphorylated and the cytosolic protein complex becomes destabilized. Thus, β -catenin gets stabilized and translocates to the nucleus where it interacts with transcription factors, thereby activating known target genes. LRP, low density lipoprotein receptor-related protein; P, phosphorylation; DVL, disheveled; APC, adenomatous polyposis coli; GSK3 β , glycogen synthase kinase 3 β ; CK1, casein kinase 1, TCF, t-cell factor; CCND1, cyclin D1; MMP7, matrix metalloprotease 7.

Abnormal regulation of the Wnt/ β -catenin signaling pathway can lead to various diseases including different types of cancer (Polakis 2000, Logan and Nusse 2004). Inappropriate β -catenin stabilization and therefore signaling is observed in hepatocellular carcinoma (HCC), hepatoblastoma (HB), colorectal carcinoma, tumors of the mammary gland and several other neoplasia (Reya and Clevers 2005, Schmidt *et al.* 2011). Nearly 40 % of human HCC harbor mutations in the proto-oncogene *CTNNB1* (encoding β -Catenin). These activating mutations are predominantly located in the codons 33, 37, 41 or 45 of exon 3 affecting the Ser-Thr-phosphorylation sites of β -catenin and thereby preventing its degradation (de La Coste *et al.* 1998, Miyoshi *et al.* 1998, Wong *et al.* 2001). As a consequence, Wnt targets like GS are overexpressed in *Ctnnb1* mutated hepatocellular tumors (Loeppen *et al.* 2002).

1.4 Chemical Carcinogenesis

Carcinogenesis, the term for malignant tumor formation, describes the stepwise transformation of a normal to a malignant cell as a multistage process. In 1990, Fearon and Vogelstein designed a model to explain the sequential genetic alterations during the multistep development of colorectal carcinoma (Fearon and Vogelstein 1990). According to their model, tumors are the result of the mutational inactivation of tumor suppressor genes linked to the activation of oncogenes. According to their model, mutations in at least five genes are required that affect signaling in cell proliferation, survival and death. Proto-oncogenes are genes, which result in a permanent active profuse expressed product upon initiation. Known examples are *Raf*, *Ras* and *Ctnnb1*, which, when constitutively activated in tumor cells, result in increased cell proliferation (Giles *et al.* 2003, Croce 2008, Wang *et al.* 2009). In contrast, tumor suppressors like APC and p53 are negative regulators; they are inactivated in tumor cells and lose their physiological function (Weinberg 1991).

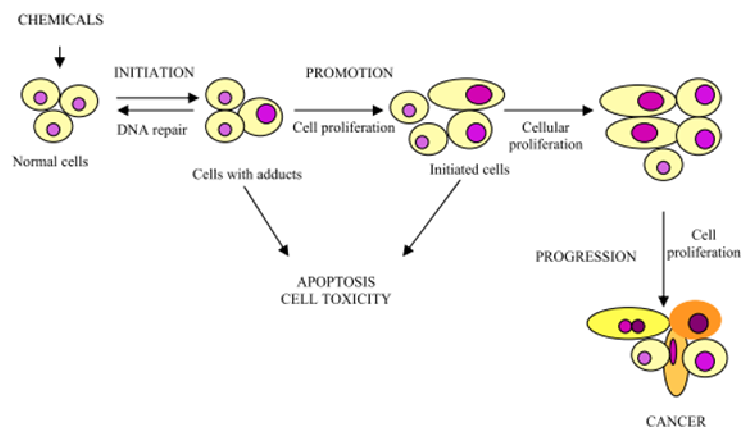


Figure 5: Chemical carcinogenesis stages (Oliveira *et al.* 2007) showing the way of a normal cell to cancer.

A tumor with a diameter of 1 mm consists of one million cells (Aktories *et al.* 2013) and descends from one initial, normal cell which passes through steps of initiation and promotion. It escapes from apoptosis and shows an enhanced cell proliferation while accumulating genetic and epigenetic alterations (Trosko 2001). DNA damage is established as the first step in chemical carcinogenesis. After this irreversible initiation, the so formed initiated cell is susceptible to tumor promoters. Promoters are non-genotoxic compounds that increase cell proliferation leading to preneoplastic lesions

(Oliveira *et al.* 2007). Tumor promotion is an at least partly reversible process and the promoter must be present for a long period of time (Butterworth *et al.* 1992). Prolonged treatment with tumor promoters or treatment with cytotoxic agents may lead to tumor formation, when the agents are given alone, probably due to the presence of spontaneously mutated initiated cells (Laskin *et al.* 1988). The transformation into a malignant cell is the last step in carcinogenesis (Klaunig *et al.* 2000).

1.4.1 Hepatocellular Malignancies

MARCAR partners focus on liver malignancies, as the liver represents the major target organ for NGC. Liver cancer incorporates various histologically different primary hepatic neoplasms which comprise hepatocellular carcinoma (HCC) and hepatoblastoma (HB) amongst others. Hepatocellular carcinoma is the major malignant tumor in the liver, most prominent risk factors are chronic hepatitis B and C infection, alcohol abuse and aflatoxin B1 exposure (Farazi and DePinho 2006). Distinct genetic events are associated with HCC formation such as inactivation of the tumor suppressor p53 and the activation of Wnt signaling through mutations in β -catenin (Polakis 2000, Farazi and DePinho 2006).

In contrast to HCC, HB is a rare liver neoplasm occurring in small infants and children (Darbari *et al.* 2003). Each year 0.5 in 100,000 children come down with this cancer (AWMFOonline 2010). Recent analysis demonstrated an 80 % prevalence of mutations in *CTNNB1* (Schmidt *et al.* 2011). More rarely, HB shelter genetic alterations affecting other members of the Wnt pathway (Oda *et al.* 1996, Koch *et al.* 2004).

In addition to the detection of cancer by blood tests, medical ultrasonics and classical diagnosis based on tissue samples, non-invasive imaging technologies like high-field magnetic resonance imaging (MRI) and high resolution positron emission tomography (PET) have opened a new tool for the early detection of liver tumors. PET uses radiolabeled biomolecules which trace non-invasively specific pathways and pathologies while MRI creates morphological pictures with a spatial resolution in the μm range by means of magnetic fields and radio waves. By applying simultaneous both

non-invasive methods, sensitivity and specificity for early tumor detection can be increased. Early detection of preneoplastic lesions by non-invasive *in vivo* imaging technologies will probably help with screenings for unwanted carcinogenic effects. In this thesis, we wanted to visualize the growth of *Ctnnb1* mutated liver tumors in a reporter mouse by non-invasive technologies.

1.4.2 Induced Hepatocarcinogenesis in Mice

In order to investigate genes involved in carcinogenesis, tumors have to be generated.

Therefore, mice that are susceptible to chemically induced carcinogenesis are a useful model to study critical alterations occurring during hepatocarcinogenesis. Previous work demonstrated that liver tumors induced in C3H mice predominantly harbor mutations in either *Ha-ras*, *B-raf* or *Ctnnb1*. The resulting type of mutation depends on the treatment regimen.

Mutations in the proto-oncogenes *Ha-ras* (Harvey rat sarcoma) and *B-raf* are attained by a single intraperitoneal application of the liver carcinogen diethylnitrosamine (DEN) to two week old mice (Jaworski *et al.* 2005). Ras proteins are small monomeric membrane bound GTPases that regulate cell division and apoptosis, processes often deregulated in tumors (Malumbres and Barbacid 2003). In contrast, about 80% of the generated liver tumors after one single DEN injection of mice at the age of 6 weeks followed by chronic administration of the prominent tumor promoter phenobarbital reveal *Ctnnb1* mutations (Aydinlik *et al.* 2001). *Ctnnb1* mutated liver tumors harbor high expression of glutamine synthetase (GS), the prototype marker for β -catenin activation (Loeppen *et al.* 2002, Cadoret *et al.* 2002). For experimental analysis the mouse strain C3H is suitable since it has been demonstrated that it is susceptible to PB promotion (Aydinlik *et al.* 2001) and shows a high incidence of spontaneous liver tumor formation (Buchmann *et al.* 1991), while C57BL/6 mice are more resistant. This susceptibility is linked to a marker called D1Mit33 on mouse chromosome 1 (Bilger *et al.* 2004).

1.5 Zonated Gene Expression in the Liver

The gene expression patterns in *Ha-ras* and *Ctnnb1* mutated tumors resembled those seen in periportally and pericentrally located hepatocytes in normal liver tissue. There, the same signaling pathways operate (Hailfinger *et al.* 2006). Periportal cells can be distinguished from pericentral cells based on their different gene expression profile (figure 6). Hepatocytes in pericentral areas exhibit high activity in metabolism of xenobiotics, bile acid synthesis and glycolysis as well as biotransformation. The signal triggering this gene expression profile is likely a Wnt-signal, presumably delivered by endothelial cells of the central veins, activating the Wnt dependent signaling cascade in the neighboring hepatocytes. Thus, marker enzymes like glutamine synthetase and several Cyps that are overexpressed in *Ctnnb1* mutated tumors also serve as markers for perivenous gene expression (Hailfinger *et al.* 2006). Periportal areas are marked by high levels of gluconeogenesis, cholesterol biosynthesis, fatty acid and amino acid degradation (Gebhardt 1992, Jungermann 1995, Braeuning *et al.* 2006, Ghafoory *et al.* 2013), displaying high expression of glucose-6-phosphatase (G6Pase) and E-cadherin, markers which are also characteristic for *Ha-ras* mutated tumors (Hailfinger *et al.* 2006, Braeuning *et al.* 2007).

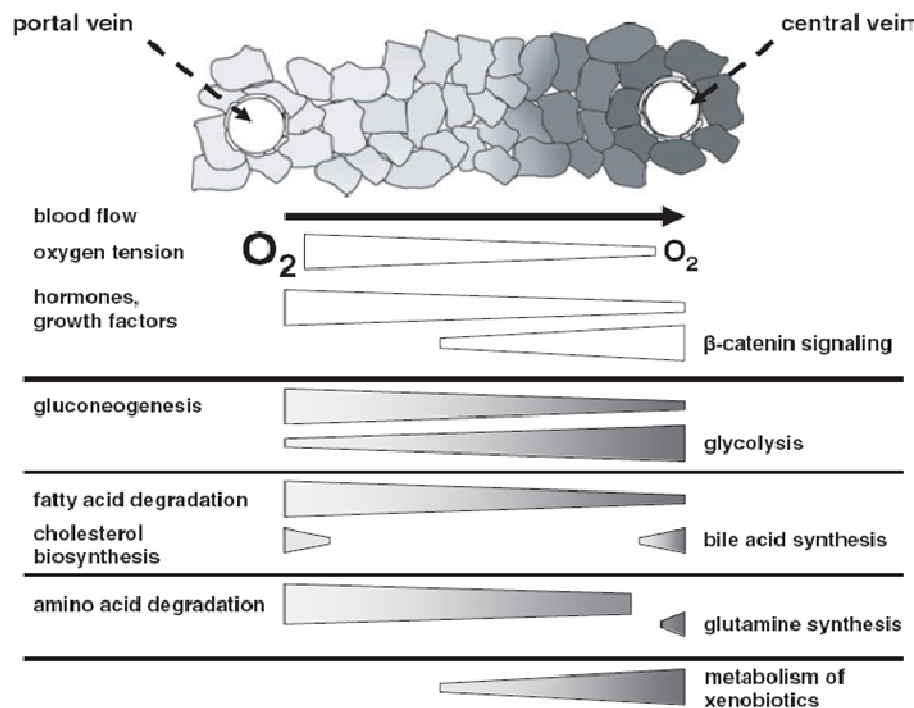


Figure 6: Schematic illustration of zoned gene expression in the liver. The figure shows the blood flow, oxygen and hormone and β -catenin signaling gradient that influences liver zonation (Braeuning *et al.* 2006).

1.6 Aims and Objectives

Aberrant expression of long non-coding RNA Gtl2/ MEG3, located on the Dlk1-Dio3 imprinting cluster, is often observed in tumors. Recently, project partners identified Gtl2 as novel biomarker candidate for liver tumor promotion in rodents. The aim of this project was to elucidate the role of Gtl2 in hepatocarcinogenesis and to verify its role as a biomarker for NGC and a tumor suppressor. For this purpose, examinations on murine liver treated with different NGC and GC compounds were performed and completed by cell culture experiments generating a switchable Gtl2 expressing system for global gene expression analysis to identify potential target genes. Due to the lack of an appropriate knockout mouse model, Gtl2 was constitutively overexpressed in murine liver by the use of adenoviral Gtl2.

Another goal was to life image the development of special liver tumors in an engineered glutamine synthetase reporter mouse by PET and MRI. This reporter mouse could also be used to generate a glutamine synthetase gene expression “atlas”, which indirectly predicts in which organs/ cells Wnt signaling is active in the adult and during development.

2. Material

2.1 Laboratory Equipment

Item	Manufacturer	product
Autoclave	Webeco, Selmsdorf, Germany	Autoclave C
Balance	Mettler-Toledo, Gießen, Germany	P1200
	Sartorius, Göttingen, Germany	Analytic
	Sartorius, Göttingen, Germany	CP922
	Mettler, Gießen, Germany	Laborwaage K7
	Mettler, Gießen, Germany	Laborwaage P1200
Burner	WLD-TEC, Göttingen, Germany	Gasprofi 1 micro
Camera	Nikon, Düsseldorf, Germany	Coolpix 950
	Raytest, Straubenhardt, Germany	CSC Chemoluminescence detection module
	Zeiss, Oberkochen, Germany	AxioCam MRC
Centrifuge	Eppendorf, Hamburg, Germany	5410
	Eppendorf, Hamburg, Germany	5415D
	Eppendorf, Hamburg, Germany	5417R
	Heraeus Instruments, Hanau, Germany	Biofuge 13
	Heraeus Instruments, Hanau, Germany	Megafuge 1.0R
	Hettich, Tuttlingen, Germany	Mikro 200R
	Labnet, Edison, USA	C1301P
Cyrostat microtome	Reichert-Jung, Wetzlar, Germany	Frigucut 2800
Drying oven	Heraeus Instruments, Hanau, Germany	
Electrophoresis chambers	GibcoBRL, Karlsruhe, Germany	H6
	Bio-Rad, Munich, Germany	Mini Protean II
Heat sterilizer	Heraeus Instruments, Hanau, Germany	VTR 5022
Homogenizer	ART, Müllheim, Germany	Micra D-9
Incubator	Heraeus Instruments, Hanau, Germany	BB 6220 CU
Laminar flow	BDK, Sonnenbühl, Germany	Sterilbank UVF 6.12 F
Magnetic separation module	Promega, Mannheim, Germany	
Magnetic stirrer	Janke & Kunkel, Staufen, Germany	IKA Combimag RCT
	Janke & Kunkel, Staufen, Germany	IKA Mag RH

	Germany	
	Heidolph Instruments, Schwabach, Germany	MR 80
Microscope	Leitz, Wetzlar, Germany	Labovert FS
	Zeiss, Oberkochen, Germany	Imager.M1
Microwave	Bosch, Stuttgart, Germany	600 W
Multiwell plate reader	Perkin Elmer, Waltham, USA	1420 Multilabel Counter Victor V ³
PCR machine	PerkinElmer, Waltham, MA, USA	GeneAmp PCR System 2400
	Bio-Rad, Munich, Germany	MyCycler™ thermal cycler
pH meter	WTW, Weilheim, Germany	pH 522
Photometer	Peqlab, Erlangen, Germany	NanoDrop ND-1000
Power supply	Pharmacia, Uppsala, Sweden	LKB EPS 500/400
	Desaga, Wiesloch, Germany	Desatronic 3x500/100
	GibcoBRL, Karlsruhe, Germany	ST 305
	GibcoBRL, Karlsruhe, Germany	ST 606 T
Quantitative real-time PCR	Roche Diagnostics, Mannheim, Germany	LightCycler 1.5
Shaker	Braun, Melsungen, Germany	Certomat HK
	Heidolph, Kelheim, Germany	Titramax 1000
Thermoblock	Eppendorf, Hamburg, Germany	5320
	Eppendorf, Hamburg, Germany	5436
UV illuminator	Biometra, Göttingen, Germany	TI 1
Vortex mixer	Bender & Hobein AG, Zurich, Switzerland	Genie 2TM
Water bath	GFL, Burgwedel, Germany	1083
Water purification system	Merck Millipore, Billerica, MA, USA	Milli Q Plus

2.2 Expandable Items and Small Devices

Item	Manufacturer	Type designation
0.2 ml reaction tubes	Peqlab, Erlangen, Germany	-
0.5 ml reaction tubes	Eppendorf, Hamburg, Germany	-
1.5 ml reaction tubes	Eppendorf, Hamburg, Germany	-
1.8 ml cyro tubes	Nunc, Wiesbaden, Germany	Cryo Tube Vials
2 ml reaction tubes	Eppendorf, Hamburg, Germany	-
6 ml polystyrene tubes	BD, Heidelberg, Germany	Falcon 2058
15 ml tubes	BD, Heidelberg, Germany	Falcon 2096
50 ml tubes	BD, Heidelberg, Germany	Falcon 2070

Cages	Techniplast, Neumarkt, Germany	Macrolon Typ 2
Capillaries (for lightcycler)	Roche Applied Science, Penzberg, Germany	LightCycler Capillaries (20 µl)
Cell culture dishes	BD, Heidelberg, Germany	Falcon 3003
Cell culture plates	BD, Heidelberg, Germany	Falcon 3224
	BD, Heidelberg, Germany	Falcon 3043
	BD, Heidelberg, Germany	Falcon 3226
Cell scraper	Corning, USA	Costar Cell Lifter
Centrifuge adapter	Roche Applied Science, Penzberg, Germany	LightCycler Centrifuge Adapters
Counting chamber	Brand, Wertheim, Germany	Fuchs-Rosenthal
Cover slips	Thermo Scientific, Schwerte, Germany	30 mm diameter, #1
Dako pen	Dako, Glostrup, Denmark	Pen S2002
Disinfectant concentrate	Braun, Melsungen, Germany	Helipur
Glassware	Schott, Mainz, Germany	-
Glass pasteur pipette	WU Mainz, Mainz, Germany	-
Glass pipette	Brand, Wertheim, Germany	5 ml, 10 ml, 20 ml
Gloves	Ansell, Munich, Germany	Micro Touch Hygrip
	Kimberly-Clark, Dallas, USA	Safeskin Purple Nitrile
Inoculating loop	Greiner, Frickenhausen, Germany	731165
Microscope glasses	R. Langenbrinck, Emmendingen, Germany	26x76 mm
Metal tweezers	Eickemeyer, Tuttlingen, Germany	-
	Schnitzer Steel, Portland, OR, USA	-
Metal scissors	Hauptner, Dietikon, Switzerland	-
Needles (0.9 x 40 mm)	BD, Heidelberg, Germany	Microlance 3™
Parafilm	Pechiney, Chicago, USA	PM-996
Q-tips	Neolab, Heidelberg, Germany	
Scalpel	Braun, Melsungen, Germany	
Sterile filter	Millipore, Eschborn, Germany	Steritop 0.22 µm
Syringes	BD, Heidelberg, Germany	1 ml BD slip-tip syringe
Syringe filter	Sartorius, Göttingen, Germany	Minisart

2.3 Chemicals and Biochemicals

Reagent	Manufacturer
(3-Aminopropyl)triethoxysilane	Sigma, Taufkirchen, Germany
3-Amino-9-ethylcarbazole	ICN Biochemicals, Aurora, USA
Acetaminophen	Sigma, Taufkirchen, Germany
Acetic acid (100 %)	Merck KgaA, Darmstadt, Germany

Acetone	Sigma, Taufkirchen, Germany
Accutase	Sigma, Taufkirchen, Germany
Acrylamide (30 %)	Roth, Karlsruhe, Germany
Agarose	Peqlab, erlangen, Germany
Ammonium persulfate	Serva, Heidelberg, Germany
Ampicillin sodium salt	Sigma, Taufkirchen, Germany
Ampuwa (sterile water)	Fresenius Kabi Deutschland GmbH, Bad Homburg, Germany
AMV Reverse Transcriptase 10 U/ μ l	Promega, Mannheim, Germany
Bacto agar	Applichem, Darmstadt, Germany
Bacto tryptone	Applichem, Darmstadt, Germany
Bacto yeast extract	Applichem, Darmstadt, Germany
Benzonase	Sigma, Taufkirchen, Germany
Biotin-16-UTP	Roche Diagnostics, Mannheim, Germany
Boric acid	Merck KgaA, Darmstadt, Germany
Bovine serum albumin	Thermo Scientific, Schwerte, Germany
Bradford protein assay	Biorad, Munich, Germany
Bromodeoxyuridine	Applichem, Darmstadt, Germany
Bromophenol blue	Serva, Heidelberg, Germany
CaCl ₂	Sigma, Taufkirchen, Germany
Calf intestinal alkaline phosphatase	Life technologies, Darmstadt, Germany
CDP-Star ready to use	Life technologies, Darmstadt, Germany
Chloral hydrate	Riedel-de Haen, Seelze, Germany
Chloroform	Merck KgaA, Darmstadt, Germany
Citric acid	Applichem, Darmstadt, Germany
Coelenterazine	PJK, Kleinblittersdorf, Germany
Coenzyme A	PJK, Kleinblittersdorf, Germany
Collagenase	Sigma, Taufkirchen, Germany
Complete Mini protease inhibitor cocktail	Roche Diagnostics, Mannheim, Germany
D-glucose-6-phosphate	Sigma, Taufkirchen, Germany
Diethylpyrocarbonate	Sigma, Taufkirchen, Germany
Digitonin	Sigma, Taufkirchen, Germany
Dimethylformamide	Merck KgaA, Darmstadt, Germany
Dithiothreitol	Sigma, Taufkirchen, Germany
D-luciferin	PJK, Kleinblittersdorf, German
DMEM/F12	Gibco, Life technologies, Darmstadt, Germany
DMSO	Applichem, Darmstadt, Germany
DNase I (10 U/ μ l)	Roche Diagnostics, Mannheim, Germany
dNTPs 100 mM	Life technologies, Darmstadt, Germany
dNTPs 2 mM	Thermo Scientific, Schwerte, Germany
Doxycycline	Sigma, Taufkirchen, Germany
dT ₂₀ primer	Genaxxon, Ulm, Germany
Dynabeads M-280 Streptavidin	Life technologies, Darmstadt, Germany
EDTA	Merck KgaA, Darmstadt, Germany
EGTA	Merck KgaA, Darmstadt, Germany
Entellan	Merck KgaA, Darmstadt, Germany

Eosin G	Merck KgaA, Darmstadt, Germany
Ethanol	Merck KgaA, Darmstadt, Germany
Ethidium bromide	Serva, Heidelberg, Germany
Ficoll type 400	Sigma, Taufkirchen, Germany
Geneticin sulfate G418	Biochrom, Berlin, Germany
GeneRuler 100 bp plus DNA Ladder	Thermo Scientific, Schwerte, Germany
GeneRuler 1 kb DNA Ladder	Thermo Scientific, Schwerte, Germany
Glucose	Roth, Karlsruhe, Germany
Glutaraldehyde	Serva, Heidelberg, Germany
Glycerol	Appllichem, Darmstadt, Germany
Glycine	Roth, Karlsruhe, Germany
H ₂ O ₂ (30 %)	Sigma, Taufkirchen, Germany
HCl	Merck KgaA, Darmstadt, Germany
Hematoxylin	Roth, Karlsruhe, Germany
Hepes (acid)	Roth, Karlsruhe, Germany
HiPerFect	Qiagen, Hilden, Germany
Hoechst 33258	Life technologies, Darmstadt, Germany
Hygromycin B	InvivoGen, San Diego, USA
I-Block	Life technologies, Darmstadt, Germany
Isopropanol	Merck KgaA, Darmstadt, Germany
Kaiser's glycerol gelatin	Merck KgaA, Darmstadt, Germany
KAl(SO ₄) ₂ · 12 H ₂ O	Merck KgaA, Darmstadt, Germany
KCl	Merck KgaA, Darmstadt, Germany
KH ₂ PO ₄	Merck KgaA, Darmstadt, Germany
K ₂ HPO ₄ · 3 H ₂ O	Merck KgaA, Darmstadt, Germany
Lead nitrate	Merck KgaA, Darmstadt, Germany
LiCl	Roth, Karlsruhe, Germany
Lipofectamine 2000	Life technologies, Darmstadt, Germany
Maleic acid	Merck KgaA, Darmstadt, Germany
Methanol	Merck KgaA, Darmstadt, Germany
MgCl ₂	Roche Diagnostics, Mannheim, Germany
MgCl ₂ · 6 H ₂ O	Merck KgaA, Darmstadt, Germany
MgSO ₄ · 7 H ₂ O	Merck KgaA, Darmstadt, Germany
Midori Green Advanced DNA stain	Nippon Genetics, Düren, Germany
Milk powder	Roth, Karlsruhe, Germany
Mouse genomic DNA	Promega, Mannheim, Germany
NaC ₂₄ H ₃₉ O ₄	Sigma, Taufkirchen, Germany
NaCl	Merck KgaA, Darmstadt, Germany
NaHCO ₃	Merck KgaA, Darmstadt, Germany
Na ₂ HPO ₄ · 2 H ₂ O	Merck KgaA, Darmstadt, Germany
NaIO ₃	Merck KgaA, Darmstadt, Germany
NaN ₃	Merck KgaA, Darmstadt, Germany
NaOH	Merck KgaA, Darmstadt, Germany
NP-40	Sigma, Taufkirchen, Germany
NTPs	Life technologies, Darmstadt, Germany
Opti-MEM I	Gibco, Life technologies, Darmstadt, Germany
Orange G	Peqlab, Erlange, Germany

Passive Lysis Buffer 5x	Promega, Mannheim, Germany
pBR322 DNA- <i>MspI</i> digest	NEB, Frankfurt, Germany
Penicillin/streptomycin	Biochrom, Berlin, Germany
Pentobarbital	Sigma, Taufkirchen, Germany
Phenobarbital	Sigma, Taufkirchen, Germany
Proteinase K	Boehringer, Mannheim, Germany
Phenol	Roth, Karlsruhe, Germany
QuantiFast Probe PCR Master Mix	Qiagen, Hilden, Germany
QuantiTect Primer Assays	Qiagen, Hilden, Germany
QuantiTect SYBR Green Mix	Qiagen, Hilden, Germany
Random hexamer primers	Genaxxon BioScience, Ulm, Germany
Restriction endonuclease <i>HindIII</i>	NEB, Frankfurt, Germany
<i>PvuII</i>	NEB, Frankfurt, Germany
<i>XbaI</i>	NEB, Frankfurt, Germany
<i>XhoI</i>	NEB, Frankfurt, Germany
Restriction 10x Buffer	NEB, Frankfurt, Germany
RiboRuler High Range RNA Ladder	Thermo Scientific, Schwerte, Germany
RNaseOUT recombinant ribonuclease inhibitor	Life technologies, Darmstadt, Germany
RNA Loading Dye	Thermo Scientific, Schwerte, Germany
SDS	Serva, Heidelberg, Germany
SOC medium	Life technologies, Darmstadt, Germany
Sodium acetate	Merck KGaA, Darmstadt, Germany
Sodium citrate	Merck KGaA, Darmstadt, Germany
Sucrose	Merck KGaA, Darmstadt, Germany
Swine serum (normal)	Dako, Glostrup, Denmark
T3 RNA Polymerase	Life technologies, Darmstadt, Germany
T7 RNA Polymerase	Life technologies, Darmstadt, Germany
Taq buffer 10x	Thermo Scientific, Schwerte, Germany
Taq polymerase (1 U/ μ l)	Thermo Scientific, Schwerte, Germany
Taq polymerase (5 U/ μ l)	Thermo Scientific, Schwerte, Germany
Tetramethylethylenediamine (TEMED)	Serva, Heidelberg, Germany
Transcription buffer 5x	Life technologies, Darmstadt, Germany
Tris-HCl	Sigma, Taufkirchen, Germany
Tris base	Sigma, Taufkirchen, Germany
TRIzol	Life technologies, Darmstadt, Germany
Trypsin-EDTA	Biochrom, Berlin, Germany
Tween 20	Sigma, Taufkirchen, Germany
X-Gal substrate	Peqlab, Erlangen, Germany
Xylene	Merck KGaA, Darmstadt, Germany
Xylene cyanol	Sigma, Taufkirchen, Germany

2.4 Buffers and Solutions

2.4.1 Eukaryotic Cell Culture

DMEM/F12

Reagent	Amount
DMEM/F12	6 g
NaHCO ₃	1,22 g
H ₂ O _{dest}	ad 450 ml

- adjust with HCl_{conc} to pH 7.2, filtrate sterile (pore size 0.22 µm), store at 4°C

before use, add:

- 10 % (v/v) FCS (heat inactivated at 56 °C for 30 min), 1 % (v/v) penicillin (10,000 U/ml)/ streptomycin (10 mg/ml) solution, store at 4 °C

- for cultivation of stably transfected cells, add 0.5 % (v/v) geneticine (20 mg/ml) and 0.1 % (v/v) hygromycin B (100 mg/ml)

DMEM/F12 freezing medium

Reagent	Amount
DMEM/F12 medium	90 ml
DMSO	10 ml

- store at 4°C

100 mM hepes buffer

Reagent	Amount
Hepes (acid)	11.92 g
H ₂ O _{dest}	ad 500 ml

- adjust with NaOH to pH 7.4

20 mg/ml geneticin solution

Reagent	Amount
Geneticin sulfate G418 (activity 701 mg/g)	1.43 g
100 mM hepes buffer pH 7.4	50 ml

- filtrate sterile (pore size 0.45 µm), store at -20°C

100 mg/ml hygromycin B solution

Reagent	Amount
Hygromycin B (activity 990 mg/g)	2.02 g
100 mM hepes buffer pH 7.4	20 ml

- filtrate sterile (pore size 0.45 μm), store at -20°C

10x PBS

Reagent	Amount	Final concentration
NaCl	80 g	1,4 M
KCl	2 g	27 mM
KH_2PO_4	2 g	15 mM
$\text{NaH}_2\text{PO}_4 \cdot 2 \text{H}_2\text{O}$	14,35 g	80 mM
$\text{H}_2\text{O}_{\text{dest}}$	ad 1000 ml	

- autoclave 40 min

- working solution 1x PBS: dilute 1:10 with $\text{H}_2\text{O}_{\text{dest}}$

2.4.2 Cell Treatment

Doxycycline

Reagent	Amount	Stock conc.	Final conc.
Doxycycline	10 mg	1 mg/ml	0.01-1 $\mu\text{g}/\text{ml}$
$\text{H}_2\text{O}_{\text{dest}}$	10 ml		

- filtrate sterile (pore size 0.45 μm), protect from light, store in aliquots at -20°C

NaCl

Reagent	Amount	Stock conc.	Final conc.
NaCl	584 mg	1 M	15 mM
$\text{H}_2\text{O}_{\text{dest}}$	10 ml		

- filtrate sterile (pore size 0.45 μm), store at 4°C

LiCl

Reagent	Amount	Stock conc.	Final conc.
LiCl	424 mg	1 M	15 mM
$\text{H}_2\text{O}_{\text{dest}}$	10 ml		

- filtrate sterile (pore size 0.45 μm), store at 4°C

Phenobarbital solution

Reagent	Amount	Stock conc.	Final conc.
Phenobarbital	25.4 mg	100 mM	30 mM
H ₂ O _{dest}	1 ml		

- prepare fresh solutions before use

5-Azadeoxycytidine solution

Reagent	Amount	Stock conc.	Final conc.
5-Azadeoxycytidine	5 mg	10 mM	10 μ M
DMSO	2190 μ l		

- store in aliquots at -20°C

2.4.3 Perfusion

Basal perfusion buffer

Reagent	Amount
NaCl	12.6 g
KCl	0.64 g
MgSO ₄ · 7 H ₂ O	0.54 g
KH ₂ PO ₄	0.3 g
NaHCO ₃	3.62 g
Hepes (acid)	7.16 g
Glucose · H ₂ O	3 g
H ₂ O _{dest}	ad 2000 ml

- adjust to pH 7.2 and store at 4°C

Perfusion buffer

Reagent	Amount
EGTA	47,5 mg
Basal perfusion buffer	500 ml

- adjust to pH 7.2 and store at 4°C

Collagenase buffer

Reagent	Amount
CaCl ₂	290 mg
Basal perfusion buffer	500 ml

- adjust to pH 7.2, store at 4°C and add 250 mg collagenase before use

Washing buffer

Reagent	Amount
CaCl ₂	290 mg
Basal perfusion buffer	500 ml
BSA	10 g

- adjust to pH 7.2 and store at 4°C

2.4.4 Prokaryotic Cell Culture

LB medium

Reagent	Amount
Bacto tryptone	10 g
Bacto yeast extract	5 g
NaCl	10 g
H ₂ O _{dest}	ad 1000 ml

- adjust with NaOH to pH 7.0, autoclave for 40 min, store at RT

- before use, add ampicillin to a final concentration of 0.1 mg/ml

LB-agar plates

Reagent	Amount
Bacto agar	15 g
LB medium	ad 1000 ml

- autoclave 40 min, add ampicillin to a final concentration of 0.1 mg/ml at most 60°C

- pour into 10 cm dishes, let cool down and store putting at the lid at 4°C

LB-glycerol storing medium

Reagent	Amount
LB medium	5 ml
Glycerol	5 ml

- filtrate sterile (pore size 0.45 µm) and store at -20°C

2.4.5 Reporter Gene Analysis

DTT

Reagent	Amount	Stock conc.	Final conc.
DTT	1.545 g	1 M	33.3 mM
H ₂ O _{dest}	10 ml		

- filtrate sterile (pore size 0.45 µm) and store at -70°C

Firefly luciferase buffer

Reagent	Amount
ATP	292 mg
Coenzym A	207 mg
Tricine	3.58 g
MgSO ₄ · 7 H ₂ O	1.32 g
Na ₂ EDTA (200 mM, pH 8.0)	500 µl
D-luciferin	132 mg
H ₂ O _{dest}	ad 1000 ml

- adjust to pH 8.0 and cool on ice before adding D-luciferin, filtrate sterile (pore size 0.22 µm), protect from light and store in aliquots at -70°C

- before use, add 333 µl 1 M DTT per 10 ml firefly luciferase buffer

1000x coelenterazine

Reagent	Amount
Coelenterazine	0.605 mg
Methanol	1 ml

- protect from light and store in 50 µl aliquots at -70°C

1 M K_xPO₄ pH 5.1

Reagent	Amount
K ₂ HPO ₄ · 3 H ₂ O	22.82 g
KH ₂ PO ₄	34.02
H ₂ O _{dest}	350 ml

Renilla luciferase buffer

Reagent	Amount
Na ₂ EDTA (200 mM, pH 8.0)	11 ml
K _x PO ₄ buffer (1 M, pH 5.1)	220 ml
NaCl	64.3 g
NaN ₃	0.845 g
BSA	0.44 g
H ₂ O _{dest}	ad 1000 ml

- adjust to pH 5.0 with KOH, filtrate sterile (pore size 0.22 µm) and store in aliquots at -70°C

- add 20 µl coelenterazine per 10 ml renilla luciferase buffer prior to use

2.4.6 Gel Electrophoresis

Agarose Gel Electrophoresis

50x TAE buffer (pH 8.5)

Reagent	Amount
Tris base	242 g
EDTA (0.5 M, pH 8)	100 ml
Glacial acetic acid	57.1 ml
H ₂ O _{dest}	ad 1000 ml

6x loading buffers

Reagent	Amount
Sucrose	50 g
SDS	1 g
Orange G dye	0.5 g
H ₂ O _{dest}	ad 100 ml

GeneRuler 1 kb DNA ladder

Reagent	Amount
1 kb DNA ladder	1 µl (1 µg/µl)
6x loading buffer	1 µl
H ₂ O _{dest}	ad 7 µl

GeneRuler 100 bp plus DNA ladder

Reagent	Amount
100 bp plus DNA ladder	1 µl (1 µg/µl)
6x loading buffer	1 µl
H ₂ O _{dest}	ad 7 µl

Acrylamide Gel Electrophoresis

5x TBE buffer pH 8.3

Reagent	Amount
Tris base	54 g
EDTA (0.5 M, pH 8)	20 ml
Boric acid	27.5 g
H ₂ O _{dest}	ad 1000 ml

10x loading buffer

Reagent	Amount
Bromophenol blue	25 mg
Xylene cyanol	25 mg
Ficoll type 405	1.5 g
EDTA (0.5 M, pH 8)	1 ml
H ₂ O _{dest}	ad 10 ml

10 % Ammonium persulfate

Reagent	Amount
APS	1 g
H ₂ O _{dest}	ad 10 ml

Ethidium bromide solution (0.5 µg/ml)

Reagent	Amount
Ethidium bromide	0.5 mg
H ₂ O _{dest}	ad 1000 ml

pBR322 DNA-*Msp*I Digest

Reagent	Amount
pBR322 DNA- <i>Msp</i> I Digest (1 µg/µl)	10 µl
10x loading buffer	10 µl
H ₂ O _{dest}	ad 50 µl

2.4.7 Immunohistochemistry

Carnoy's fixative

Reagent	Amount
Ethanol	60 ml
Chloroform	30 ml
Glacial acetic acid	10 ml

- prepare shortly before use

Coating solution

Reagent	Amount
(3-Aminopropyl)triethoxysilane	4 ml
Acetone	ad 200 ml

10x 0.1 M citrate buffer pH 6

Reagent	Amount
Citric acid (sodium salt)	29.41 g
H ₂ O _{dest}	ad 1000 ml

Glucose-6-phosphatase staining solution

Reagent	Amount
Tris-maleate (0.2 M)	100 ml
H ₂ O _{dest}	133 ml
2% lead nitrate	25 ml

- add 250 mg D-glucose-6-phosphate (monosodium salt) shortly before use

Lead nitrate (2 %)

Reagent	Amount
Lead nitrate	2 g
H ₂ O _{dest}	ad 100 ml

TB buffer pH 8.7

Reagent	Amount
Tris base	6 g
MgCl ₂ · 3 H ₂ O	406 mg
H ₂ O _{dest}	ad 1000 ml

TBS/ T pH 7.4

Reagent	Amount
Tween 20	1 ml
NaCl	8.76 g
Tris base	2.42 g
H ₂ O _{dest}	ad 1000 ml

PBS/ S

Reagent	Amount
NaCl	2.03 g
BSA	1 g
1x PBS	ad 100 ml

PBS/ T

Reagent	Amount
Tween-20	0.2 ml
1x PBS	ad 100 ml

Acetate buffer

Reagent	Amount
Sodium acetate	6.48 g
Glacial acetic acid	1.21 ml
H ₂ O _{dest}	ad 1000 ml

3-Amino-9-ethylcarbazole (AEC) solution

Reagent	Amount
3-Amino-9-ethylcarbazole	4 mg
N,N-Dimethylformamide	1 ml
Acetate buffer	14 ml
H ₂ O ₂ (30 %)	15 µl

- dissolve first 2 components before adding acetate buffer

- add H₂O₂ before use

Alcoholic eosin solution

Reagent	Amount
Eosin Y	0.8 g
Ethanol (60 %)	ad 200 ml

- filter through fluted filter paper

Mayer's Hematoxylin

Reagent	Amount
Hematoxylin	1 g
NaIO ₃	0.2 g
KAl(SO ₄) ₂ · 12 H ₂ O	50 g
Chloral hydrate	50 g
Citric acid	1 g
H ₂ O _{dest}	ad 1000 ml

- dissolve first 3 components in H₂O_{dest} before adding chloral hydrate and citric acid

0.2 M tris/ maleate buffer

Reagent	Amount
Tris (base)	24.2 g
Maleic acid	23.2 g
H ₂ O _{dest}	ad 1000 ml

- adjust pH with 1 N NaOH to 6.5

X-Gal staining solution

Reagent	Amount	Stock conc.	Final conc.
X-Gal	100 mg	100 mg/ml	1 mg/ml
DMF	1 ml		

- store at -20°C

X-Gal staining buffer

Reagent	Amount
K ₄ [Fe ^(III) (CN) ₆]	210 mg
K ₃ [Fe ^(III) (CN) ₆]	160 mg
MgCl ₂ · 6 H ₂ O	40.6 mg
NP-40	20 µl
SDS	10 mg
PBS	ad 100 ml

- add 1 % X-Gal staining solution before use

2.4.8 Western Blot

10x Assay buffer

Reagent	Amount
MgCl ₂ · 6 H ₂ O	2.03 ml
Tris (base)	24.2 g
H ₂ O _{dest}	ad 100 ml

- adjust to pH 9.5 before adding MgCl₂ · 6 H₂O

- for 1x Assay buffer dilute 1:10 with H₂O_{dest}

2x Lämmli buffer

Reagent	Amount
Glycerol	20 ml
Tris (base)	1.51 g
H ₂ O _{dest}	25 ml
Bromphenol blue	4 mg
β-Mercaptoethanol	10 ml
SDS	4 g
H ₂ O _{dest}	ad 100 ml

- adjust to pH 6.8 with HCl before adding bromphenol blue, β-mercaptoethanol and SDS

- add H₂O_{dest} to a final volume of 100 ml and store in 1 ml aliquots at -20°C

10x SDS-PAGE running buffer

Reagent	Amount
Glycine	144 g
Tris (base)	30 g
SDS (20 % solution)	50 ml
H ₂ O _{dest}	ad 1000 ml

- for 1x SDS-PAGE running buffer dilute 1:10 with H₂O_{dest}

10x Transfer buffer

Reagent	Amount
Glycine	144 g
Tris (base)	30 g
H ₂ O _{dest}	ad 1000 ml

- for final working dilute 100 ml of 10x Transfer buffer with 200 ml methanol and 700 ml H₂O_{dest}

2.4.9 RNA-Protein-Pulldown

0.1 % DEPC-H₂O

Reagent	Amount	Final conc
Diethylpyrocarbonate	1 ml	1 % (v/v)
H ₂ O _{dest}	ad 1000 ml	

- dissolve until stirring; incubate overnight at RT, autoclave 20 min

Solution A

Reagent	Amount	Final conc
NaOH	1 g	0.1 M
NaCl	0.73 g	0.05 M
DEPC-H ₂ O	ad 250 ml	

Solution B

Reagent	Amount	Final conc
NaCl	0.73 g	0.1 M
DEPC-H ₂ O	ad 250 ml	

1 M Tris pH 7.5

Reagent	Amount	Final conc
Tris base	121.1 g	1 M
DEPC-H ₂ O	ad 1000 ml	

- adjust to pH 7.5

- for 20 mM Tris dilute 1:50 with DEPC-H₂O

2x BW (binding and washing) buffer

Reagent	Amount	Final conc
Tris-HCl pH 7.5	1 ml 1 M Tris-HCl	10 mM
EDTA	1 ml 0.1 M EDTA	1 mM
NaCl	11.69 g	2 M
DEPC-H ₂ O	ad 100 ml	

-for 1x BW buffer dilute 1:2 with DEPC-H₂O

10x RNA-protein binding buffer

Reagent	Amount	Final conc
Tris-HCl pH 7.5	2 ml 1 M Tris-HCl	0.2 M
NaCl	1.25 ml 4 M NaCl	0.5 M
MgCl ₂	0.2 ml 1 M MgCl ₂	20 mM
Tween	100 µl	1 %
DEPC-H ₂ O	ad 10 ml	

2.4.10 Cell Fractionation**Basic buffer**

Reagent	Amount	Final conc
NaCl	8.776 g	150 mM
Hepes	13.015 g	50 mM
DEPC-H ₂ O	ad 1000 ml	

- adjust to pH 7.4 with HCl, filtrate sterile (pore size 0.45 µm), store at 4°C

Digitonin buffer (cytosolic protein fractionation)

Reagent	Amount	Final conc
Digitonin (50 mg/ml)	10 µl	50 µg/ml
Basic buffer	ad 10 ml	

-dissolve 50 mg digitonin in 1 ml of total buffer by heating the solution for 2 min on 95°C, add dissolved digitonin to basic buffer and add 1 tablet Complete Mini protease inhibitor cocktail/ 7 ml basic buffer

NP-40 buffer (organelle membrane-bound fractionation)

Reagent	Amount	Final conc
NP-40	1 ml	1 % (v/v)
Basic buffer	ad 100 ml	

- store at 4°C

RIPA buffer (nuclear protein fractionation)

Reagent	Amount	Final conc
NaC ₂₄ H ₃₉ O ₄	250 mg	0.5 % (v/v)
SDS (20 % solution)	250 µl	0.5 % (v/v)
Basic buffer	ad 50 ml	

- shortly before use, add appropriate volume of Benzonase (1 U/ ml) and store at 4°C

2.5 Primers

2.5.1 Genotyping

PCR-ID	Forward primer (5'→3')	Reverse primer (5'→3')	Amplicon
7656	CAGTTCAGACTCAAGGATCA TGC	CGAGCAAACCTACTGTGTAGAT AGC	304 bp (wt) 403 bp (ki)

2.5.2 Mutation analysis and sequencing

Gene	Forward primer (5'→3')	Reverse primer (5'→3')	Amplicon
<i>Ctnnb1</i>	ACTCTGTTTTACAGCTGACCT	GAGCGCATGATGGCATGTCTG	248 bp

2.5.3 Gtl2-T3 PCR

Primer	sequence (5'→3')	length	T _m [°C]	GC [%]	Amplicon
Gtl2_F1	AGCACAGAAGACGAAGAGCTG	21 bp	59.8	52.4	1924 bp
Gtl2_R1	CAAGAAATTTATTGAAAGCACCAT	24 bp	54.2	29.2	

2.5.4 Gtl2 upstream region PCR

Primer	sequence (5'→3')	length	T _m [°C]	GC [%]	Amplicon
Gtl2_T1 _F2	CACCAGCGAGGACAAGCGACAA	23 bp	66	60.9	1.3 kb
Gtl2_T1 _R1	CAAGAAATTTATTGAAAGCACCAT	24 bp	62.7	50	
Gtl2_T2 _3_F2	CACCGAGTCACAGTGGCATCC	21 bp	63.7	61.9	1.3 kb
Gtl2_T2 _3_R	GCTGGCTGGGTGGGGTTTA	19 bp	61	63.2	
Gtl2_fw 160	GTTGCTGGACTTTCAGGTTATG	22 bp	58.4	45.5	1.6 kb
Gtl2_rev 1980	CAGACCAGTGGCTTGCCTA	19 bp	58.8	57.9	
Gtl2_fw 1966	CAAGCCACTGGTCTGGAAAT	20 bp	57.3	50	1.8 kb
Gtl2_rev 3611	CCTAGGATGCCACTGTGACTC	21 bp	61.8	57.1	

2.5.5 Sequencing

Primer	sequence (5'→3')
CMV_for	CAAATGGGCGGTAGGCGTGTA
Gtl2Seq_388F	ACAGCGAGGGACAAGCGACAA
Gtl2Seq_1096F	CGGAGGACACTTGGACTCTTGCC
Gtl2Seq_1286R	ACGAAGACGGCGACGGGAT
pCMV4_Rneu	CCAGCTTGGTTCCCGAATAGA
Gtl2PromA_426R	CAGAATTAGCCCTTGCTTTATC
Gtl2PromA_845F	GACCCTCCTTGTCTATGCTTG
Gtl2PromA_994R	CCATGCTGAGGGCTATTGT
Gtl2PromA_1876R	AGCCTTCTCCGCCTCCTC
Gtl2PromM_306R	GGAAGAAGCCAAACCTATGCTAA
Gtl2PromM_987R	GGGCCTCCACAGCAAAGT
Gtl2PromM_1594R	CGATGCACTTCGGAGGGTG
M13-uni	GTAAAACGACGGCCAGT
M13-rev	AACAGCTATGACCATG
Gstm3_delR1	CCCGACTGCATCTGCGTGTT

2.5.6 LightCycler PCR

Gene	Forward primer (5'→3')	Reverse primer (5'→3')	Amplicon
18s rRNA	Mm_Rn18s_3_SG QuantiTect Primer Assay		143 bp
Dio3	Mm_Dio3_1_SG QuantiTect Primer Assay		143 bp
Dlk1	Mm_Dlk1_1_SG QuantiTect Primer Assay		120 bp
Meg3	Mm_Meg3_1_SG QuantiTect Primer Assay		148 bp
Mirg	Mm_Mirg_4_SG QuantiTect Primer Assay		168 bp
Rian	Mm_Rian_2_SG QuantiTect Primer Assay		149 bp
Rtl1	Mm_Rtl1_2_SG QuantiTect Primer Assay		88 bp
Meg3	Rn_RGD1566401_va.1_SG QuantiTect Primer		125 bp
MEG3	Hs_MEG3_QF_1 QuantiFast Probe Assay		85 bp
18s rRNA	CGGCTACCACATCCAAGGAA	GCTGGAATTACCGCGGCT	187 bp
hCAR1	TGCAACTGAGTAAGGAGCAA GAA	AAGGGCTGGTGATGGATGAA	273 bp
mCcmd1	GCGCCCTCCGTATCTTACTT	TCCTCTCGCACTTCTGCTC	113 bp
mCdk2	CCCTGGATGAAGATGGACG	ATCAGAGCCGAAGGTGGG	138 bp
mCdk4	CACGCCTGTGGTGGTTAC	GAGATTCGCTTATGTGGGTTA	342 bp
mCyp2b10	TACTCCTATTCCATGTCTCCA AA	TCCAGAAGTCTCTTTTCACATG T	118 bp
rCyp2b1	TATCTTGCTCCTCCTTGCTCTC	AACTCCTCTTTCCCATCCC	413 bp
rCyp4a3	CAAGGCTGTCGAGGATCTAA AC	GATGCACATGGTGGTGTAAAG GT	474 bp
rGls2	GCACAAGTTCGTGGGCAAG G	GTGCATGAGGCTGAGGGTGTT	469 bp
mGtl2-T1	TTTCTGTCTTGCCGAGTGG	AGGAAGCAGTGGGTTGGAG	455 bp

mGtl2-T2	GGACTCTTGCCACATTAGCC C	ATTTTCTCCTCAGCCCTTTGTT	497 bp
mGtl2-T3	GTCTTCCTGTGCCATTTGCT	TTCATCAGTCAGTAGGTGGGT CT	416 bp
mNr4a2	TCTCCCAAGCACGTCAAAGA	ATTTCCCATCATACTAGCAA TC	340 bp
mOlf612	CTCCCTATCCTCTTGAAGAGA TTG	TCACGGATCTGCTTGGTTTT	428 bp
mPcna	GATAAAGAAGAGGAGGCGG TAA	CTGGCATCTCAGGAGCAATC	277 bp
rSds	AAACAAGGCTGTAAACATTT CGTC	GTGATCTTGGGCAGGGTGA	491 bp
mWdr20a	AAGGCTGCCGACCTGAGTA	AGAAACCCGTCCTGGCTCA	484 bp

2.6 Antibodies

Antigen	Cyp1a2
Manufacturer	Gift of Dr. Roland Wolf, University of Dundee, Dundee, UK
Catalog number	-
Source	rabbit, polyclonal
Application	IHC, 1:1000 in PBS/ S

Antigen	Cyp2c
Manufacturer	Gift of Dr. Roland Wolf, University of Dundee, Dundee, UK
Catalog number	-
Source	rabbit, polyclonal
Application	IHC, 1:300 in PBS/ S

Antigen	GAPDH
Manufacturer	Millipore, Merck KGaA, Darmstadt, Germany
Catalog number	2145925
Source	mouse, polyclonal
Application	WB, 1:1000 in I-Block PBS/ T

Antigen	Glutamine synthetase (GS)
Manufacturer	Sigma, Taufkirchen, Germany
Catalog number	G2781
Source	rabbit, polyclonal
Application	IHC, 1:1000 in PBS/ S

Antigen	Histone H3
Manufacturer	Cell signaling, Danvers, USA
Catalog number	D1H2
Source	rabbit, polyclonal
Application	WB, 1:2000 in 5 % milk powder TBS/ T

Antigen	Mouse IgG
Manufacturer	Sigma, Taufkirchen, Germany
Catalog number	A2554
Source	goat, polyclonal
Application	IHC, 1:20 in blocking buffer, HRP conjugated

Antigen	Rabbit IgG
Manufacturer	Dako, Glostrup, Denmark
Catalog number	P0217
Source	swine, polyclonal
Application	IHC, 1:20 in blocking buffer, HRP conjugated

Antigen	Anti mouse
Manufacturer	Life technologies, Darmstadt, Germany
Catalog number	T2192
Source	goat, polyclonal
Application	WB, 1:10,000 in I-Block PBS/ T, AP conjugated

Antigen	Anti rabbit
Manufacturer	Life technologies, Darmstadt, Germany
Catalog number	T2191
Source	goat
Application	WB, 1:10,000 in 5 % milk powder TBS/ T, AP conjugated

2.7 Vectors

pCR3 mCAR1

Information: Vector expressing mCAR1 under the control of the constitutively active promoter.

Resistance: Ampicillin

Manufacturer: Negishi, NIEHS, Durham, USA

pTAluc/STF

Information: Vector expressing Firefly luciferase reporter under the control of 8x TCF/ LEF binding sites.

Resistance: Ampicillin

Manufacturer: Source of the backbone: Clontech, Mountain View, USA

pRL-CMV

Information: Vector expressing Renilla luciferase under the control of the constitutively active cytomegaly virus promoter.

Resistance: Ampicillin

Manufacturer: Promega, Mannheim, Germany

pCMV4-Gtl2

Information: Vector expressing Gtl2-T3 under the control of a constitutively active cytomegaly virus promoter, cloned by Viktoria Kramer-Potapenja

Resistance: Ampicillin

Manufacturer: Source of the backbone: Poellinger, Karolinska Institute, Stockholm, Sweden

pTRE-Tight-Gtl2

Information: Vector containing a modified Tet response element consisting of the tet operator sequence (tetO) and a minimal CMV promoter allowing rtTA-inducible expression of Gtl2-T3.

Resistance: Ampicillin

Manufacturer: Source of the backbone: Clontech, Mountain View, USA

pTK-Hyg

Information: Vector containing a hygromycin-resistance gene for selection of stably transfected cell clones.

Resistance: Ampicillin, hygromycin

Manufacturer: Clontech, Mountain View, USA

pSV2-neo

Information: Vector containing a neomycin-resistance gene for selection of stably transfected cell clones.

Resistance: Neomycin, geneticin and ampicillin

Manufacturer: Clontech, Mountain View, USA

pTet-on advanced

Information: Component of the Tet-On Advanced expression system, expressing the reverse tetracycline-controlled transactivator protein (rtTA) under the control of the constitutively active CMV promoter.

Resistance: Ampicillin

Manufacturer: Clontech, Mountain View, USA

pBlueScript SK(-)/ Gtl2-T3

Information: Vector containing Gtl2-T3, flanked by T7 and T3-RNA polymerase binding sites, allowing *in vitro* transcription of Gtl2-T3.

Resistance: Ampicillin

Manufacturer: Source of the backbone: Stratagene, La Jolla, USA

2.8 Cell lines

Cell line	Cell type	Mutation status (<i>Ctnnb1</i> exon 3)	Reference
70.4	mouse hepatoma, strain C3H/ He	<i>Ctnnb1</i> wt/wt	Kress <i>et al.</i> 1992
70.4 Tet on K23	stably transfected subclone of 70.4	<i>Ctnnb1</i> wt/wt	Stiegler 2009
70.4 UT K54	stably transfected subclone of 70.4	<i>Ctnnb1</i> wt/wt	Köber 2013
70.4 STF K15	stably transfected subclone of 70.4	<i>Ctnnb1</i> wt/wt	Braeuning <i>et al.</i> 2007
53.2b	mouse hepatoma, strain C57BL/ 6J	<i>Ctnnb1</i> wt/wt	Kress <i>et al.</i> 1992
Hepa 1c1c.7	mouse hepatoma, strain C57BL/ J	<i>Ctnnb1</i> del/---	Bernhard <i>et al.</i> 1973
55.1c	mouse hepatoma, strain C57BL/ 6J	<i>Ctnnb1</i> wt/del	Kress <i>et al.</i> 1992
HC-AFW1	human HCC	<i>CTNNB1</i> del	Armeanu-Ebinger <i>et al.</i> 2012

2.9 Rodent strains

Strain	Sourcer
C3H/ He N	Charles River, Sulzfeld, Germany
GS reporter mouse	Taconic Artemis, Köln, Germany

2.10 Kits

Kit	Manufacturer
AdEasy Adenoviral Vector System	Agilent Technologies, Böblingen, Germany
Biotin Luminescent Detection Kit	Roche Diagnostics, Mannheim, Germany
Easyprep Pro Plasmid Mini Kit	Biozym, Hessisch Oldendorf, Germany
Expand Long Template PCR System	Roche Diagnostics, Mannheim, Germany
FastStart DNA Master ^{PLUS} SYBR Green I Kit	Roche Diagnostics, Mannheim, Germany
Genopure Plasmid Maxi Kit	Roche Diagnostics, Mannheim, Germany
High Pure RNA Isolation Kit	Roche Diagnostics, Mannheim, Germany
peqGOLD Cycle Pure Kit	Peqlab, Erlangen, Germany
peqGOLD Gel Extraction Kit	Peqlab, Erlangen, Germany
QuantiFast Probe PCR Kit	Qiagen, Hilden, Germany
QuantiTect SYBR Green PCR Kit	Qiagen, Hilden, Germany
TOPO TA Cloning Kit	Life technologies, Darmstadt, Germany

2.11 Tissue Samples

Mouse liver samples from a tumor promotion experiment (Rignall *et al.* 2013) were available, in which the treatment with two PCBs (PCB 126 and PCB 153) lasted for 34 weeks.

Samples from chemically induced mouse liver tumors were available from an experiment previously conducted in our laboratory (unpublished). There, C3H mice have been treated with a single dose of DEN to induce *Ras* and *Raf* mutated tumors. After 6 months, animals received 0.05 % PB for 4 weeks. Tumors had been analyzed in terms of mutations of the *Ha-ras* and *B-raf* proto-oncogenes according to (Aydinlik *et al.* 2001, Jaworski *et al.* 2005).

Liver samples from wild type mice as well as hCAR/ hPXR mice (Braeuning *et al.* 2014) treated with two different fungicides were available in our laboratory (unpublished).

Also samples from rats, treated with two NGC (PB and CF) as well as two GC (AAF, NNM) were available (Ittrich *et al.* 2003).

2.12 Software

Software	Manufacturer
AxioVision 4.5	Zeiss, Oberkochen, Germany
Adobe Photoshop	Adobe Systems, San Jose, USA
BioDraw Ultra 12.0	PerkinElmer, Waltham, USA
Chromas Lite	Technelysium, Brisbane, USA
Corel Draw Graphics Suite 12	Corel Corporation, Ottawa, Canada
CSC Camera Controller 1.11	Raytest, Traubenhardt, Germany
EndNote X2	EndNote, Carlsbad, USA
NanoDrop ND-1000 V3.2.1	PerkinElmer, Waltham, USA
Office 2007	Microsoft, Redmond, USA
OriginPro 8G	Origin Lab Cooperation, Northampton, MA, USA
Primer Premier 5.00	Premier Biosoft, Palo Alto, USA
Roche LightCycler Run 5.32	Roche Diagnostics, Mannheim, Germany
Victor Workout 1.5	Perkin Elmer, Waltham, USA
Windows XP	Microsoft, Redmond, USA
Windows 7	Microsoft, Redmond, USA

3. Methods

3.1 Animals

3.1.1 Animal Housing

Mice were singly kept in Makrolon type 2 cages at a 12 hour light/ dark cycle with water and food available *ad libitum*. The animals were treated with human care and all protocols were in compliance with institutional guidelines.

3.1.2 Breeding of the GS Reporter Mouse

Taconic Artemis generated a GS (glutamine synthetase) reporter mouse expressing three reporters (β -galactosidase, LacZ; thymidine kinase 1, Tk-1; and Firefly luciferase, FLuc) under the control of a GS promoter specifically activated in cells with active β -catenin signaling and therefore also in *Ctnnb1* mutated cells. For higher tumor susceptibility, C57BL/ 6 GS mice were interbred with C3H/ He N every generation. Existence of the knock in the reporter allele (KI) was determined by PCR (3.1.3).

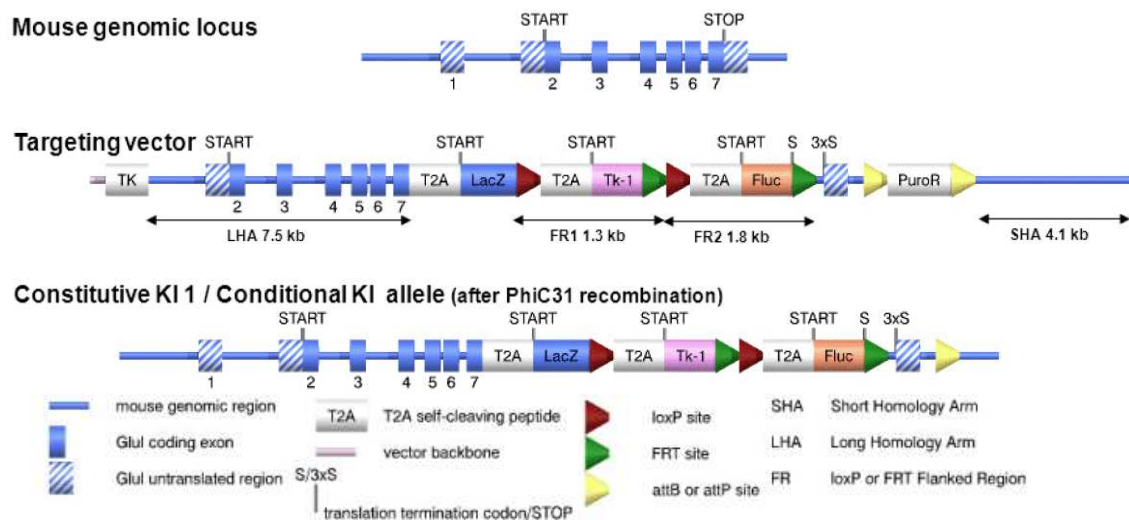


Figure 7: Schema of the GS (glutamine synthetase, Glul) reporter mouse generation. The targeting strategy allows the generation of a constitutive Knock in (KI) of LacZ and a conditional and constitutive KI of Tk-1 and/or FLuc in the *Glul* gene. The constitutive KI 1 / conditional KI allele is obtained after PhiC31-mediated removal of the puromycin resistance selection marker. This allele expresses a chimeric transcript encoding the *Glul* protein fused to T2A, LacZ, loxP, T2A, Tk-1, FRT, loxP, T2A, FLuc and FRT sequences. A cleavage at the T2A site results in the expression of *Glul*, LacZ-loxP, Tk-1-FRT-loxP and a FLuc-FRT protein under the control of the endogenous *Glul* promoter (TaconicArtemis 2012).

3.1.3 Genotyping

Genotyping was performed from mouse genomic DNA via PCR. Animals were sedated with isoflurane to cut out a small piece of ear. DNA isolation was carried out by overnight proteinase K digestion followed by heat inactivation at 95°C for 15 min.

Table 1: Proteinase K digestion for genotyping

Reagent	Amount
10x PCR buffer	8 µl
Proteinase K (20mg/ml)	2 µl
H ₂ O sterile	70 µl
Total volume	80 µl

Cell fragments were pelletized by centrifugation at 13,000 rpm for 5 min. 5 µl of the DNA-containing supernatant was used for the genotyping PCR.

Primers are listed in 2.5.1.

Table 2: PCR protocol for detecting the knock in reporter allele in the GS mouse

Reagent	Amount
10x PCR buffer	5 µl
MgCl ₂ (25 mM)	4 µl
dNTPs (10 mM)	1 µl
Primer 7656_F	1 µl
Primer 7656_R	1 µl
Taq polymerase (1 U/µl)	1 µl
H ₂ O sterile	35 µl
DNA	5 µl
Total volume	50 µl

Table 3: PCR conditions for detecting the knock in reporter allele in the GS mouse

Step	Temp.	Time
Activation	95°C	5 min
Denaturation	95°C	30 sec
Annealing	60°C	30 sec
Elongation	72°C	1 min
	35 cycles	
	72°C	10min

PCR product formation was determined by acrylamide gel electrophoresis. The wt allele showed a product at 304 bp, the constitutive knock in allele at 403 bp.

3.1.4 Organ Harvesting

For organ harvesting, mice were anesthetized with a mixture containing 95 % CO₂ and 5 % O₂ and killed by cervical dislocation around 10 a.m. to exclude circadian influences. The abdomen was opened, the liver bled by opening the *vena cava*, weighed and washed in cold PBS. Liver lobes were isolated and shock-frozen on dry ice before stored at -70°C or fixed in Carnoy's solution or in 4 % paraformaldehyde for later paraffin embedment.

3.1.5 Preliminary Reporter Testing in the GS Reporter Mouse

Before further experiments, each of the three reporter genes was tested for its functionality. For FLuc reporter testing, activity of Firefly luciferase enzyme was measured in organ homogenates (3.8.1). For LacZ reporter testing, shock-frozen organs were processed and stained with X-Gal as described in 3.9.5. The Tk-1 measurement was performed by Dr. Andreas Schmid at the laboratory of Preclinical Imaging and Imaging Technology in Tübingen according to 3.13.

3.1.6 Section of the GS Reporter Mouse

In cooperation with the Institute of Pathology and Neuropathology, Department Pathology, University of Tübingen, Prof. Dr. med. Bence Sipos and Dr. med. vet. Ursula Kohlhofer, 30 organs from male and female GS reporter mice were isolated, rolled in tissue-tek and shock-frozen on dry ice before cutting slices and staining with X-Gal (3.9.5).

3.1.7 Induction of *Ctnnb1* mutated Liver Tumors in the GS Reporter Mouse

Generation of liver tumors in male GS reporter mice was conducted as previously described (Moennikes *et al.* 2000). Mice were injected a single intraperitoneal dose of DEN (90 µg/g body weight) at the age of 8-9 weeks followed by a treatment-free period of 2 weeks. Animals were then treated with 0.05 % PB in the drinking water for 25 weeks. Tumor formation was reported every 2-4 weeks starting at week 12 after DEN.

3.1.8 Mutation Analysis

Tumor areas were punched out with a cannula and digested with proteinase K for 1 h at 50°C followed by a heat inactivation step at 95°C for 20 min.

Table 4: Proteinase K digestion for mutation analysis

Reagent	Amount
10x PCR buffer	5 µl
Proteinase K (10 mg/ml)	2 µl
H ₂ O sterile	32 µl
Total volume	39 µl

DNA was amplified by PCR to screen for mutations in exon 3 of the *Ctnnb1* gene using the following reaction mix (table 5) and PCR conditions (table 6).

Table 5: Reaction mix for the *Ctnnb1* PCR

Reagent	Amount
Genomic DNA	39 µl
dNTPs (2 mM)	5 µl
Primer_fwd (10 µM)	2.5 µl
Primer_rev (10 µM)	2.5 µl
BSA (20 mg/ml)	1 µl
Taq polymerase (2 U/µl)	1 µl
Total volume	51 µl

Table 6: Temperature program used for the *Ctnnb1* PCR

Gene	Activation	Denat and Elongation	Annealing	Cycles
<i>Ctnnb1</i>	95°C 5 min	95°C, 58°C, 72°C à 1 min	72°C 10 min	40

Aliquots of PCR products were checked on an acylamide gel for correct product amplification. Mutations in the *Ctnnb1* gene were determined by sequencing the PCR product spanning exon 3 of the gene which encodes the critical phosphorylation sites. Sequencing was performed at 4baselab GmbH, Reutlingen, using primer pairs listed in table 2.5.2.

3.1.9 Adenoviral Gene Transfer into C3H Mice

The Gtl2 adenoviral construct was created in cooperation with Michael Mc Mahon, (Dundee, Scotland) using the AdEasy Adenoviral Vector System Kit (Agilent Technologies, Berkshire, United Kingdom).

12 6 week old male C3H mice were injected with $6.2 \cdot 10^8$ IFU in 200 μ l PBS via tail vein. 6 animals received a GFP containing adenovirus as a control, 6 animals received the Gtl2 containing adenovirus. They were killed at two different time points (4 and 8 days after injection) and the liver was harvested (3.1.4).

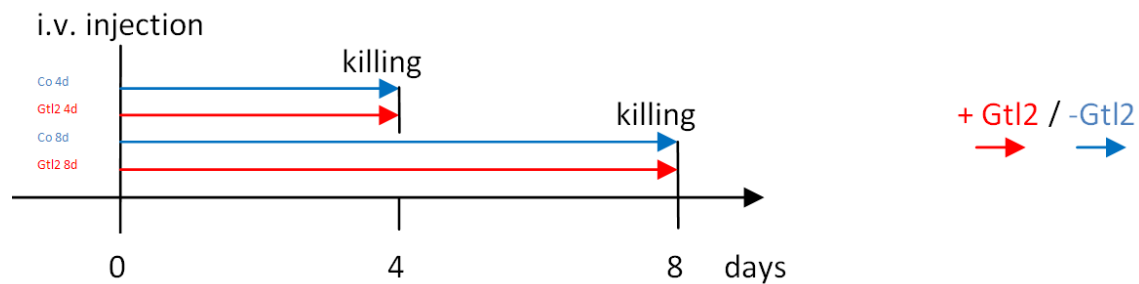


Figure 8: Schema of the AdGtl2 study. 3 mice per group were injected with an adenovirus containing Gtl2 or GFP as a control. They were killed 4 or 8 days after injection.

3.2 Cell Culture

3.2.1 General Remarks

In order to prevent contaminations, all working steps had to be performed under sterile conditions. Therefore, culture media and solutions as well as consumables were either autoclaved (121°C, 1 bar, 40 min) or, if heat sensitive, sterile filtered. Glassware was sterilized for 4 h at 180°C. Additionally, work material was disinfected with 70 % ethanol before putting under the clean bench. Cultivation took place at 37°C and 5 % CO₂ with almost saturated humidity.

3.2.2 Medium Change and Cell Passaging

When cells reached a confluence of about 90 %, they were passaged in order to prevent growth inhibition. Cells were washed with 1x PBS and detached from the dish using trypsin-EDTA. Enzyme activity was stopped by adding the culture medium before cells were singularized by pipetting up and down using an injection needle. A few drops of the cell suspension were dripped on a new dish filled with fresh culture medium. For experiments, cells had to be counted using a Fuchs-Rosenthal chamber to reach defined cell number before plating.

3.2.3 Thawing and Freezing of Cells

Frozen cells were thawed at room temperature. The suspension was transferred into prewarmed medium and centrifuged for 5 min at 900 rpm. Supernatant was sucked off and the cell pellet was resuspended in fresh culture medium. After 24 hours, the first medium change had to be conducted.

For storage, confluent cells were detached as described in 3.2.2 and centrifuged for 5 min at 900 rpm. After aspirating the supernatant, the cell pellet was resuspended in 3 ml freezing medium containing 10 % DMSO whereof 1 ml was filled into one prechilled cryo vial. The vials stayed 1 h on ice and overnight at -70°C. The following day they could be preserved in liquid nitrogen.

3.2.4 Transfection

Plasmids expressing Gtl2 are introduced into cells via lipofection-based transient or stable transfection. Lipofectamine 2000 was used according to manufacturer's manual. Cells were seeded in antibiotic-free medium 24 h prior to transfection. When they reached 60 % confluence, 0.8 µg plasmid and 1.6 µg Lipofectamine 2000 dissolved in Opti-MEM I were gently dropped onto the cells. Medium change stopped transfection 4 h later. Cells were treated 24 h after transfection.

Plasmids carrying reporter genes were introduced into the cells similarly.

Stably transfected cell line 70.4 STF K15 (Braeuning *et al.* 2007), 70.4 Tet on K23 (Stiegler 2009) and 70.4 UT K54 (Köber 2013) had been generated by cotransfection of selection markers:

Table 7: Stably transfected cell line with included plasmids and resistance

Cell Line	Plasmid transfected	Resistance
70.4 STF K15	pTALuc/ STF pSV2-neo	Geneticin
70.4 Tet on K23	pTet-On Advanced pSV2-neo	Geneticin
70.4 UT K54	pTRE-Tight-Gtl2 pTK-Hyg	Hygromycin

3.2.5 Tet-On Advanced Inducible System

The Tet-On Advanced Inducible Gene Expression System (Clontech, Mountain View, USA) provides an opportunity for on-demand expression of a desired gene, in this case Gtl2. Gtl2 expression is thereby controlled by the tetracycline derivate doxycycline. The system consists of a Tet-on Advanced transactivator and a P_{Tight} inducible promoter. In the presence of doxycycline, Tet-On Advanced binds to the tetracycline response element P_{Tight} thus activating high level transcription from the inducible promoter. This promoter controls the transcription of downstream Gtl2 (figure 9).

70.4 cells had been stably transfected with these vectors (see 3.2.4) and named 70.4 UT K54.

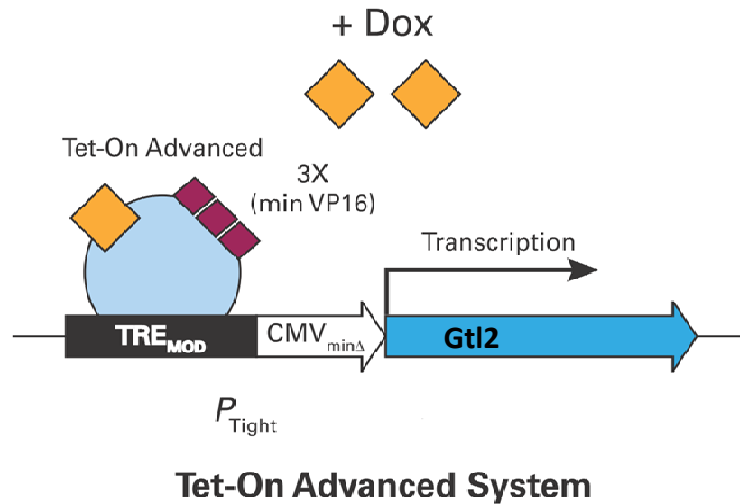


Figure 9: Induction in the Tet-On Advanced System. The system consists of a Tet-on Advanced transactivator and a P_{Tight} inducible promoter. In the presence of doxycycline (Dox), Tet-On Advanced binds to the tetracycline response element P_{Tight} thus activating high level transcription from the inducible promoter. This promoter controls the transcription of downstream Gtl2. Modified after Clontech 2012.

3.2.6 Transduction

The Gtl2 adenoviral construct was created adapted from pTRE-Tight-Gtl2 in cooperation with Michael Mc Mahon (Dundee, Scotland) using the AdEasy Adenoviral Vector System Kit (Agilent Technologies, Berkshire, United Kingdom). 10 or 100 MOI (multiplicity of infection) were dropped on the cells followed by a medium change after 4 h. RNA isolation took place 24 h after transduction.

3.2.7 Treatment

Culture medium was sucked off and replaced by fresh medium with 1 % FCS containing the reagent in end concentration. Cells were treated for 24 or 48 h. Mode of action of the different compounds as well as their final concentration are listed in table 8.

Table 8: Treatment compounds with their mode of action and final concentration

Reagent	Mode of action	Final con.
5-Aza-dC	Demethylation	10 μ M
Doxycycline	Activation of the Tet system	0.01-1 μ g/ml
LiCl	Inhibition of GSK3 β	15 mM
Phenobarbital	indirect CAR activator	30 mM

3.3 Isolation and Cultivation of Primary Cells from Mouse Liver

3.3.1 Preparation of Collagen-Coated Culture Dishes

Sterile collagen fibers from rat tails were stirred overnight in sterile filtrated 0.05 % acetic acid at 4°C. Unsolved fibers were removed by centrifugation at 5000 g for 4 h and 4°C. Culture dish coating was carried out by pipetting the collagen solution onto the dish, let drying and incubating overnight with UV.

3.3.2 Isolation of Primary Hepatocytes

Mice were anesthetized with pentobarbital and disinfected at the abdominal area, before the abdominal wall was cut open. Liver had to be flushed through the *vena porta* to the open *vena cava inferior*. As soon as the blood had fully removed, the liver became soft, bright and showed structure while collagenase buffer rinsed in. The dissected hepatocytes were washed with washing buffer and pelletized by centrifugation at 50 g for 2 min before resuspended in washing buffer. Viability was checked and cells were seeded on collagen-coated dishes. After 5 h, they were attached to the dish.

3.4 Quantitative Real-time PCR

3.4.1 Isolation of RNA from Frozen Liver

RNA was isolated from frozen liver tissue using TRIzol reagent according to the manufacturer's protocol. The concentration of eluted RNA was measured on a NanoDrop ND-1000 photometer. After RNA isolation, DNase I digestion was performed in order to remove genomic DNA. 100 µg of RNA were treated with 25 U DNase I in a total volume of 100 µl for 1 h at 37°C and purified by phenol/ chloroform extraction and subsequent ethanol precipitation.

3.4.2 Isolation of RNA from Cell Culture

RNA was isolated from cell culture using Roche High Pure RNA Isolation Kit according to the manufacturer's protocol. The concentration of eluted RNA was measured on a NanoDrop ND-1000 photometer. After RNA isolation, DNase I digestion was performed in order to remove genomic DNA. Complete RNA was treated with 25 U DNase I in a total volume of 50 μ l for 1 h at 37°C and purified by phenol/ chloroform extraction and subsequent ethanol precipitation.

3.4.3 Reverse Transcription

Reverse transcription of isolated RNA was carried out using the GeneAmp PCR System 2400 (PerkinElmer, Waltham, USA) or MyCycler™ thermal cycler (Bio-Rad, Munich, Germany) for 1 hour at 42 °C followed by a heat inactivation step of 15 min at 95°C. The following reaction mix was used:

Table 9: Reaction mix for reverse transcription of isolated RNA

Reagent	Amount
10x PCR buffer	1.5 μ l
MgCl ₂ (25 mM)	3 μ l
dNTPs (10 mM)	1.5 μ l
dT ₂₀ (500 ng/ μ l)	0.38 μ l
dN ₆ (500 ng/ μ l)	0.38 μ l
AMV-RT (10 U/ μ l)	0.39 μ l
H ₂ O sterile	4.85 μ l
RNA (125 ng/ μ l)	3 μ l
Total volume	15 μl

3.4.4 LightCycler PCR

Quantitative real-time PCR was carried out on a LightCycler 1.5 instrument (Roche Applied Science, Penzberg, Germany) using either the FastStart DNA Master^{PLUS} SYBR Green I kit (Roche) or the QuantiTect SYBR Green PCR kit or QuantiFast Probe PCR kit (both Qiagen, Hilden, Germany). Primers were either synthesized by Eurofins MWG GmbH (Ebersberg, Germany) or obtained as predesigned primer assays from Qiagen and used with the QuantiTect or QuantiFast PCR kits according to the manufacturer's instructions. The temperature programs for the designed primers are listed in table 10 (for primer sequences see 2.5.6).

Table 10: Temperature programs used for LightCycler PCR

Gene	Activation	Denaturation	Elongation	Annealing	Cycles
18s rRNA	95°C 10 min	95°C 5 s	68°C 5 s	72°C 8 s	35
hCAR1	95°C 10 min	95°C 7 s	62°C 6 s	72°C 6 s	45
mCcmd1	95°C 10 min	95°C 6 s	65°C 6 s	72°C 4 s	50
mCdk2	95°C 10 min	95°C 6 s	65°C 6 s	72°C 5 s	45
mCdk4	95°C 10 min	95°C 7 s	65°C 6 s	72°C 12 s	50
mCyp2b10	95°C 10 min	95°C 0 s	57°C 5 s	72°C 5 s	60
rCyp2b	95°C 10 min	95°C 7 s	63°C 6 s	72°C 17 s	50
rCyp4a	95°C 10 min	95°C 7 s	66°C 6 s	72°C 18 s	50
rGls2	95°C 10 min	95°C 7 s	66°C 6 s	72°C 17 s	50
mGtl2-T3	95°C 10 min	95°C 7 s	64°C 6 s	72°C 15 s	45
mNr4a2	95°C 10 min	95°C 5 s	62°C 6 s	72°C 8 s	50
mOlfr612	95°C 10 min	95°C 7 s	59°C 6 s	72°C 19 s	45
mPcna	95°C 10 min	95°C 5 s	58°C 6 s	72°C 10 s	50
rSds	95°C 10 min	95°C 7 s	66°C 6 s	72°C 17 s	50
mWdr20a	95°C 10 min	95°C 7 s	66°C 6 s	72°C 17 s	45

3.5 Global Gene Expression Analysis

Global gene expression analysis was performed on Affymetrix Mouse Gene ST 2.1 Array chips by Dr. Michael Bonin, Microarray Gene Chip Facility, Institute of Medical Genetics, Tübingen. Michael Römer, Department of Computer Science, Cognitive Systems, Tübingen, conducted the analysis, where he filtered out genes with less than 50 % deregulation.

3.6 Electrophoresis

3.6.1 Agarose Gel Electrophoresis

Agarose was dissolved in 1x TAE by boiling in a microwave for 2 min. After cooling down, 0.003 % Midori Green Advanced DNA stain (Nippon Genetics, Düren, Germany) was added for later visualization and the gel was poured in the chamber. DNA samples were prepared with 6x DNA loading buffer while 2x RNA loading dye was used for RNA samples and applied in parallel with a size marker. Gel run was performed in 1x TAE with 90 V for 60 min. Afterwards, the gel was photographed under UV light using a CSC Chemoluminescence detection module (Raytest, Straubenhardt, Germany).

3.6.2 Acrylamide Gel Electrophoresis

Acrylamide gel mix was prepared according to table 11. After polymerization, the gel was poured into a rack. DNA samples were prepared with 6x DNA loading buffer and applied in parallel with a size marker. Gel run was performed in 1x TBE with 300 V for 70 min. Afterwards, the gel was stained with ethidiumbromide (0.5 µg/ml) for 10 min and photographed under UV light using a CSC Chemoluminescence detection module (Raytest, Straubenhardt, Germany).

Table 11: Mix for acrylamide gels

Reagent	Amount
H ₂ O _{dest}	16.6 ml
5x TBE	7.2 ml
Acrylamide (30 %)	12 ml
10 % APS	200 µl
TEMED	30 µl

3.7 Plasmid Preparation

3.7.1 Amplification of Gtl2-T3

Gtl2-T3 was amplified of cDNA transcribed from *Cttnb1* mutated mouse liver tumor tissue using the Expand Long Template PCR System (Roche Diagnostics, Mannheim, Germany) and the following PCR conditions:

Table 12: PCR protocol for amplification of Gtl2-T3

Reagent	Amount
10x buffer 1	5 μ l
dNTPs (10 mM)	1.75 μ l
Primer Gtl2_F1 (20 μ M)	1 μ l
Primer Gtl2_R1 (20 μ M)	1 μ l
Polymerase-mix	0.75 μ l
H ₂ O sterile	37.5 μ l
cDNA	3 μ l
Total volume	50 μl

Table 13: PCR conditions or amplification of Gtl2-T3

Step	Temp.	Time
Activation	94°C	2 min
Denaturation	94°C	10 sec
Annealing	59°C	30 sec
Elongation	68°C	2 min
	10 cycles	
Denaturation	94°C	15 sec
Annealing	59°C	30 sec
Elongation	68°C	2 min + 2 sec
	25 cycles	
	72°C	7 min

PCR product formation was determined by agarose gel electrophoresis, showing Gtl2-T3 at 1.9 kb.

3.7.2 Amplification of Gtl2 upstream regions

Gtl2 upstream regions were amplified of mouse genomic DNA (Promega, Mannheim, Germany) using the Expand Long Template PCR System (Roche Diagnostics, Mannheim, Germany), the following primer pairs and PCR conditions:

Table 14: PCR primer combinations for amplification of Gtl2 upstream regions

Fragment	Primer F	Primer R
Prom_T1	Gtl2_T1_F2	Gtl2_T1_R1
Prom_T2_3_A	Gtl2_fw160	Gtl2_rev1980
Prom_T2_3_M	Gtl2_fw1966	Gtl2_rev3611
Prom_T2_3_E	Gtl2_T2_3_F2	Gtl2_T2_3_R

Table 15: PCR protocol for amplification of Gtl2 upstream regions

Reagent	Amount
10x buffer 1	5 µl
dNTPs (10 mM)	1.75 µl
Primer F (20 µM)	1 µl
Primer R (20 µM)	1 µl
Polymerase-mix	0.75 µl
H ₂ O sterile	39 µl
gen. mouse DNA	1.5 µl
Total volume	50 µl

Table 16: PCR conditions for amplification of Gtl2 upstream regions

Step	Temp.	Time
Activation	94°C	2 min
Denaturation	94°C	10 sec
Annealing	59°C	30 sec
Elongation	68°C	2 min
	10 cycles	
Denaturation	94°C	15 sec
Annealing	59°C	30 sec
Elongation	68°C	2 min + 2 sec
	25 cycles	
	72°C	7 min

PCR product formation was determined by agarose gel electrophoresis, both Prom_T1 and Prom_T2_3 showing a product at 1.3 kb, while Prom_T2_3_A was 1.6 kb and Prom_T2_3_M was 1.8 kb.

3.7.3 Cloning Strategy

All four fragments of the Gtl2 upstream region were cloned into pT81luc by means of the TOPO TA Cloning Kit (Life technologies, Darmstadt, Germany) according to manufacturer's instruction. First, fragments were subcloned into pCR2.1-TOPO by the advantage of the terminal transferase activity of Taq polymerase adding a single A overhang to the PCR product, thus cloning it directly into the linearized vector. Ligation activity was raised by the presence of topoisomerase I. Positive clones could then be selected via blue-white-screening before desired fragments were cut out through overnight digestion using *HindIII* and *XhoI*. Subsequent dephosphorylation and purification of the backbone prepared Prom_T1, Prom_T2_3_A, Prom_T2_3_M and Prom_T2_3_E for their introduction into pT81luc target vector. Correct insertion was determined by sequencing.

3.7.4 Plasmid Progeny and Isolation

Bacteria can be easily used to propagate desired vectors using frozen stocks. A small amount of a stock was transferred into LB medium containing vector specific selective antibiotics. Bacteria culture grew overnight at 37°C. Depending on the quantity, plasmid isolation was performed with Easyprep Pro Plasmid Mini Kit (Biozym, Hessisch Oldendorf, Germany) or Genopure Plasmid Maxi Kit (Roche Diagnostics, Mannheim, Germany) according to manufacturer's instruction. Both isolation procedures are based on a modified alkaline lysis protocol followed by binding of the plasmid DNA to the anion-exchange material in the column, washing with high salt buffers and subsequent elution in H₂O_{dest}.

If no glycerol stock was available, vectors had to be transformed into One Shot TOP10 chemically competent *e.coli* (Life technologies, Darmstadt, Germany) as described by the manufacturer.

3.7.5 DNA Quantification

Determination of the DNA concentration and purity was carried out measuring the optical density at 260 nm with the NanoDrop ND-1000 (Peqlab, Erlangen, Germany).

$$c(DNA) \left[\frac{\mu g}{ml} \right] = Extinction_{260\text{ nm}} \cdot 50 \frac{\mu g}{ml} \cdot dilution\ factor$$

The $\frac{Extinction_{260\text{ nm}}}{Extinction_{280\text{ nm}}}$ ratio indicates the purity of the DNA solution; it shall reside between 1.8 and 2. Such pure DNA could be used for further experiments.

3.8 Luciferase Assays

3.8.1 Firefly Luciferase Measurement in Homogenate of GS mice

To measure FLuc reporter activity in GS mice, desired organs were isolated, weighed and washed in cold PBS. Every shock-frozen organ was homogenated in PBS. After lysis of cells with 1x PLB, the activities of Firefly luciferase enzyme was detected via measurement of generated luminescence at the multiwell plate reader 1420 Multilabel Counter Victor V³ (Perkin Elmer, Waltham, USA). The assay was calibrated with recombinant luciferase to allow an estimation of the amount of enzyme per tissue unit.

3.8.2 Duale Luciferase Reporter System

Reporter systems are important tools for the analysis of eukaryotic gene expression. Thereby, a reporter plasmid is used expressing the Firefly luciferase gene under the control of a promoter of interest. Enhanced activation of the gene of interest can easily be detected concerning to increased Firefly luciferase activity accompanied with luminescence. Due to varying transfection efficiencies, Renilla luciferase controlled by a constitutive active CMV promoter is used as a standard.

For preparation, cells were washed with 1x PBS. Lysis took place for 20 min under gentle shaking with 1x PLB. Generated luminescence was measured at the multiwell plate reader 1420 Multilabel Counter Victor V³ (Perkin Elmer, Waltham, USA). Since Firefly luciferase reaction is quenched by adding Renilla buffer and luminescence is detected at different wavelengths, both luciferases could be detected in one assay.

3.9 Immunohistochemistry and *in situ* Hybridization

3.9.1 Frozen Liver Sections

Sections were prepared in a microtome from frozen organs. Slices (10 µm) were fixed with 3 % formaldehyde, while unspecific binding was blocked by incubation with swine serum (1:20 dilution, Dako, Glostrup, Denmark) and subsequently stained immunohistochemically.

3.9.2 Carnoy Fixation

Liver tissue was incubated in Carnoy fixative overnight. The fixative was removed by overnight incubation in isopropanol followed by embedding of the tissue samples in paraffin.

3.9.3 Formalin Fixation

Liver tissue was fixed in 4 % formalin overnight and washed for 1 h with water. Dehydration took place overnight (50-100 % isopropanol) before embedment in paraffin.

3.9.4 Preparation

5 µm sections were performed from Carnoy (3.9.2) and formalin (3.9.3) fixed, paraffin embedded tissues. Before staining, slices were deparaffinized in xylene and rehydrated (50-100 % ethanol).

3.9.5 X-Gal Staining

Mouse organs were fixed by 2 % paraformaldehyde/ 0.25 % glutaraldehyde in PBS. Fixation buffer was removed by washing in 1x PBS for 1 h. β -Galactosidase positive cells were stained by an incubation in X-Gal staining buffer at room temperature.

3.9.6 Glucose-6-phosphatase Staining

Cryo sections were dipped in 0.5% glutaraldehyde in H_2O_{dest} and incubated for 20 min in the staining solution at 37°C. After short precipitation in 1 % ammonium sulfide, they were fixed for 5 min in 5% glutaraldehyde-glacial acetic acid. Sections were washed with H_2O_{dest} and subsequently stained with Mayer's haematoxylin for 5 min. They were rinsed with water for 15 min and dehydrated in graded alcohols followed by repeated incubation in xylene for 5 min and embedment in entellan.

3.9.7 HE Staining

Cryo sections were washed with H_2O_{dest} and subsequently stained with Mayer's haematoxylin for 5 min. They were rinsed with water for 10 min, equilibrated in 50 % ethanol for 30 s and stained with alcoholic eosin solution for 3 min. Afterwards, ethanol dehydrated the sections followed by repeated incubation in xylene for 5 min and embedment in entellan.

3.9.8 Staining of Cyps and GS

Cryo sections were incubated in methanol/ H_2O_2 for 15 min to inactivate peroxidases. Unspecific binding was blocked before primary antibody binding was performed overnight at 4°C in humid atmosphere. Then, horseradish peroxidase conjugated secondary antibody was added for 1 h at RT. Sections were stained with 3-amino-9-ethylcarbazole/ H_2O_2 .

3.9.9 Meg3/ Gtl2 *in situ* Hybridization

In situ Hybridization (ISH) was performed at the Department for Discovery and Investigative Safety, Novartis Institutes for Biomedical Research, Basel, Switzerland, using the fully automated instrument Ventana Discovery Ultra (Roche Diagnostics, Schweiz AG, Rotkreuz, Switzerland) according to Lempiainen *et al.* 2013.

3.10 Digitonin Based Cell Fractionation

In order to determine the cellular localization of Gtl2, RNA was fractionated and the expression was measured. At once, Histone H3 and GAPDH (glyceraldehyde 3-phosphate dehydrogenase) proteins were used for purity control of the nuclear and cytosolic fractions. A well established protein fractionation protocol of Holden *et al.* was adapted to RNA fractionation (Holden and Horton 2009). Thereby, digitonin (Sigma, Taufkirchen, Germany) was used to permeabilize the cell membrane, thus lysing the cells.

Cells were scraped off in 1x PBS and pelletized by centrifugation (15 min, 300 g, 4°C). The pellet was resuspended in digitonin buffer. After 60 min of incubation at 4°C, cytosolic protein fraction was separated by centrifugation (30 min, 2000 g, 4°C). The supernatant (cytosolic protein fraction) was divided, half for RNA isolation with TRIzol and half for purity control of the cytosolic fraction via western blot. NP-40 buffer was used to dissolve the remaining cell pellet and incubated on ice for 45 min. Separation of the organelle membrane bound fraction was conducted by centrifugation (30 min, 7000 g, 4°C). The pellet was dissolved in RIPA buffer containing benzonase and incubated on ice for 3 h with recurrent mixing. Nuclear fraction was gained after centrifugation (30 min, 7000 g, 4°C) and subsequently divided for RNA and protein isolation.

3.11 Western Blot

Polyacrylamide gels are used to separate proteins according to their length and charge. Therefore, proteins are denatured with β -mercaptoethanol while SDS imparts a negative charge to linearized proteins.

The running gel was first filled into the assembled chamber and let polymerize covered with isopropanol. Then the stacking gel was casted (table 17).

Table 17: Mix for two SDS polyacrylamide gels

Reagent	12.5 % running gel	4 % stacking gel
Acrylamide solution	15 ml	10 ml
10 % APS	150 μ l	100 μ l
TEMED	15 μ l	10 μ l

Samples were mixed with an equal volume of 2x Lämmli buffer and heated for 10 min at 90°C. SDS-PAGE was performed at 100 V to separate proteins. Then, proteins were blotted on a PVDF membrane via wet electroblotting at 400 mA and 4°C for 150 min. The membrane was dried and activated with methanol. Blocking followed for 1.5 h to avoid unspecific binding of the antibodies. The blocking solution was replaced by the primary antibody and the membrane incubated overnight at 4°C. The next day, the membrane was washed twice before the secondary antibody was added for 2 h. After twice washing and incubation with 1x assay buffer, the membrane was covered with CDP-Star ready to use (Life technologies, Darmstadt, Germany) and laminated. Photos were captured using a CSC Chemoluminescence detection module (Raytest, Straubenhardt, Germany) after 1 h incubation in the dark.

For antibody dilutions, washing and blocking conditions see chapter 2.6.

3.12 RNA protein pulldown

3.12.1 *In vitro* Transcription

Linearized plasmid pBlueScript SK(-)/Gtl2-T3 containing Gtl2 DNA flanked of T3 and T7 RNA polymerase promoters was used as a template for *in vitro* transcription. The following reaction mix (table 18) was incubated at 37°C for 2 h before RNA synthesis was stopped by the addition of 2 µl 0.5 M EDTA pH 8.0 and incubation at 65°C for 10 min. T7 RNA polymerase synthesized Gtl2 in sense orientation, T3 polymerase synthesized Gtl2 in antisense orientation.

Table 18: Reaction mix for *in vitro* transcription

Reagent	Amount
5x Transcription buffer	10 µl
NTPs (10 mM) containing Biotin-16-UTP (3.5 mM)	10 µl
RNase inhibitor	1.25 µl
T7 or T3 RNA polymerase	1.5 µl
Linearized template DNA	1 µg
DEPC-treated H ₂ O	ad 50 µl
Total volume	50 µl

RNA precipitation took place after adding 4 µl 4 M LiCl and 150 µl EtOH overnight at -75°C. RNA was washed with 70 % EtOH and dissolved in DEPC-H₂O containing an RNase inhibitor. RNA length was determined on an agarose gel, while Biotin Luminescent Detection Kit (Roche Diagnostics, Mannheim, Germany) was used to detect biotin-labeled nucleic acids by enzyme immunoassay with luminescence according to manufacturer's instruction.

3.12.2 RNA Protein Pulldown

Streptavidin coupled Dynabeads have been extensively used for isolation of biotinylated molecules due to their very high binding affinity and the replacement of centrifugation by a magnet. Here, Gtl2 binding proteins were isolated and identified via mass spectrometry.

In preparation for the pulldown, Dynabeads M-280 Streptavidin (Life technologies, Darmstadt, Germany) were washed twice with 1x BW buffer, solution A and solution B before resuspended in 2x BW buffer. The beads were preincubated with 70.4 UT K54 proteins and washed once again. RNA binding took place by adding 4 µg sense or antisense RNA and RNase inhibitor dissolved in the similar volume to that of 2x BW buffer and followed by a subsequent incubation on a shaker for 30 min. Unbound RNA was washed away three consecutive times with 20 mM Tris-HCl pH 7.5. For protein binding, a protein-premix (table 19) was added to the beads dissolved in 1x RNA protein binding buffer and incubated for 60 min at 4°C with gentle agitation.

Table 19: Protein-premix for RNA-protein pulldown

Reagent	Amount
10x RNA protein binding buffer	10 µl
Glycerol	15 µl
Protein (of 70.4 UT K54)	500 µg
RNase inhibitor	1 µl
DEPC-treated H ₂ O	ad 100 µl
Total volume	100 µl

Beads had been washed three times with an equal volume of 1x BW buffer. Boiling the beads in SDS sample buffer for 15 min eluted bound proteins. Eluate was appended to the same amount of water and applied to a SDS-PAGE gel. Bart van den Berg (NMI, Protein Analytic, Reutlingen) performed the in-gel digestion and adjacent mass spectrometry. A schematic representation of the procedure is given in the figure below.

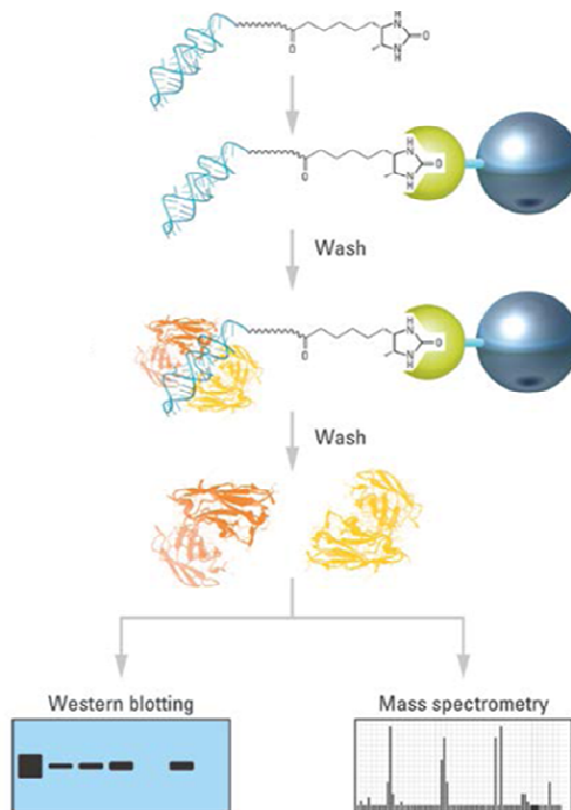


Figure 10: Schematic procedure summary for the RNA-protein pulldown using magnetic beads. First, the RNA was labeled with biotin and bound to the streptavidin coupled beads. RNA bound beads were then equilibrated in buffer before protein mix was added. Unbound proteins were washed away. Samples were eluted by boiling the beads in SDS sample buffer. Finally, mass spectrometry was used to identify eluted proteins. This could be determined by western blotting (modified after Pierce Magnetic RNA-Protein Pulldown Kit, Thermo Scientific, Schwerte, Germany).

3.13 PET Imaging

Positron emission tomography (PET) was performed at the laboratory of Prof. Bernd Pichler by Dr. Andreas Schmid (Laboratory for Preclinical Imaging and Imaging Technology of the Werner Siemens-Foundation, Department of Preclinical Imaging and Radiopharmacy, Tübingen) using ^{18}F -FHBG as a reporter probe for imaging thymidine kinase 1 reporter gene in the GS mouse.

3.14 MRI Imaging

Magnetic resonance imaging (MRI) was carried out at the laboratory of Prof. Bernd Pichler by Dr. Andreas Schmid (Laboratory for Preclinical Imaging and Imaging Technology of the Werner Siemens-Foundation, Department of Preclinical Imaging and Radiopharmacy, Tübingen) according to Schmid *et al.* 2013 from week 12 after DEN every 2-4 weeks with a 7 Tesla MR scanner (ClinScan, Bruker BioSpin MRI, Ettlingen, Germany).

3.15 Statistic data processing

Statistic processing of the datasets including mean value, standard deviation and standard error of mean were conducted in excel. Two groups were compared using the paired or unpaired student's t-test. Differences were considered significant in groups with five or more independent experiments or animals when $p < 0.05$ (indicated by *). $P < 0.01$ is indicated by **, $p < 0.001$ by ***.

4. Results

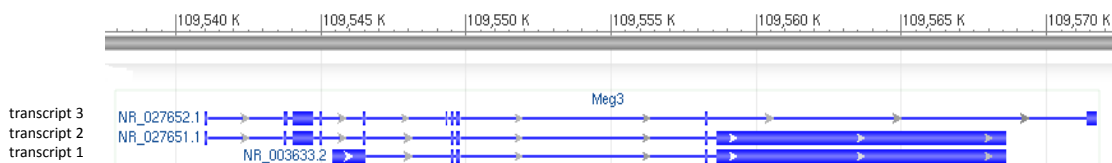
4.1 Gtl2 Expression in Different Tumor Tissues

4.1.1 Expression of Gtl2 Transcript Variant 3 in Murine Liver

Recent work of our MARCAR project partners showed that several non-coding RNAs encoded in the imprinted Dlk1-Dio3 gene cluster are upregulated in wild type mouse liver after PB treatment (Lempiainen *et al.* 2013, Phillips *et al.* 2009). Long non-coding RNA Gtl2, the human orthologue is known as MEG3 (maternally expressed gene 3), is the main topic in this thesis and located within this cluster.

Three Gtl2 transcript variants of varying length were documented in the NCBI database, but only transcript variant 3 (NR_027652.1), the shortest one with 1.9 kb, could be detected in the above mentioned PB promoted liver tumors and in PB treated normal liver (figure 11). Thus, Gtl2 transcript variant 3 (Gtl2-T3) expression was determined from now on, in the following only named Gtl2.

A



B

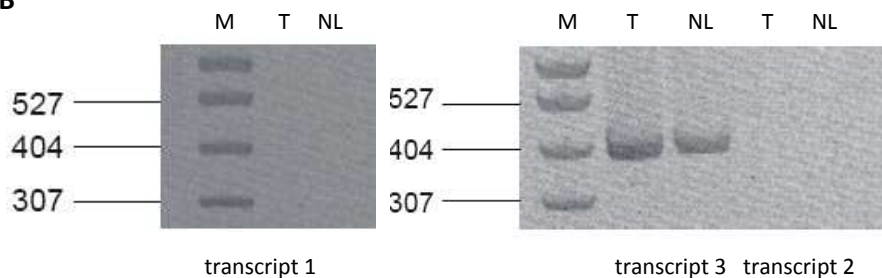


Figure 11: Gtl2 transcript variants expressed in murine tissue. (A) Three different Gtl2 transcript variants of varying length are documented in the NCBI database, **(B)** but only Gtl2 transcript 3 (NR_027652.1, Gtl2-T3) could be detected in phenobarbital (PB)-treated normal liver (NL) and *Ctnnb1* mutated tumor tissue (T). M, marker.

As recapitulated in figure 12, Gtl2 expression was upregulated both in normal murine liver after PB treatment and in *Cttnb1* mutated liver tumors compared to untreated controls, although the increase was much higher in *Cttnb1* mutated tumors. *Ras/ Raf* mutated liver tumors showed a decrease in Gtl2 expression compared to *Cttnb1* mutated tumors.

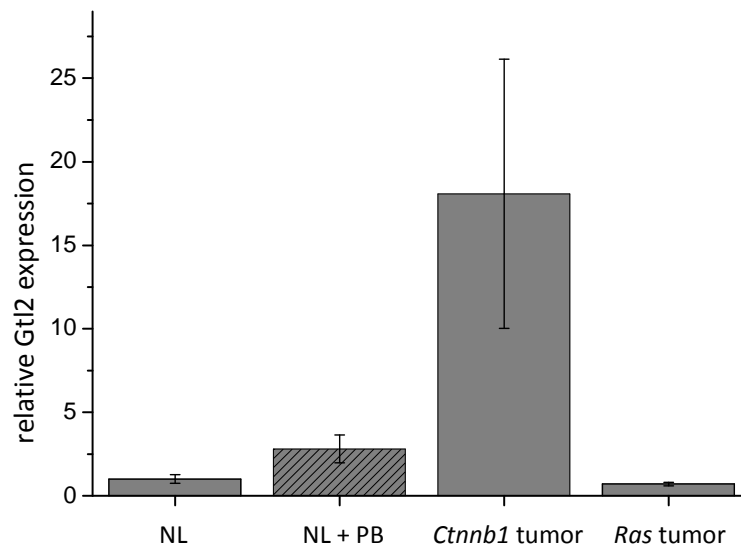


Figure 12: Relative Gtl2 expression in normal liver (NL) compared to phenobarbital treated liver (NL + PB) for 12 weeks, *Cttnb1* mutated tumor and *Ras/ Raf* mutated tumor tissue. Gtl2 was upregulated after phenobarbital (PB) treatment, in *Cttnb1* mutated liver tumors, but downregulated in *Ras/ Raf* mutated tumors. PB treatment is indicated by hatching. n=3-5, \pm SEM are given.

4.1.2 Induction of Gtl2/ MEG3 Expression in Human, Mouse and Rat Liver

To check the transferability to other species with tumors comprising *Cttnb1* mutations, MEG3 expression was ascertained in human hepatoblastoma (HB), a rare liver neoplasm occurring in small infants and children. Samples were obtained from the University Children's Hospital, Tübingen. Recent analysis by Dr. Andreas Schmidt demonstrated 80 % prevalence of mutations in *CTNNB1* in those tumor samples (Schmidt *et al.* 2011). Only tumor samples comprising these mutations were used for the following measurement. As shown in figure 13, MEG3 was elevated in most *CTNNB1* mutated hepatoblastoma samples compared to adjacent normal liver tissue.

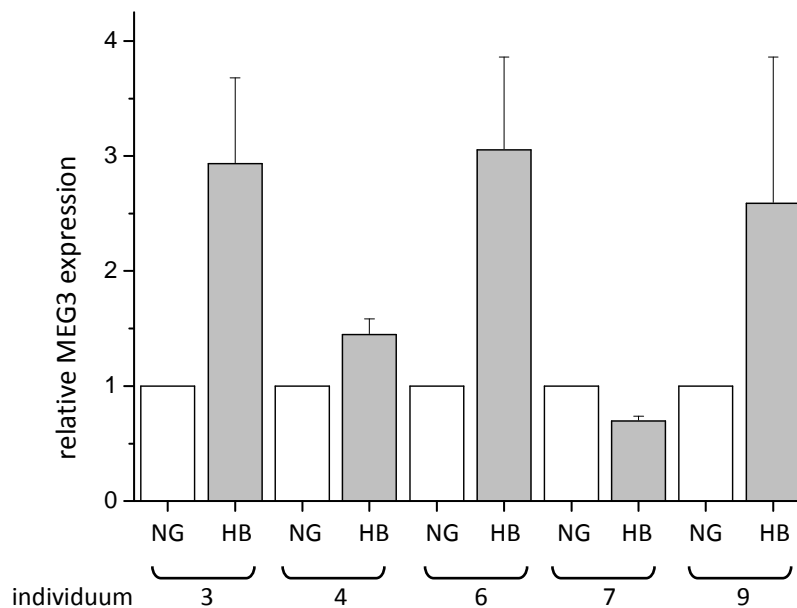


Figure 13: Relative MEG3 expression in *CTNNB1* mutated human hepatoblastoma compared to normal tissue. Tumors were represented by grey bars, normal tissue by colorless bars. MEG3 was upregulated in most mutated hepatoblastoma. Presented data result from three measurements; mean \pm SEM are given. NG, normal liver surrounding the respective tumor; HB, hepatoblastoma.

Lempiainen *et al.* 2013 revealed altered gene expression in the whole *Dlk1-Dio3* cluster in *Cttnb1* mutated liver tumors growing under PB treatment. As evident from figure 12, *Gtl2* expression was reduced in *Ras/Raf* mutated liver tumors compared to those tumors harboring a *Cttnb1* mutation, selected by the tumor promoter PB. To clarify whether PB treatment of mice would lead to a reexpression of *Gtl2* in *Ras* and *Raf* mutated liver tumors, mice that had been treated at 2 weeks of age with DEN were treated with PB for 4 weeks at the age of 6 months, when *Ras/Raf* mutated tumors were expected to be manifest. Interestingly, in response to PB, *Ras* and *Raf* mutated tumors expressed significantly less *Gtl2* and expression of *Rian* and *Mirg*, two other non-coding RNAs from the maternal allele, was also downregulated. These changes were accompanied by decreased mRNA levels of two protein coding genes on the cluster, *Rtl1* and *Dio3*, as it is depicted in figure 14. *Dlk1* could not be detected. These result also clearly shows that PB alone cannot explain the upregulation of *Gtl2* in *Cttnb1* mutated liver tumors since such an effect was not seen in their *Ras/Raf* mutated counterparts.

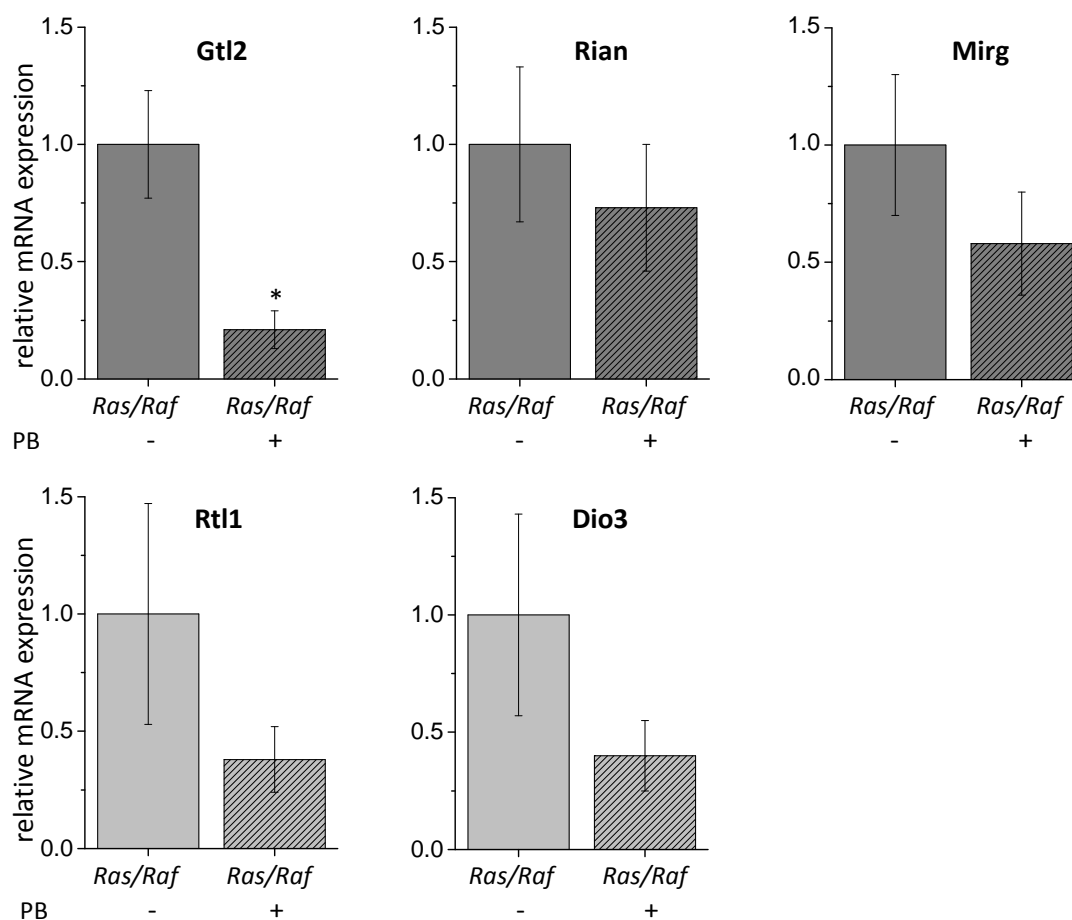


Figure 14: Relative expression of Dlk1-Dio3 cluster genes in murine *Ras* or *Raf* mutated tumors treated with or without phenobarbital. The maternal genes *Gtl2*, *Rian* and *Mirg*, represented by dark grey bars, were downregulated in *Ras/Raf* tumors of animals treated with phenobarbital (PB) for 4 weeks at the age of 6 months as well as the paternal genes *Rtl1* and *Dio3*, represented by light grey bars. PB treatment is indicated by hatching. 5-6 animals per group; mean \pm SEM are given. Unpaired student's t-test *... p-value < 0.05.

In the following, Dlk1-Dio3 cluster alterations were examined administrating additional NGC to mice to decide whether the foregoing observed perturbations were attributable only to PB or also to other NGC. In a previous study, equipotent doses of the polychlorinated biphenyls PCB 153 and PCB 126, and a combination of both were administered to mice for 22 weeks. PCB 153 is a prototype PB-like PCB acting through CAR while PCB 126 is a dioxin-like PCB which acts via the Ah-receptor. Because recent studies had shown that the potency of PCBs are correlated to their Cyp inducing capacity, induction of Cyp2b10 and Cyp1a1 isoforms respectively were used as an indicator of their outcome, as indicated in figure 15. In response to PCB 153 and PCB 126, hepatocytes expressed significantly higher levels of maternally expressed *Gtl2*, *Mirg* and *Rian* and the paternal *Rtl1*, while the other paternal protein coding gene *Dio3* was downregulated. Once again, *Dlk1* could not be detected.

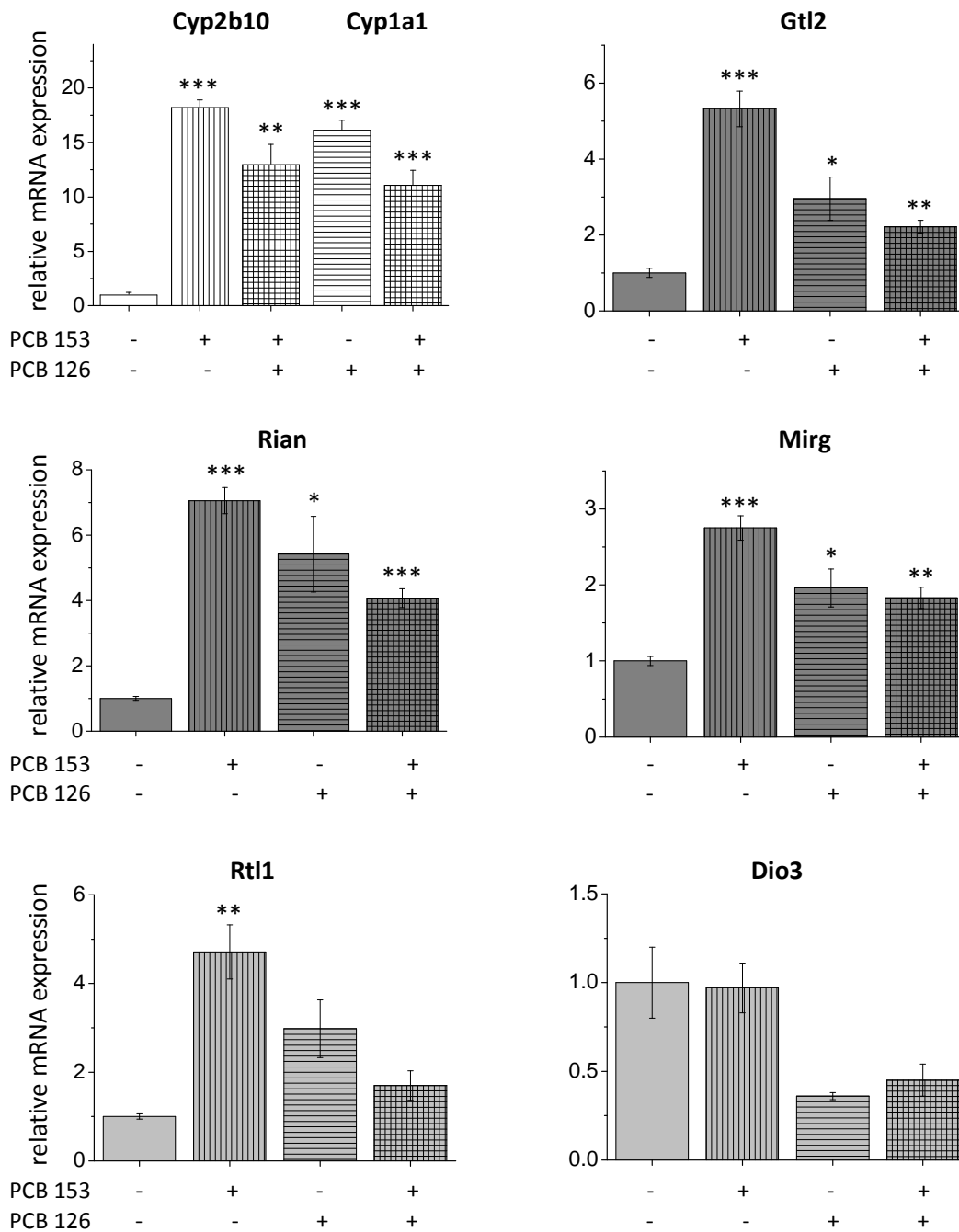


Figure 15: Relative expression of Dlk1-Dio3 cluster genes and Cyp2b10 and Cyp1a1 in murine liver treated with PCB 153, PCB 126 or a combination of both for 22 weeks. The aryl hydrocarbon receptor (AhR) agonist PCB 126 and PCB 153, acting via activation of the constitutive androstane receptor (CAR) led to enhanced Gtl2, Mirg and Rtl1 expression. The corresponding Cyp isoform was also upregulated. Paternal gene Rtl1 was upregulated but Dio3 was downregulated. Maternal genes are represented by dark grey bars, while paternal genes are represented by light grey bars. PCB treatments are indicated by different hatching. 5 animals per group; mean \pm SEM are given. Unpaired student's t-test *... p-value <0.05, ** < 0.01, *** < 0.001.

Since PB is a non-genotoxic hepatocarcinogen in rodents (Lee 2000, Whysner et al. 1996), there is toxicological concern about the relevance of this effect for humans. In this case, the development of humanized mouse models provides a powerful approach for understanding pathways of human diseases. To analyze potential species differences in receptor dependent Dlk1-Dio3 cluster regulation underlying liver tissue molecular responses to other CAR activators to which man may be exposed, humanized CAR/ PXR (hCAR/ hPXR) and wt mice obtained two different doses of cyproconazole (cypro) or prochloraz (procl) in the diet for 4 weeks. Both compounds are part of the conazole fungicides with cypro belonging to the larger group of triazol fungicides while procl is characterized by the presence of an imidazole ring and is thus member of the imidazole fungicides. Samples were available from a recently conducted study in our lab (Braeuning, unpublished).

Induction of Cyp2b10 expression was used, as in the PCB-study, as an indicator of CAR activation caused by the fungicides cyproconazole and prochloraz. Analogous to other CAR agonists, cypro induced mRNA levels of all three lncRNAs, namely Gtl2, Rian and Mirg quite differently in a concentration dependent manner. Surprisingly, the highest concentration was less effective in altering their expression than the lower one. As illustrated in figure 16, procl had the ability to augment maternal Gtl2, Rian and Mirg expression, too, while in contrast, paternal protein coding genes Rtl1 and Dio3 showed extenuated expression levels after treatment with both fungicides. Upon comparison of wt with humanized mice, the latter displayed a fewer impact of procl and cypro on all maternal Dlk1-Dio3 cluster genes above mentioned, while paternal genes were downregulated to an equal or even greater extent.

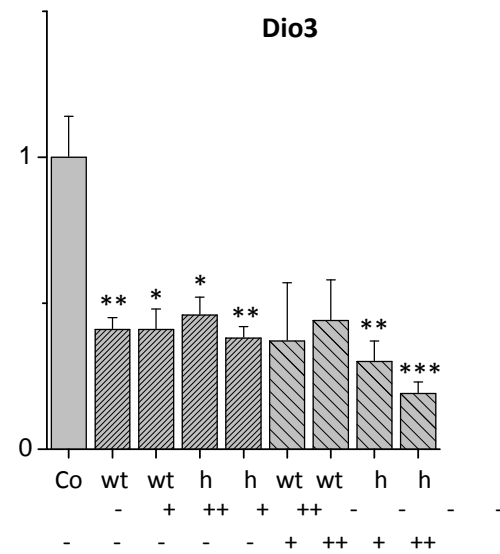
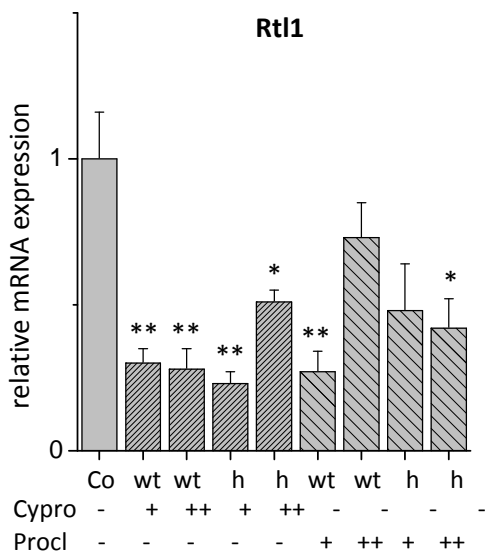
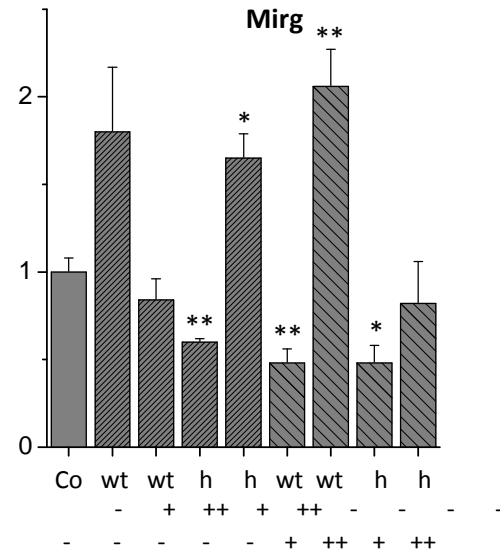
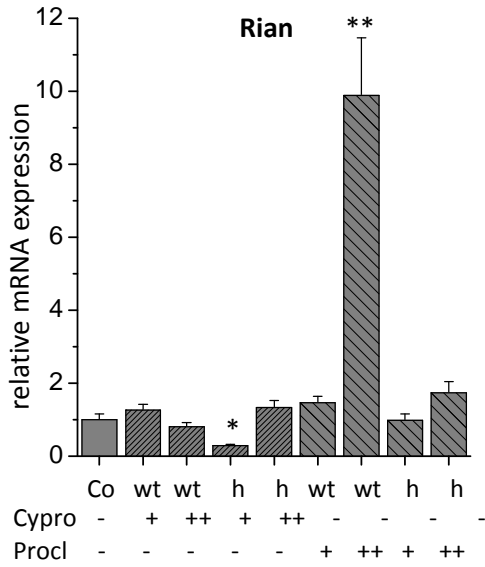
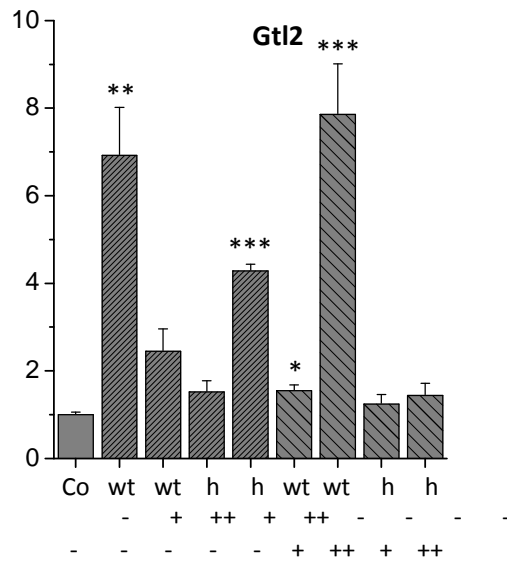
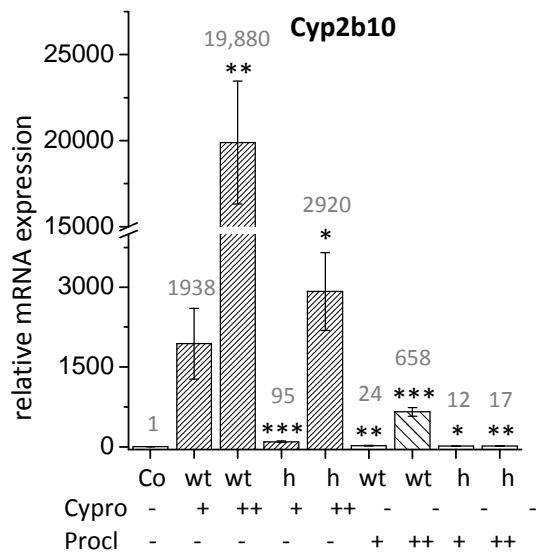


Figure 16: Relative expression of Dlk1-Dio3 cluster genes and Cyp2b10 in the liver of wt and hCAR/ hPXR animals treated with different concentrations of two fungicides, cyproconazole (cypro) and prochloraz (procl) for 4 weeks. Paternal protein coding genes Rtl1 and Dio3 were downregulated, while the maternal Gtl2 was upregulated. The other two maternal genes, Rian and Mirg showed a varying expression. Cyp2b10 was upregulated. Maternal genes are represented by dark grey bars, while paternal genes are represented by light grey bars. Conazole fungicide treatments are indicated by different hatching. 6 animals per group; mean \pm SEM are given. Unpaired student's t-test *... p-value < 0.05, ** < 0.01, *** < 0.001.

At present, most toxicological studies and long term experiments are performed in rodents, often mice, but more frequently in rats as they pose a more transferrable model to humans. Therefore, analysis of liver samples of Wistar rats fed with PB and clofibrate (CF) were included in this work. As already described by Ittrich *et al.* 2003, male and female rats developed preneoplastic foci of altered hepatocytes when feeding them with the mentioned NGC (0.05 % PB or 0.5 % CF) for 10 consecutive weeks. Augmented Cyp2b10 expression could be regarded as the indicator for CAR activation whilst Cyp4a posed as a marker for peroxisome proliferation (figure 18). As it is depicted in figure 17, CF and PB were able to influence Gtl2 expression in male and female rats only very moderately without statistical significance. These findings of NGC action were compared to GC effects caused by N-nitrosomorpholine (NNM) and 2-acetylaminofluorene (AAF). NNM diminished Gtl2 level in both genders, but AAF revealed significant gender differences (figure 17). Interestingly, AAF induced Gtl2 expression in liver of males which also were much more sensitive to the aromatic amine with respect to the development of preneoplastic foci while no such effect were seen in the comparatively insensitive females (Ittrich *et al.* 2003).

Hereinafter, expression of Wnt target genes was monitored by qPCR. All treated rats displayed homogenous augmented Cyp7a1 expression in their livers. The enzyme catalyzes the rate limiting step of bile acid synthesis from cholesterol. Serine dehydratase (Sds), converting serine into pyruvate, and glutaminase 2 (Gls2), an isoform of glutaminase normally expressed in kidney, were said to be downregulated in *Cttnb1* mutated mouse liver tumors (Unterberger *et al.* 2014). In rat liver foci, Sds and Gls2 mRNA levels were upregulated after PB and CF treatment and downregulated after AAF treatment as illustrated in figure 18. NNM, however, showed an inverted pattern of Sds and Gls2 expression in male and female Wistar rats.

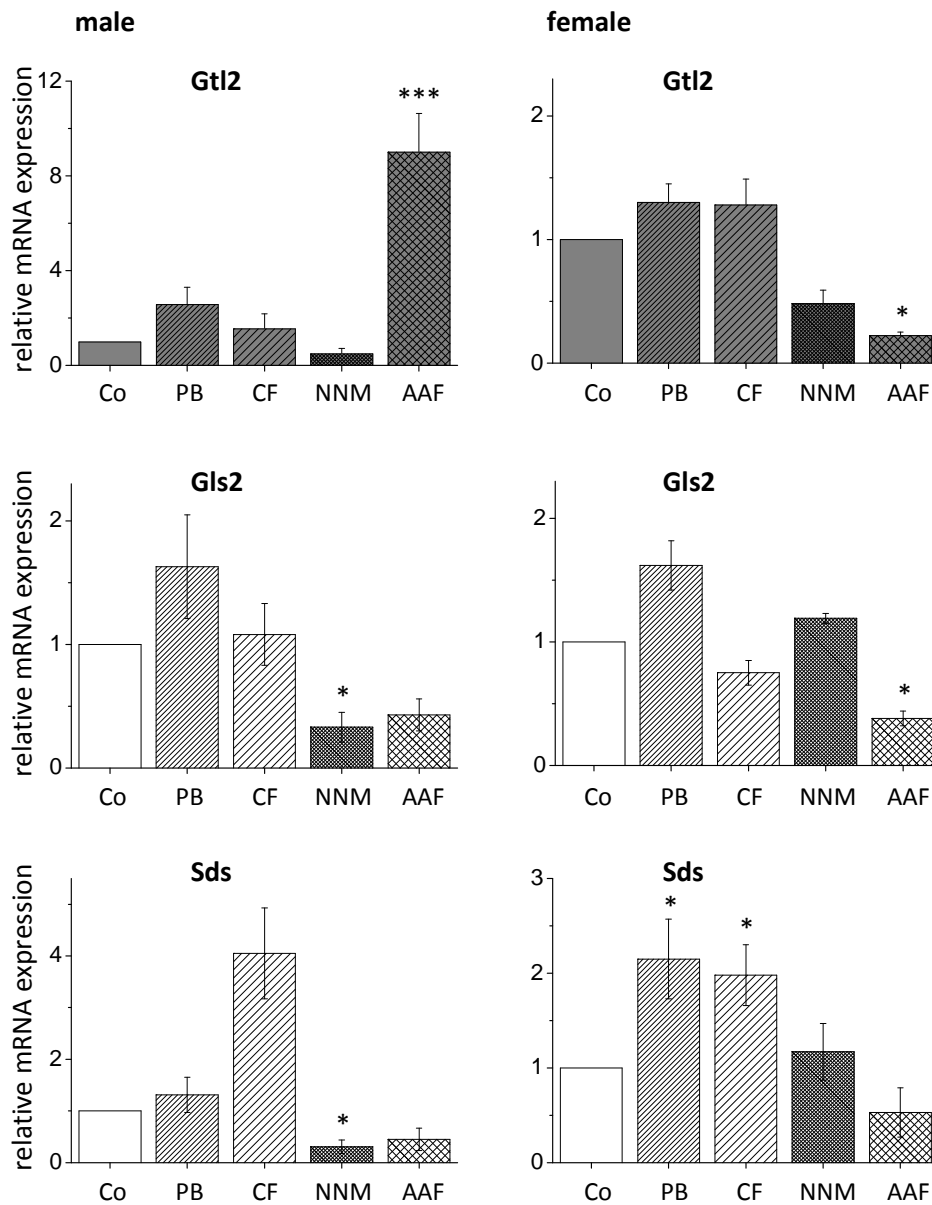


Figure 17: Relative Gtl2, Gls2 and Sds expression in liver tissue from rats treated with NGC (PB, CF) or GC (NNM, AAF) for 10 consecutive weeks. 0.05 % phenobarbital (PB) and 0.5 % clofibrate (CF) treatment induced Gtl2 expression in both genders, but only moderate without any significance, while NNM (N-nitrosomorpholine, 5 mg/kg bwt) led to a downregulation. Gtl2 showed a gender specific different expression after AAF (2-acetylaminofluorene, 10 mg/kg bwt) treatment. Gls2 and Sds, known to be negative Wnt target genes, were expressed diverse concerning to NGC and GC treatment. Sds was upregulated after PB and CF, but downregulated after NNM and AAF treatment. Gls2 shows various expressions. Treatment groups are indicated by different hatching. 4-5 animals per group; mean \pm SEM are given. Unpaired student's t-test *... p-value < 0.05, *** < 0.001.

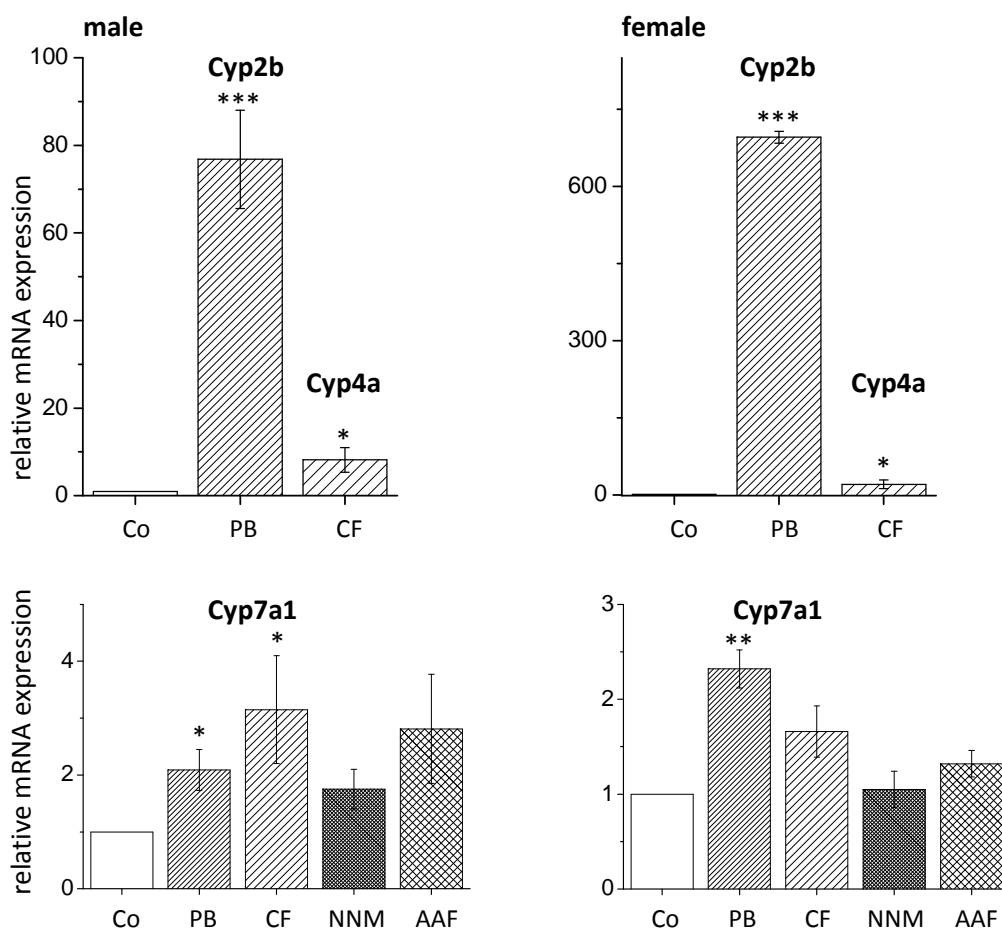


Figure 18: Relative Cyp expression in liver tissue from rats treated with NGC (PB, CF) or GC (NNM, AAF) for 10 consecutive weeks. 0.05 % phenobarbital (PB) and 0.5 % clofibrate (CF) treatment were used to induce Cyp2b10 or Cyp4a expression. Cyp7a1, known to be upregulated with active β -catenin signaling, was also upregulated under PB and CF treatment, as well as after administration of the two GC NNM (N-nitrosomorpholine, 5 mg/kg bwt) and AAF (2-acetylaminofluorene, 10 mg/kg bwt). Treatment groups are indicated by different hatching. 4-5 animals per group; mean \pm SEM are given. Unpaired student's t-test *... p-value < 0.05, ** < 0.01, *** < 0.001.

4.1.3 Gtl2 Expression in Murine Primary Hepatocytes

One of the aims of modern toxicology is to reduce, refine and replace experimental animal use. For this reason, further experiments on Gtl2 were carried out with cultures of freshly isolated hepatocytes. Primary hepatocytes are frequently used *in vitro* models for investigating drug metabolism and signaling pathways (Klingmuller *et al.* 2006). Dissected hepatocytes were grown on collagenase coated plates and treated for 24 h and 48 h with PB to activate CAR dependent gene expression. As illustrated in figure 19, Cyp2b10 expression, as an indicator for CAR activation, was elevated after 24 h of treatment but returned to nearly basal level at the later time point of investigation. Gtl2 levels were unchanged at all time points studied.

Thus, primary hepatocytes do not serve as an adequate system for investigating Gtl2 targets and Gtl2 regulation.

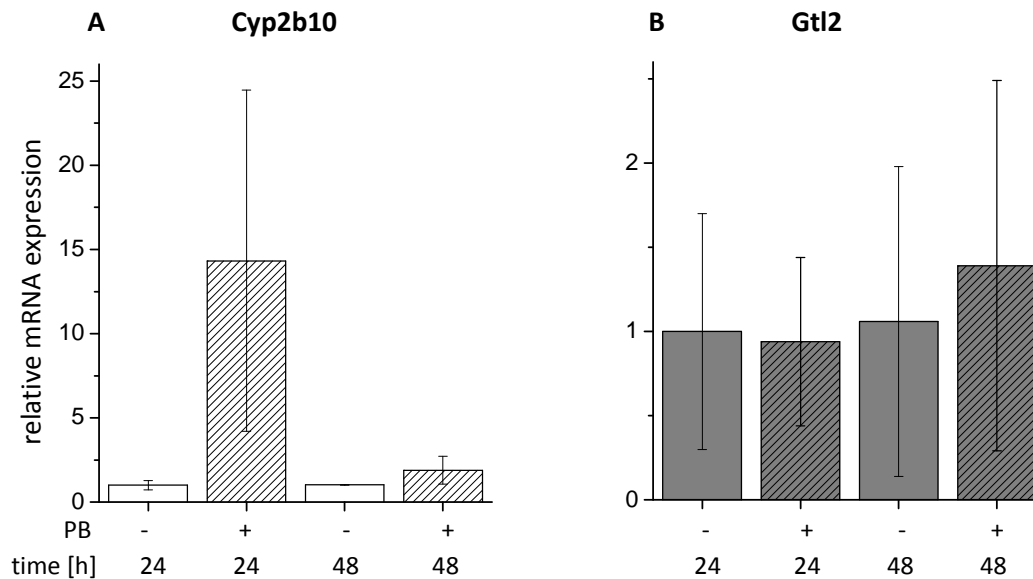


Figure 19: Relative Cyp2b10 (A) and Gtl2 (B) expression in primary hepatocytes treated with or without 3 mM phenobarbital for 24 h and 48 h. Cyp2b10 levels were upregulated after 24 h of phenobarbital (PB) treatment, while no effects on Gtl2 expression were visible. PB treatment is indicated by hatched bars. n=2; mean \pm SD are given.

4.1.4 Gtl2/ MEG3 Expression in Hepatoma Cell Lines

Cell lines with hepatic characteristics have been isolated from mouse liver tumors (Kress *et al.* 1992, Bernhard *et al.* 1973). The hepatocellular cell lines 70.4, 53.2b, 55.1c and Hepa1c1c.7 employed in this work were characterized in terms of mutations in the *Ctnnb1*, *Ha-ras* and *B-raf* proto-oncogenes by former group members as previously described (Aydinlik *et al.* 2001, Jaworski *et al.* 2005).

Unfortunately, expression of Gtl2 could not be detected in any of the various cell lines investigated, which were derived from liver tumors of C57BL/6 or C3H/ He mice or from man (not shown). Surprisingly, a recently published pediatric human hepatocellular cell line, named HC-AFW1, showed MEG3 expression accompanied by strong β -Catenin expression (figure 20). This cell line shows a deletion of 49 bp in exon 3 of CTNNB1 (Armeanu-Ebinger *et al.* 2012). These cells are special as they express CAR receptor (figure 20 A) what few cell lines do.

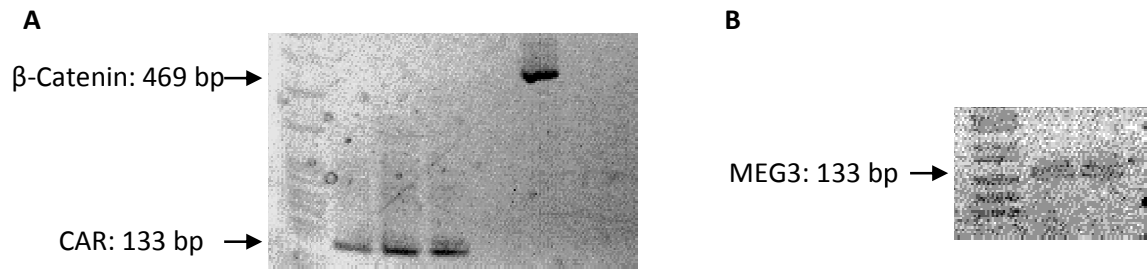


Figure 20: (A) CAR and β-Catenin expression and (B) MEG3 expression in human HC-AFW1 cell line.

As it turned out not to be possible to manipulate MEG3 expression in HC-AFW1 via siRNA, another way to alter gene expression had to be tested.

There is evidence that the lack of Gtl2 expression is due to hypermethylation in the Gtl2 gene promoter and in the intergenic differentially methylated region (IG-DMR), which regulates imprinting of the gene (Takada *et al.* 2002, Qu *et al.* 2013). Since methylation inhibitors are able to influence methylation patterns by remodeling the chromatin structure, experiments were performed to further analyze the potential ability to switch on Gtl2 expression by 5-azadeoxycytidine (5-Aza-dC), a known methylation inhibitor (Jones and Taylor 1980). As a result of this treatment, there was a slight improvement in Gtl2 expression in mouse hepatoma cells of line 53.2b, which were used for this experiment, but on a very low level.

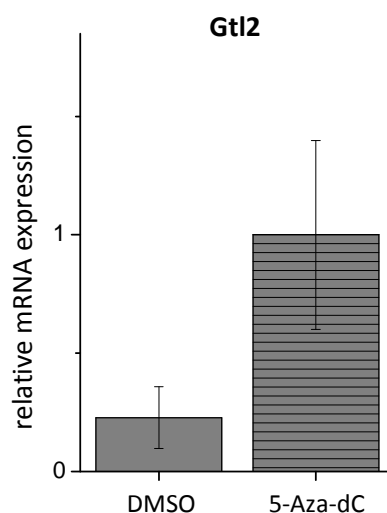


Figure 21: Methylation dependent Gtl2 expression in mouse hepatoma cells. 10 μM of the epigenetic modifier 5-Aza-dC (5-azadeoxycytidine) for 4 days turned on Gtl2 expression in murine hepatoma cell line 53.2b; n=3, mean ±SD are given.

4.1.5 CAR Regulation of Gtl2 Upstream Regions

Since it is known that both β -catenin signaling and CAR receptor are necessary for a stable Gtl2 expression (Lempiainen *et al.* 2013), Gtl2 reporter vectors were created and transfected in a murine hepatoma cell line harboring physiologically activated β -catenin and conditionally expressed CAR receptor. Gtl2 reporter vectors were constructed containing 5' upstream sequences of the transcription start of the 3 different transcripts according to the NCBI database. Transcript 1 (T1) transcription start was more downstream than the starting point of transcripts 2 and 3 (T2_3). For illustration of the upstream regions, see figure 22.

Four reporter vectors were generated: Prom_T1 spanning 1.3 kb before T1, and Prom_T2_3, subdivided into Prom_T2_3_A (beginning), Prom_T2_3_M (middle) and Prom_T2_3_E (end), together nearly 5 kb. T2_3 upstream region had been chosen larger, given that T3 was the detected transcript variant at mRNA level (figure 11).

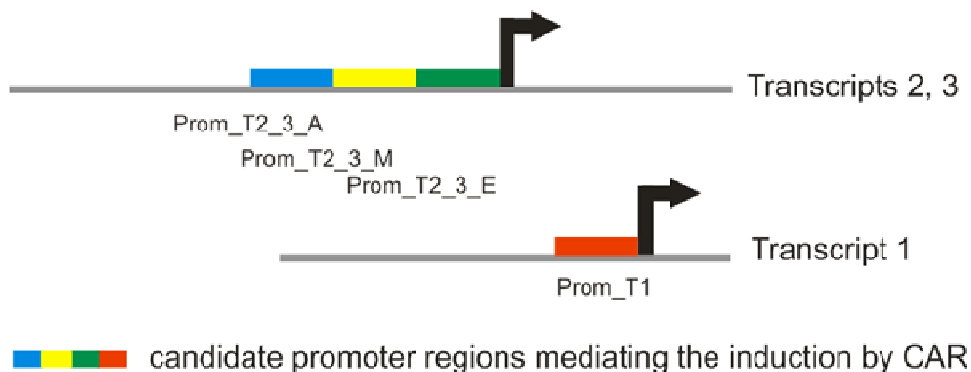


Figure 22: Schematic representation (not at scale) of murine Gtl2 upstream regions. Indicated sequences were cloned into pT81luc to analyze CAR dependent regulation of these sequences. Different parts of Gtl2 upstream regions were indicated by different colors.

These reporters were, together with an expression vector for CAR, co-transfected into 55.1c mouse hepatoma cells, a cell system that had already been used successfully in recent promoter studies (Loeppen *et al.* 2005). At 24 h after transfection, the Prom_T1 reporter construct responded to the co-transfected CAR expression vector with an approximately 3.6 fold induction of luciferase activity, as it is depicted in figure 23. Prom_T2_3_E and A showed a significant difference in CAR response, but these effects were very low. Contrastingly, β -catenin-mediated induction of luciferase activity failed in all reporter constructs (not shown).

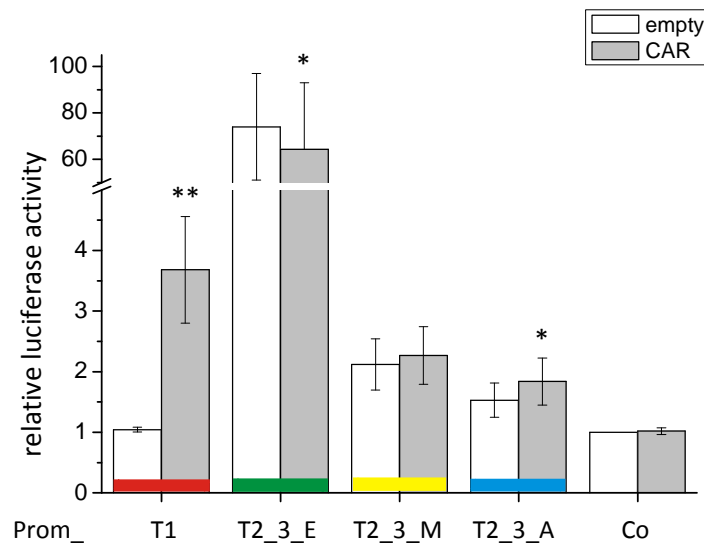


Figure 23: Relative activity of the four Gtl2 reporter vectors in 55.1c mouse hepatoma cells, as determined by firefly luciferase measurement. Cells were co-transfected with CAR (constitutive androstane receptor) for 24 h. Gtl2 transcript 1 promoter activity was upregulated by cotransfection of CAR, while transcript 2/3 promoters showed a significant difference in CAR response, but these effects were very low. Presented data result from five independent experiments performed in quadruplicates; mean \pm SEM are given. Unpaired student's t-test * ... p-value < 0.05, ** < 0.01.

4.1.6 Role of Gtl2 in β -Catenin Signaling Regulation

β -Catenin signaling plays a crucial role in proliferation of cancer cells and is often deregulated in these cells. To identify a possible participation of Gtl2 in Wnt/ β -catenin signaling, a vector has been created constitutively expressing Gtl2 under the control of a CMV promoter. Through transfection of murine hepatoma cells with this construct, Gtl2 got transiently expressed. Mouse hepatoma cells containing a 7x TCF/ LEF driven luciferase vector (SuperTopflash; STF) stably or transiently expressed were co-transfected with the Gtl2 construct or the corresponding empty vector and treated either with LiCl, to activate β -catenin signaling, or NaCl as a control, respectively. Firefly luciferase activity was measured and normalized to Renilla. β -Catenin dependent luciferase activity was increased upon activation of Wnt signaling, and even more increased under the influence of Gtl2, indicating a connection between β -catenin signaling and Gtl2 expression (figure 24). This correlation could not be substantiated, however, on the mRNA level (not shown).

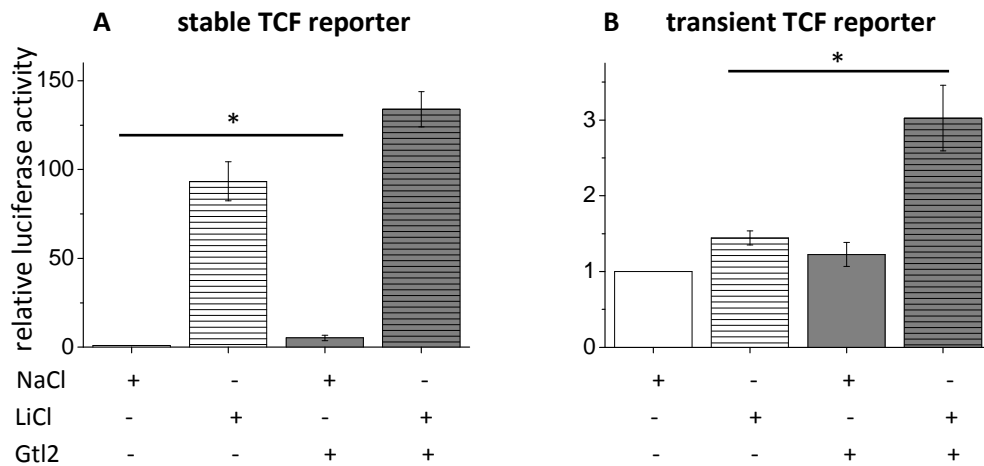


Figure 24: Activation of a β -catenin dependent TCF/LEF driven reporter vector in different mouse hepatoma cell lines. (A) 70.4 K15 cells stably transfected with a 7x TCF/LEF driven luciferase vector (SuperTopflash; STF) were transiently transfected with Gtl2 (grey bars) or the empty vector (unfilled bars) and treated with 15 mM NaCl or 15 mM LiCl (hatched bars) for 24 h. Firefly luciferase activity was normalized to Renilla. n=5. (B) 53.2b cells transiently transfected with STF and additional Gtl2 (grey bars) or the empty vector (unfilled bars) and treated with 15 mM NaCl or 15 mM LiCl (hatched bars) for 24 h. Firefly luciferase activity was normalized to Renilla. n=5, mean \pm SEM are given. Paired student's t-test * ... p-value < 0.05, the respective bars are indicated with lines above.

To improve standardization and reproducibility, two additional Gtl2 expression systems have then be established and tested.

4.2 Generation and Characterization of Engineered Gtl2 Expressing Cell Lines

A way of overexpressing a gene is its delivery by an adenovirus. Recombinant adenovirus vectors delete genes from the wt adenovirus, making a replication impossible and the system safe for use. Due to its high transduction efficiency and high expression level, adenovirus vectors have been widely used for transduction experiments. In cooperation with Michael McMahon, University of Dundee, Scotland, a Gtl2 expressing adenoviral construct has been generated and successfully introduced into Hepa1c1c.7 mouse hepatoma cells. The amount of adenoviruses used is expressed by the multiplicity of infection (MOI). MOI is the ratio of the number of virus particles to the number of target cells. As visualized in figure 25 A, Gtl2 was expressed MOI dependent, 100 MOI showing a ten time greater expression than 10 MOI. Transient expression, not integrating the DNA into the nuclear genome, has the disadvantage that a variable number of cells are transfected in each passage, resulting in divergent measurement values. If it is desired that the transfected gene actually remains in the

genome of the cell and its descendants and therefore reaching cellular homogeneity, a stable transfection must be achieved.

Clontechs Tet-On Advanced Inducible Gene Expression System is a tightly regulated system that produces by request expression of a gene of interest in target cells. The system was established in 70.4 mouse hepatoma cells by sequentially transfecting them with a Tet-On Advanced transactivator and a vector containing Gtl2 under the control of a P_{Tight} inducible promoter and selecting a stable cell line. Target cells expressed high levels of Gtl2 when cultured in the presence of the system's inducer doxycycline in a dose dependent manner, as shown in figure 25 B. Cells were termed 70.4 UT K54.

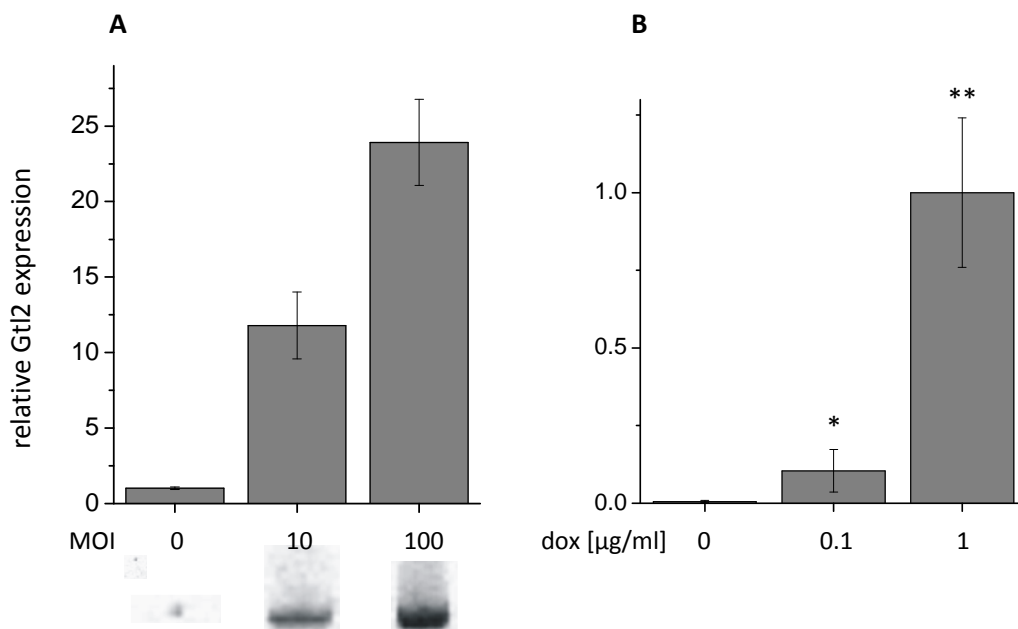


Figure 25: Two mouse hepatoma cell culture systems with induced Gtl2 expression. (A) Hepa1c1c.7 cells were transduced with 10 or 100 MOI of an adenoviral Gtl2 vector for 24 h to express Gtl2, n=3, mean \pm SD are given. **(B)** 70.4 UT K54 cells stably transfected with a Gtl2 vector were treated with 0.1 μ g/ml and 1 μ g/ml doxycycline (dox) for 24 h to turn on Gtl2 expression, n=5, mean \pm SEM are given. Paired student's t-test *... p-value < 0.05, ** < 0.01.

Two systems expressing Gtl2 had been generated as described above. For further studies, substantiation of the physiological location of long non-coding RNA Gtl2 was inevitable. Physiologically, Gtl2 was more abundant in the nucleus of mouse hepatocytes (figure 26 B). Therefore, *in situ* hybridization experiments were carried out in the laboratory of Valérie Dubost at the Novartis Institutes for Biomedical Research, Basel. The experiments were conducted in fixed and paraffin embedded

murine liver tissue. To examine the intracellular localization of Gtl2 in 70.4 UT K54 cells, digitonin based cell fractionation was performed in doxycycline treated (24 h) or untreated cells. The results demonstrated that the majority of the transcript was located in the nucleus, hence in analogy to the physiological situation *in vivo*. GAPDH and Histone H3 proteins served as controls for cytoplasmic and nuclear fractions, respectively (figure 26 A).

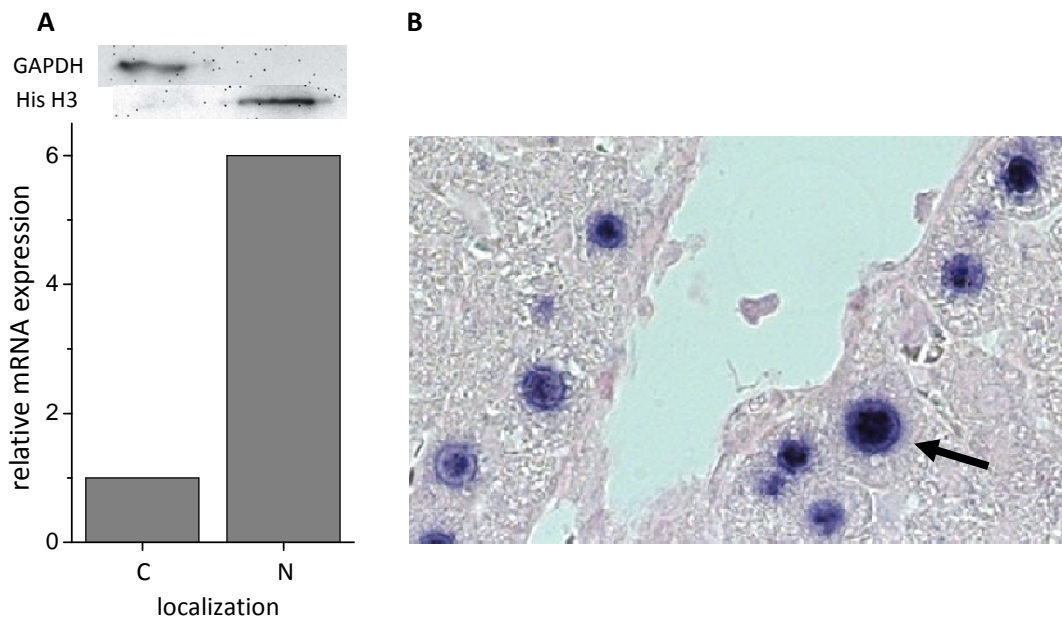


Figure 26: Nuclear localization of Gtl2 *in vitro* and *in vivo*. (A) Digitonin based cell fractionation with 70.4 UT K54 cells after doxycycline treatment for 24 h, where GAPDH and Histone H3 (His H3) served as controls for cytoplasmic (C) and nuclear (N) fraction, respectively; and (B) Gtl2 ISH in normal murine liver showed that Gtl2 was more abundant in the nucleus. n=3, one representative experiment is given.

After having demonstrated that Gtl2 shows nuclear localization in 70.4 UT K54 cells, the cells were then used to search for potential Gtl2 targets on both RNA and protein level. The RNA expression patterns of engineered Gtl2 expressing cells were analyzed by use of the Affymetrix GeneChip Mouse Gene 2.1 ST Array which contains approximately 35,240 probe sets, including more than 26,000 well established mouse genes and more than 3,300 non-coding transcripts. Genes were selected with minimum 50 % deregulation. These cutoffs were chosen to minimize false positive results of genes identified as being differentially regulated. In total, 211 genes were identified that were variably expressed. Under these genes were a striking number of immunoglobulin J genes, olfactory receptors (Olfir), and non-coding RNAs like miRNA, snoRNA and snRNA. The gene distribution of 50 % deregulated genes is visualized in figure 27. In contrast, protein coding genes were underrepresented (table 20).

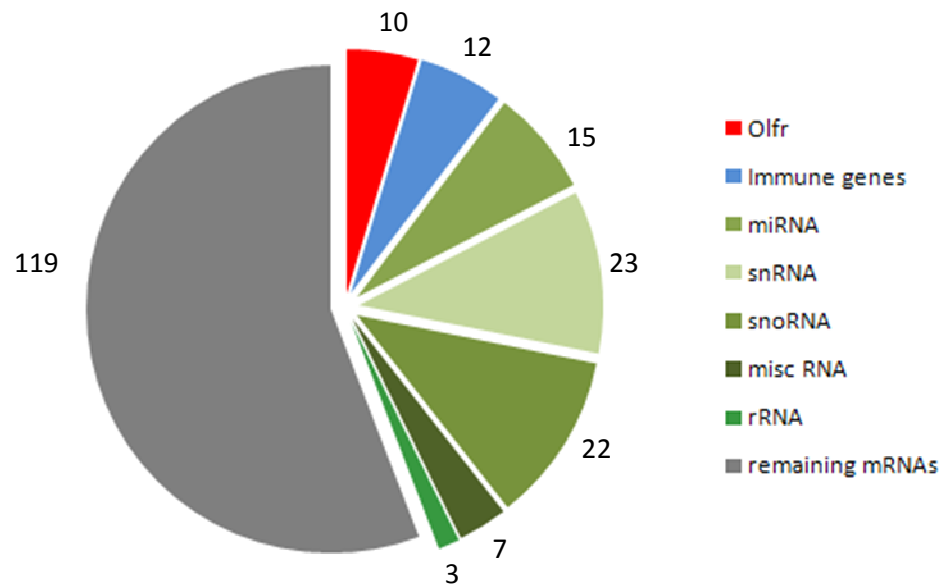


Figure 27: Gene distribution of 50 % deregulated genes in UT K54 cells (doxycycline vs. without doxycycline). Many non-coding RNAs were deregulated, olfactory receptors and immune genes were additionally clustered, small RNAs not.

Table 20: Affymetrix analysis with group enrichment in 70.4 UT K54 (doxycycline vs. without doxycycline). Protein coding genes were underrepresented, IG_J, miRNAs, snoRNAs and snRNAs were overrepresented.

#	transcript_type	total_count	diff_count	p.over	p.under
1	antisense	1097	4	1	0.61
2	IG_C_gene	12	0	1	0
3	IG_D_gene	4	1	0.33	1
4	IG_J_gene	83	6	0.0003	1
5	IG_V_gene	346	5	0.90	1
6	lincRNA	1110	3	1	0.21
7	miRNA	347	17	5.11 E-09	1
8	misc_RNA	444	7	0.37	1
9	polymorphic_pseudogene	8	0	1	0
10	processed_transcript	184	3	1	1
11	protein_coding	23126	108	1	2.29 E-14
12	pseudogene	270	1	1	1
13	rRNA	279	2	1	1
14	sense_intronic	72	0	1	0
15	snoRNA	1185	22	0.0003	1
16	snRNA	1123	24	1.28 E-05	1

A heatmap showing the most deregulated genes in 70.4 UT K54 cells with Gtl2 compared to the same cells without Gtl2 is illustrated in figure 28.

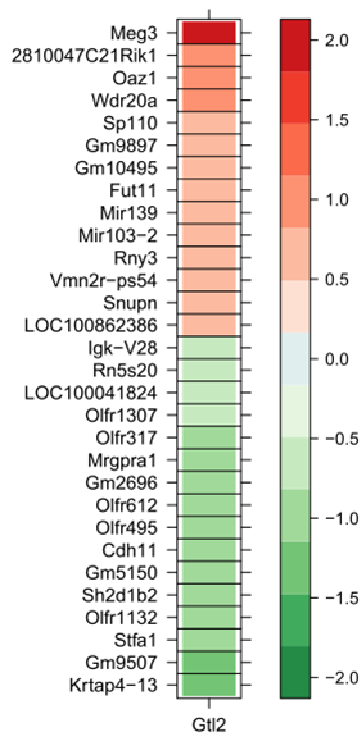


Figure 28: Heatmap showing the 30 most deregulated genes in 70.4 UT K54 cells with Gtl2 compared to the same cells without Gtl2.

To validate the microarray data, expression of several of the deregulated genes was additionally analyzed by qPCR. However, the PCR data did not resemble the findings of the microarray analysis. Either no differences were visible or as in the case of Olf612, Olf495, Oaz1 and Wdr20a, the corresponding RNA could not be detected (not shown).

Gtl2 target search was also performed on protein level. Magnetic RNA protein pulldown provides an efficient way of isolating proteins bound to the bait RNA. In this case, Gtl2 RNA was *in vitro* transcribed, biotin labeled and used to capture Gtl2 binding proteins via streptavidin magnetic beads. Washing fractions 1 and 3 as well as the eluted protein fraction were separated according to weight as indicated in figure 29.

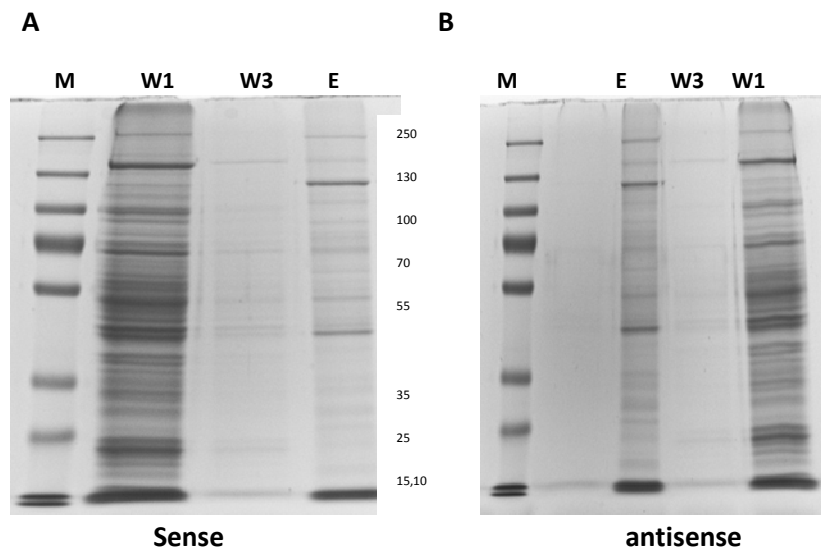


Figure 29: Output of the RNA-protein pulldown assay. (A) sense Gtl2-RNA: Lane 1: M, marker; lanes 2, 3: W, washing fractions 1, 3; lane 4: E, eluate. **(B)** antisense Gtl2-RNA: Lane 1: M, marker; lane 3: E, eluate; lanes 4,5: W, washing fractions 3, 1.

Bart van den Berg, NMI, Natural and Medical Sciences Institute at the University of Tübingen, carried out the in gel digestion, mass spectrometry and data analysis to identify Gtl2 binding proteins. A striking number of ribosomal proteins were detected, but known proteins with Gtl2 interaction like JARID, part of the PRC2 complex (Kaneko *et al.* 2014), were missing.

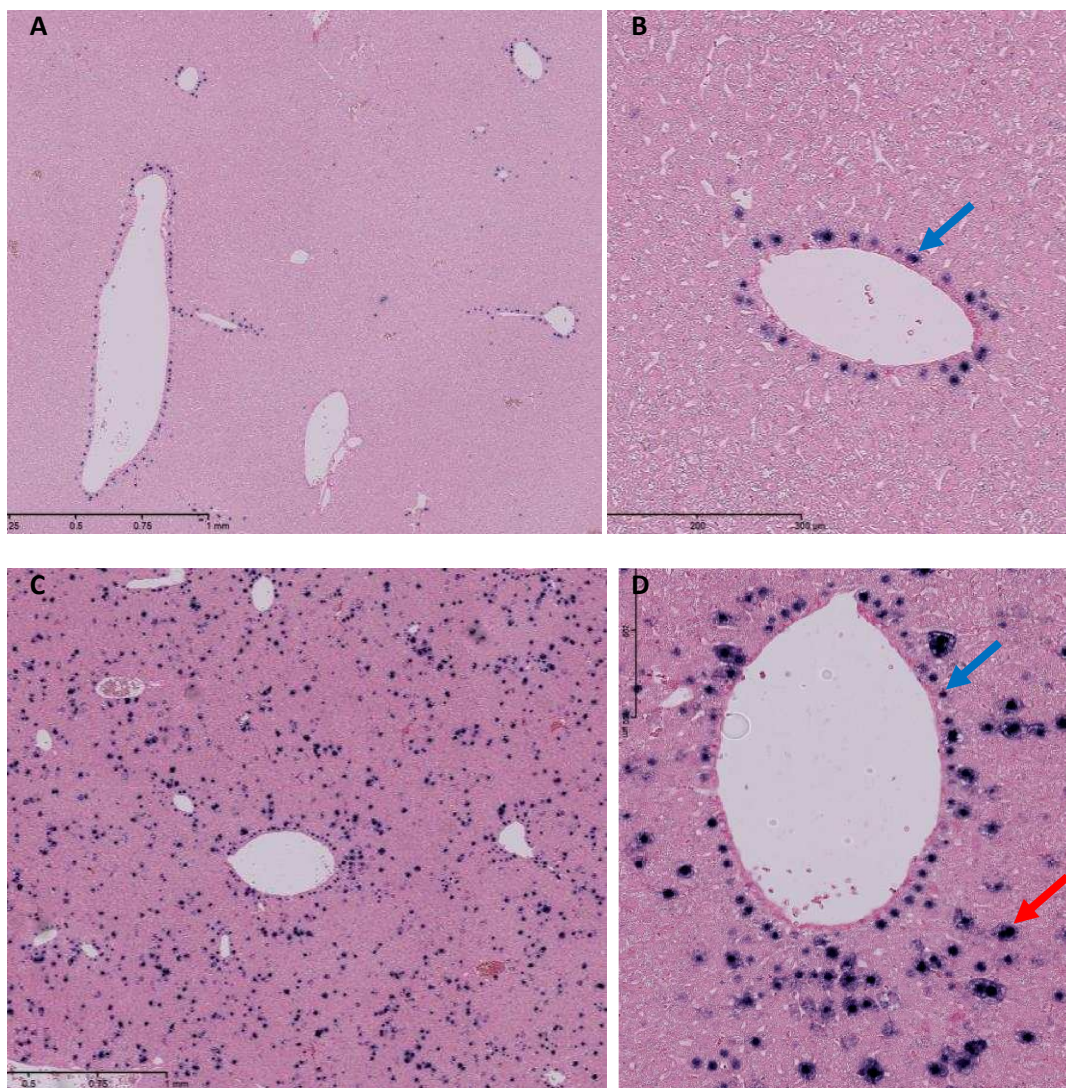
4.3 Adenoviral Overexpression of Gtl2 *in vivo*

Cell culture results were not viewed as sufficient for identifying cellular or biochemical consequences resulting from Gtl2 overexpression. Despite the effort to work with non-animal alternatives, mice offer a more realistic system to study liver functions.

4.3.1 Determination of Gtl2 Expression after Adenoviral Transduction *in vivo*

Gtl2 containing adenoviral constructs were already successfully tested in cell culture to conditionally overexpress Gtl2. Thus, these viral particles were virtually predestined to introduce Gtl2 into murine liver. After injection into the tail vein, particles migrate with

the blood flow into the liver lobule, entering via the portal vein. To prove increased Gtl2 expression, mice were sacrificed 4 or 8 days after injection. The liver was cut out and Gtl2 *in situ* hybridization using DIG-labeled single stranded riboprobes targeting a conserved 500 bp region in the Gtl2 transcript was carried out to localize Gtl2 in adenoviral treated liver sections in the laboratory of Valérie Dubost, Novartis Institutes for Biomedical Research, Basel. The experiments were conducted in fixed and paraffin embedded liver tissue. Physiologically, Gtl2 expressing nuclei surrounded the central vein (blue arrow) as it is depicted in figure 30 A, B. Four days after adenoviral Gtl2 transduction (figure 30 C, D), Gtl2 was additionally expressed in hepatocytes far away from the central vein (red arrow) in large quantities. The Gtl2 transcript was more abundant in the nuclei, as it is physiologically. Adenoviral Gtl2 expression disappeared, however, at day 8 (figure 30 E, F) and returned to a physiological level.



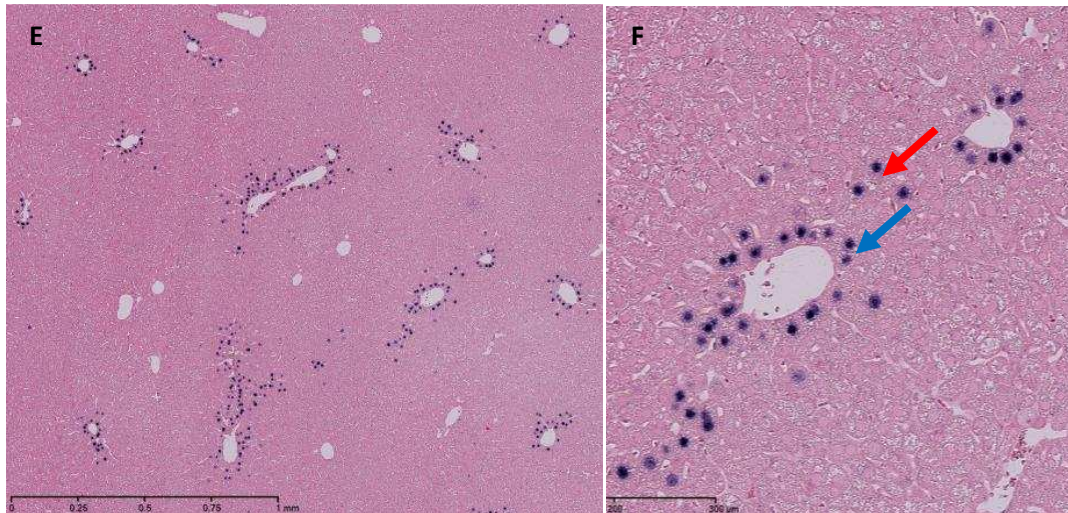


Figure 30: Gtl2 ISH in adenoviral treated murine liver. (A, B) Control, (C, D) Gtl2 4d and (E, F) Gtl2 8d animals are shown. Physiologically, Gtl2 was expressed around the central vein (blue arrows), but after adenoviral Gtl2 transduction, it was also expressed far away from the central vein (red arrow). Adenoviral Gtl2 expression disappeared till day 8. Pictures were taken with 5x (left) and 20x (right) magnification at Novartis, Basel.

In order to confirm elevated Gtl2 expression 4 days after adenoviral transduction, mRNA levels were analyzed, too. At the 4-day time point, Gtl2 RNA was clearly enhanced in liver. Control mice, which only received a GFP containing vector, remained at basal level. Animals that had received the Gtl2 vector returned to the physiological pattern 8 days after transduction (figure 31).

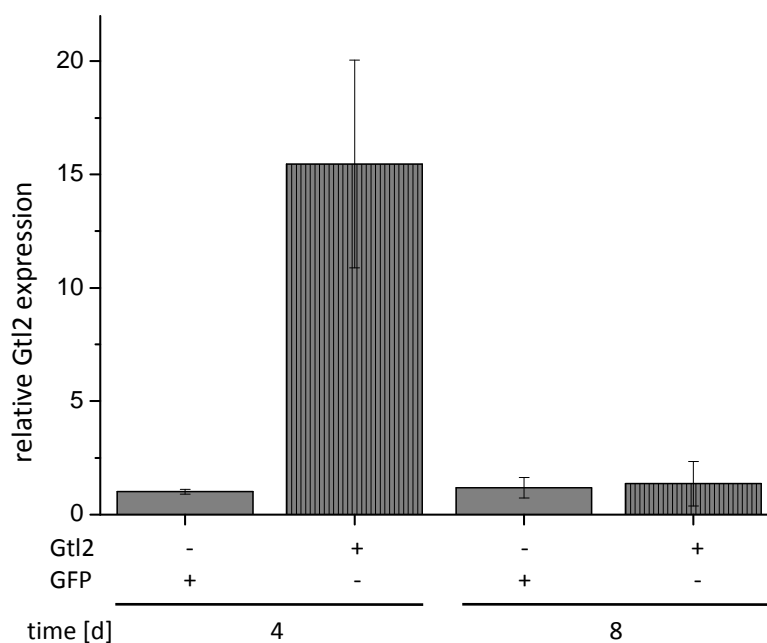


Figure 31: Relative Gtl2 expression in adenoviral treated mice. Control animals received a GFP vector, Gtl2 animals received a Gtl2 containing vector (hatched bars). Animals were killed 4 days or 8 days after injection. 3 animals per group, 3 samples per animal, mean \pm SEM are given.

4.3.2 Phenotype of Gtl2 Transduced Murine Liver

To uncover a potential phenotype change mediated by Gtl2 overexpression, Carnoy fixed liver slices were stained for glutamine synthetase (GS), Cyp1a2 and Cyp2b. Glutamine synthetase was chosen because reporter gene experiments indicated a connection between β -catenin signaling and Gtl2 expression. GS is also the most prominent marker for perivenous hepatocytes and β -catenin overexpression, since a direct correlation has been demonstrated in mouse liver tumors (Loeppen *et al.* 2002). Cyp1a2 is a representative enzyme of phase I metabolism, preferentially expressed in the perivenous zone of the liver, too. Cyp2b is a known target of PB mediated CAR activation (Honkakoski *et al.* 1998).

Immunohistochemical analyses of liver sections from adenoviral treated mice were performed, which demonstrated a perivenous expression of GS accompanied by Cyp1a2 expression in the same areas, prevailing the classic picture of zonation in the liver lobule. No difference between Gtl2 and control group could be detected, neither after 4 days (figure 32) nor after 8 days (not shown). Cyp2b, representing the PB like phenotype, was also unaffected by Gtl2 (figure 32).

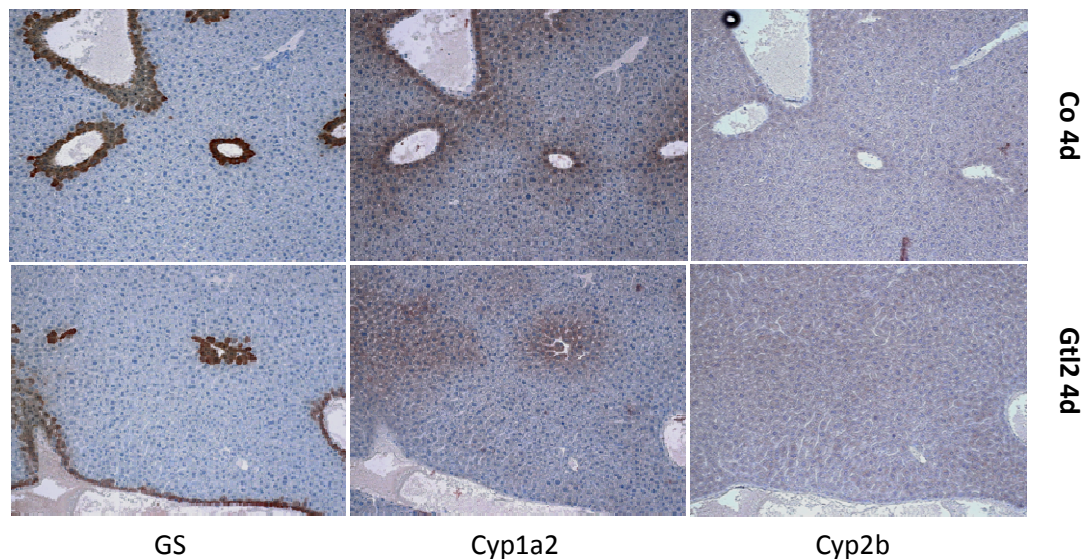


Figure 32: Immunostaining of Gtl2 treated vs. control mice. There is no difference between Gtl2 and control animals in perivenous glutamine synthetase (GS), Cyp1a2 and Cyp2b expression. Pictures were taken with 20x magnification, representative of n=3.

By having a closer look on the cell morphology visualized by haematoxylin and eosin (HE) stain, some apoptotic cells could be seen in the Gtl2 group as well as in the control group after 8 days. Additionally, 8 days of adenoviral exposure led to clustered small foci of inflammation (figure 33).

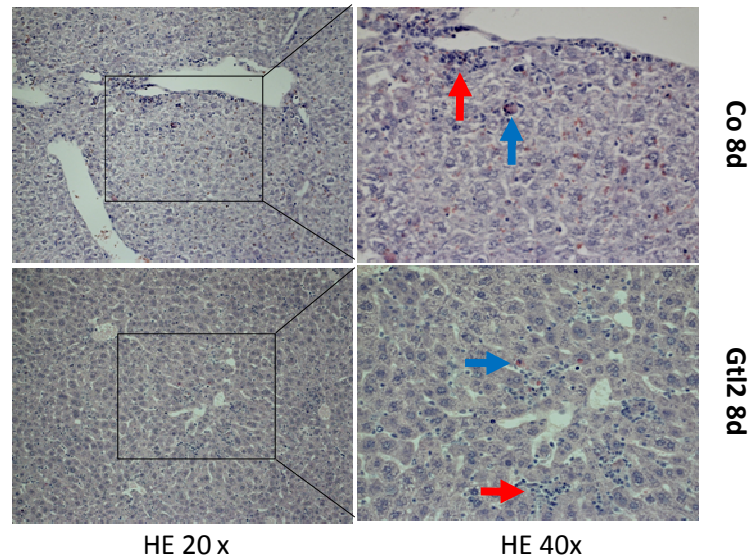


Figure 33: HE-staining of Gtl2 treated vs. control mice. Adenoviral gene transfer led to some apoptotic cells (blue arrow) and foci of inflammation (red arrow) after 8 days of adenoviral exposure to Gtl2 and GFP (control). Pictures were taken with 20x and 40x magnification, representative of n=3.

4.3.3 Quantification of Dlk1-Dio3 Cluster Genes

Gtl2 is located on one of the largest imprinting gene clusters close to other imprinted genes deregulated upon NGC treatment in mice. Since it is known that Dlk1 is directly regulated by Gtl2 (Zhao *et al.* 2010), a correlation between Gtl2 expression and expression of other genes on the same cluster would be conceivable.

Since the Gtl2 level was only increased after 4 days of transduction, 8 day samples were disregarded. Relative expression of Dlk1-Dio3 cluster genes is illustrated in figure 34. Maternally expressed Rian and Mirg were only slightly upregulated in parallel to Gtl2 overexpression. In contrast to the findings with CAR activation *in vivo*, paternal Rtl1 and Dio3 revealed an induction, too. Large standard deviations were obtained due to small sized animal groups and differences between animal responses.

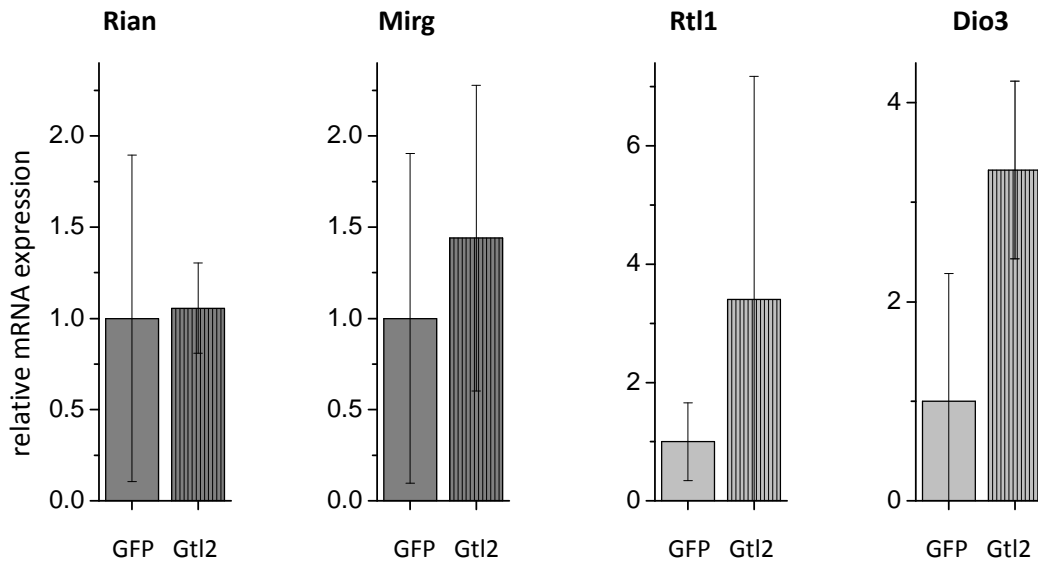


Figure 34: Relative expression of Dlk1-Dio3 cluster genes in adenoviral treated mice. Control animals received a GFP vector, Gtl2 animals received a Gtl2 containing vector (hatched bars). Animals were killed 4 days after injection. 3 animals per group, 2 groups; mean \pm SEM are given.

4.3.4 Effects of Gtl2 Overexpression on Proliferation

In contrast to normal cells, which only divide a restricted number of times before entering into growth arrest, cancer cells never cease to proliferate. The loss of negative cell cycle control can promote tumorigenesis. Due to the fact that Gtl2 was postulated as a potential tumor marker, Gtl2 might directly or indirectly affect cell proliferation. Two key classes of regulatory proteins, cyclins and cyclin dependent kinases (Cdk) determine the cell cycle (Nigg 1995). Cdk are among the most important and phosphorylate their substrate. As their name says, they require the presence of cyclins to be active.

Cyclin D1 (Cnd1) expression was downregulated upon Gtl2 overexpression in murine liver, just as Cdk2 and Cdk4. Similarly, proliferating nuclear antigen (Pcna), which is essential for replication by forming a DNA clamp and encircling the DNA, augmenting DNA polymerase's processivity, was downregulated, too (figure 35).

Summarizing the above, it appears that cell cycle activity was decreased by Gtl2 overexpression in murine hepatocytes.

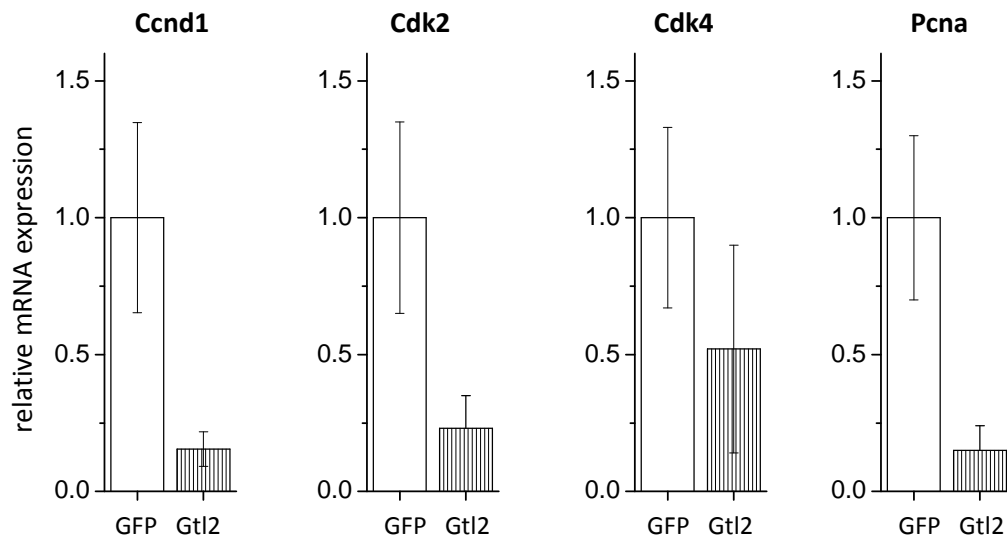


Figure 35: Relative Cyclin D1, Cdk2, Cdk4 and Pcna expression in adenoviral treated mice. Control animals received a GFP vector, Gtl2 animals received a Gtl2 containing vector (hatched bars). Animals were killed 4 days after injection. 3 animals per group, 2 groups; mean \pm SEM are given. Cell proliferation genes were downregulated in the presence of Gtl2. Ccnd1, Cyclin D1; Cdk2, Cyclin dependent kinase 2; Cdk4, Cyclin dependent kinase 4; Pcna, proliferating cell nuclear antigen.

4.4 GS Reporter Mouse

The second main topic of this work is a specific reporter mouse, harboring 3 different reporters, namely FLuc, LacZ and Tk-1, under the control of the glutamine synthetase promoter. As GS is a target for β -catenin signaling, this promoter is specifically activated in tissues, where β -catenin dependent signaling is active, as for example in perivenous hepatocytes and in *Ctnnb1* mutated liver tumors.

Transgenic GS reporter mice were born at the expected ratio of ~50 % after interbreeding Taconic GS-2A-LacZ-2A-Tk-1-2A-FLuc multi reporter model mice with mice of strain C3H/ He N. PCR analysis was performed to detect germline transmission of wt and konst Ki locus in GS mice (figure 36).

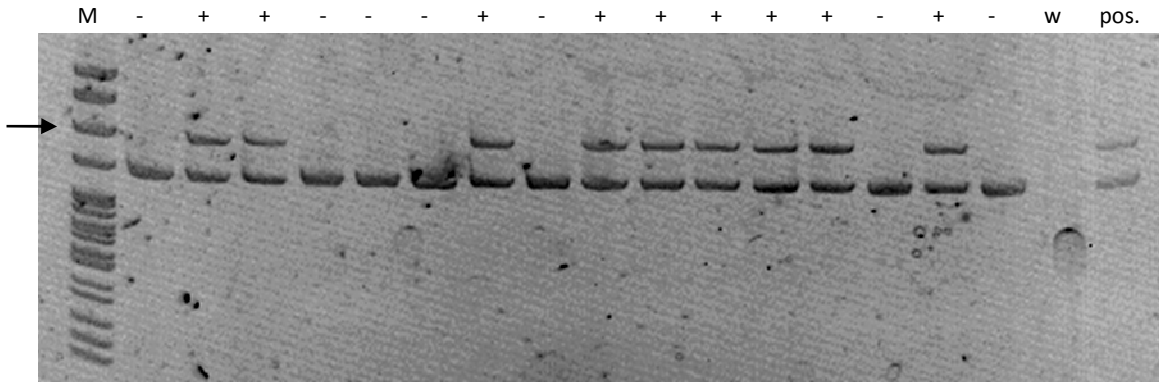


Figure 36: PCR analysis to detect germline transmission of wt and konst Ki locus in GS mice: DNA isolated from GS mice progeny was analyzed via PCR with primers 7656_68 and 7656_69. Mice harboring the GS transgene (konst Ki) were detected by the presence of an additional PCR fragment of 403 bp (indicated by the black arrow). M, marker; -, wt; +, Ki; w, negative probe; pos, positive probe.

4.4.1 Preliminary Testing of Reporter Genes in GS Mice

The functionality of the Firefly luciferase reporter (FLuc) was investigated first. Male GS mice and their wt littermates were used to generate homogenates of different organs, including heart, liver, kidney, lung and gut. Luciferase activity was first determined in heart homogenate using serial dilutions and a firefly luciferase inhibitor to quench luciferase activity. In comparison, activity of the recombinant enzyme was measured. As shown in figure 37, luciferase activity in the GS mice was clearly dependent on homogenate concentration and could be repressed by the enzyme inhibitor, demonstrating the specificity of the assay system.

Additionally, the assay was calibrated with recombinant luciferase to allow an estimation of the amount of enzyme per tissue unit.

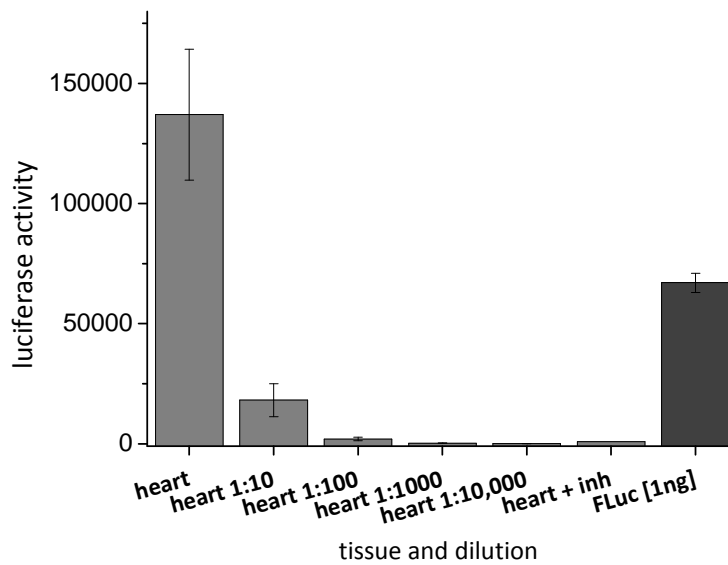


Figure 37: Firefly luciferase activity in the heart of the GS reporter mouse. Several dilutions of heart homogenate were used for determining firefly luciferase activity. A luciferase inhibitor attenuated luciferase activity, recombinant enzyme is shown for comparison; n=3 animals, mean \pm SD are given.

Firefly luciferase to tissue ratio is depicted in figure 38. GS mice showed a strong luciferase signal compared to the unspecific signal seen with organ homogenates from wt mice, implying that the artificial GS promoter was activated in all tested organs. Among these, the heart revealed the highest activity of the measured organs, while gut and lung had the lowest.

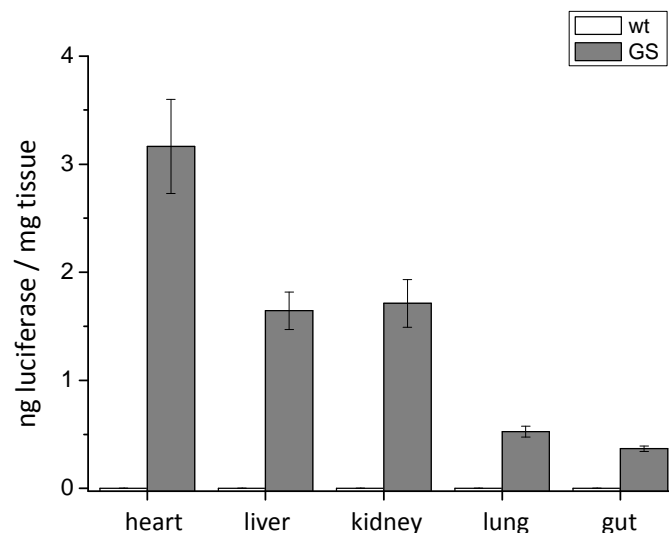
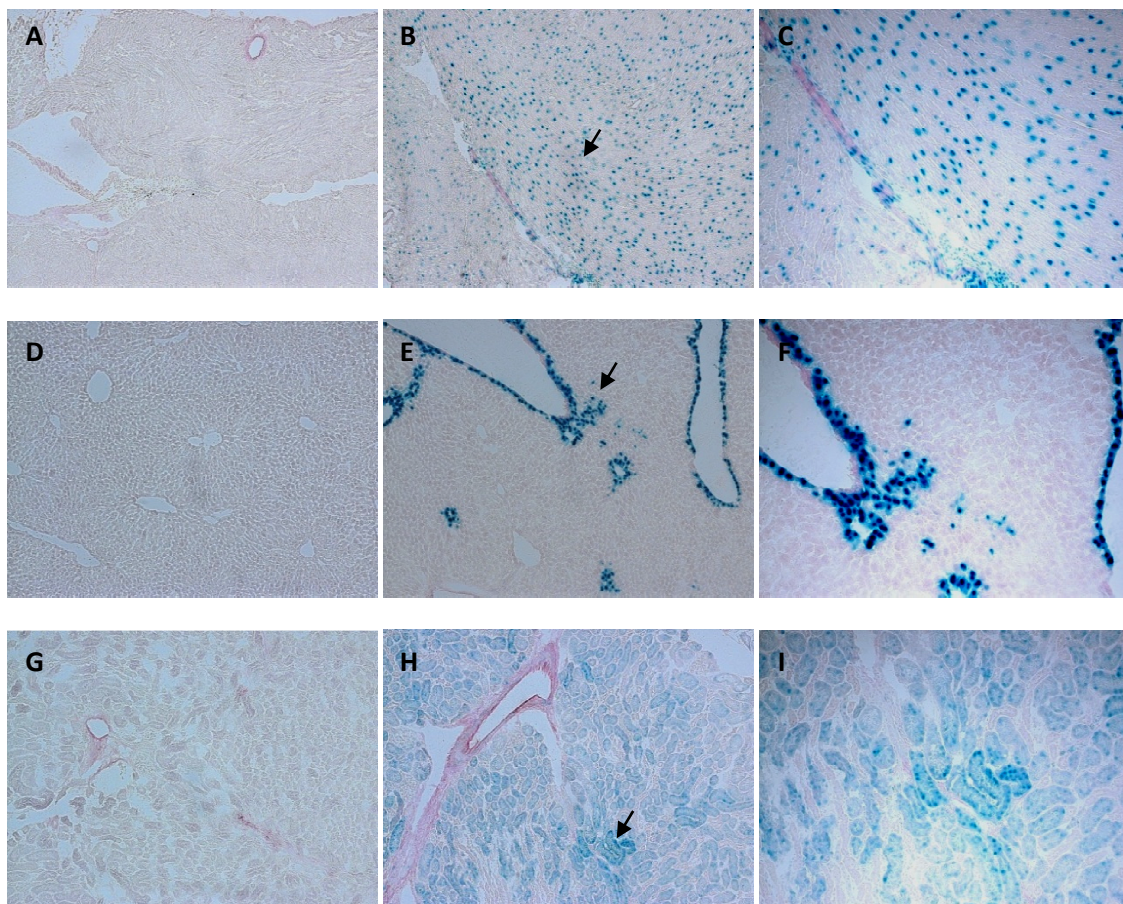


Figure 38: Amount of firefly luciferase in the homogenate of heart, liver, kidney, lung and gut from male GS mice versus wt mice. Luciferase activity was detected in the heart, liver, kidney, lung and gut of GS mice (black bars), implying GS promoter activation in all tested organs. n=3, mean \pm SD are given.

The second reporter gene in the GS mouse is LacZ, encoding β -galactosidase, which can be detected by use of the chromogenic substrate 5-bromo-4-chloro-3-indolyl-beta-D-galacto-pyranoside (X-Gal). X-Gal is hydrolyzed to colorless galactose and 4-chloro-3-brom-indigo, forming an intense blue precipitate. In this case, organs of the same animals as for determining FLuc activity were analyzed for LacZ expression via X-Gal staining. Once again, tissues from wt littermates served as controls. While no background staining occurred, the heart of GS mice displayed the most intensive reporter activity, followed by liver and kidney, as already seen with the FLuc reporter. Liver zonation was observed by LacZ reporter expression in the areas around the central vein. Lung and gut exhibited lesser LacZ activity, while the latter possessed a strong staining in the outer surrounding muscle layer (figure 39). Therefore, these results showed that the X-Gal reporter was also functional.



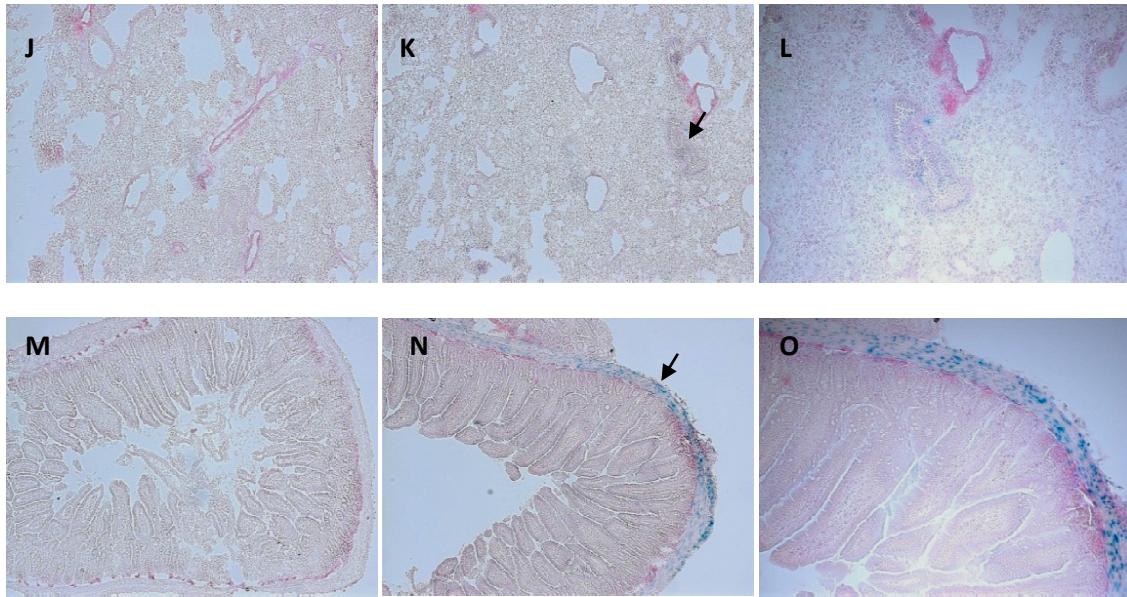


Figure 39: Male GS reporter (middle, right) and wt (left) mice stained with β -galactosidase reflecting GS promoter activity. Heart (A-C), liver (D-F), kidney (G-I), lung (J-L) and gut (M-O) are shown. Expression of glutamine synthetase could be seen in the areas around the central vein in the liver, extensive expression of glutamine synthetase was in heart and kidney and to a lower extent in gut and lung. Same animals as used for determining firefly luciferase activity in the homogenate. Pictures were taken with 10x and 20x magnification, representative of n=3.

The herpes simplex virus type 1 thymidine kinase (Tk-1) reporter gene was used to visualize GS promoter activation via PET. ^{18}F -FHBG is a thymidine analogue whose uptake is regulated by Tk-1 while ^{18}F can be detected in PET measurements. For preliminary testings, two female GS mice were scanned with PET by Dr. Andreas Schmid from the Laboratory for Preclinical Imaging and Imaging Technology of the Werner Siemens-Foundation, Department of Radiology, University of Tübingen. As shown in figure 40, the tracer displayed a rapid diffusion in the whole body except that it did not cross the blood brain barrier after tracer injection into the tail vein. ^{18}F -FHBG remained longer in the kidney and gut than in the other organs because the tracer was cleared via the renal system and the gastrointestinal tract. The reporter signal could be detected for more than 150 min after administration due to its long half life of 110 min. MRI was used to determine location of internal organs and to assemble with PET measurements. These results showed a low background signal in the liver and GS activity in the heart and validated the reporter model for further experiments. Only with a low background signal, *Cttnb1* mutated liver tumors will be detected exactly.

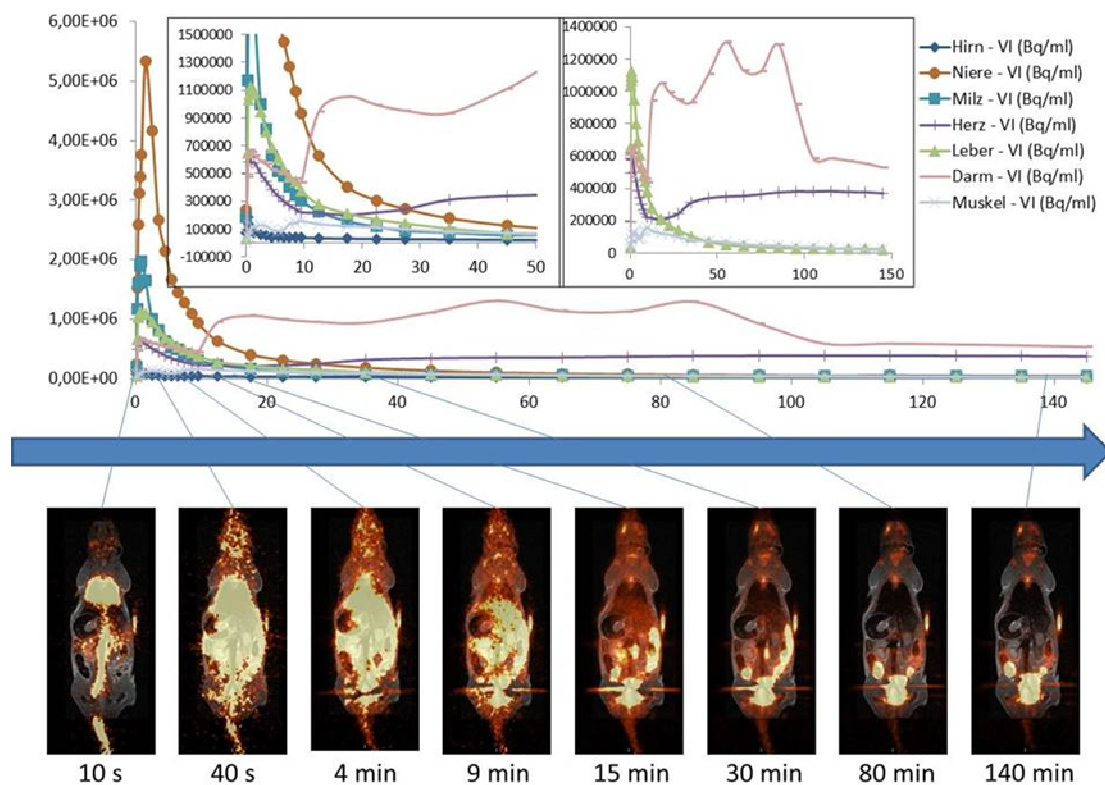


Figure 40: Female GS mouse scanned with PET. The tracer ^{18}F -FHBG rapidly diffused in the whole body, producing a strong signal in gut and heart after 60-120 min. MR imaging was used to determine the position of organs. Representative of $n = 2$. Pictures were taken by A. Schmid.

4.4.2 Glutamine Synthetase Gene Expression “Atlas” in Murine Organs

Since GS is a direct target of Wnt/ β -catenin signaling, the GS reporter mouse could be used to generate a glutamine synthetase gene expression “atlas”, which indirectly predicts in which organs and cells Wnt signaling is active.

Knowing from preliminary testings that glutamine synthetase was found in liver, kidney, gut and heart, the first question was wherever else it is expressed. Therefore, a close collaboration with Prof. Bence Sipos and Dr. Ursula Kohlhofer, Department of Pathology and Neuropathology, General Pathology, University Hospital Tübingen, was carried out to isolate 30 organs from male and female GS mice to create a GS gene expression atlas (table 21, figure 49). Cryo slices of all organs were stained with X-Gal. Strikingly, most GS was expressed in the brain area-of-interest cerebellum, hippocampus and caudate/ putamen, more precisely confined to the nuclear and cytoplasmic areas. As already known from previous studies of our group (Braeuning *et*

al. 2006), GS was expressed in pericentral hepatocytes. The digestive tract displayed GS expression in the squamous epithelium of the esophagus, in parietal and chief cells in the stomach, in smooth muscle cells of the colon and less in basal cells of the tunica mucosa in the medial and distal colon while nearly no GS promoter activity was monitored in the mucosa of the salivary gland. No GS promoter activity was reported in the three parts of the small intestine, duodenum, jejunum and ileum, in pancreas, spleen and in the proximal colon. The gall bladder lacks in the slides. Organs which have to do with urine excretion were different in their GS expression. The kidney had a high GS level in cells of the outer medulla and the cortex. GS expression was detected in the adrenal gland in the zona fasciculata of the cortex, but the urinary bladder showed nearly no GS expression. Reproductive organs were examined, too. Leydig cells of the testis displayed a high amount of GS expression, while only less GS was in the granulosa cells in the ovary. Cardiomyocytes, smooth myocytes and myocytes in the skeletal muscles also displayed a strong GS expression, which was consistently located nuclear, while less GS was expressed in the nucleus of the bronchial epithelium in the lung. Additionally, GS promoter activity was found in adipocytes of the thymus and not in thymus parenchyma. Finally, the sternum displayed no GS promoter activity. The staining on this slide was attributable to the remaining skeletal muscle cells. No differences between male and female were observed in all organs.

Figure 49 with LacZ stained organ slices is attached in the supplementary.

Table 21: Localization of glutamine synthetase in mice, which indirectly predicts in which organs and cells Wnt signaling is active. GS expression was determined via LacZ staining of more than 30 organs from male and female GS reporter mice; N, nuclear; C, cytoplasmatic; 0, no GS promoter activity.

#	organ	Male GS mouse	Female GS mouse
1	Cerebellum	brain in general (N & C)	
2	Hippocampus		
3	Caudate/ putamen		
4	Salivary gland	cells of the mucosa	
5	Thyroid gland	0	
6	Esophagus & trachea	squamous epithelium	
7	Stomach	parietal cells and chief cells	
8	Duodenum	0	
9	Jejunum	0	
10	Ileum	0	
11	Coecum	smooth muscle cells (N)	
12	Colon proximal	0	

13	Colon medial	less in basal cells of the tunica mucosa
14	Colon distal	less in basal cells of the tunica mucosa
15	Pancreas	0
16	Liver	pericentral hepatocytes (N & C)
17	Gall bladder	lacks in the slide
18	Spleen	0
19	Kidney	outer medulla and cortex
20	Adrenal gland	zona fasciculata of the cortex
21	Urinary bladder	0
22	Ovary	- less in granulosa cells
23	Uterus	- 0
24	Cervix	- 0
25	Testis	Leydig cells -
26	Heart	cardiomyocytes (N)
27	Thymus	0, but in adjacent adipocytes
28	Lung	less in bronchial epithelium (N)
29	Muscle	skeletal myocytes (N)
30	Sternum	skeletal muscle cells, but nothing in bone marrow

4.4.3 Monitoring Tumor Formation in GS Reporter Mice

In the following experiment, formation of *Ctnnb1* mutated liver tumors should be traced with non-invasive imaging technologies in GS reporter mice. In order to generate *Ctnnb1* mutated liver tumors, mice were given a single intraperitoneal DEN dose of 90 µg/g body weight followed by chronic treatment with 0.05 % PB for 25 weeks as previously described (Moennikes *et al.* 2000, also see 3.1.7). When complying the protocol, nearly 80 % of liver tumors harbor activating mutations in *Ctnnb1* (Aydinlik *et al.* 2001), while only few tumors are mutated in *Ras* or *Raf*. The special thing about the GS reporter mice used in this experiment is that they express thymidine kinase 1 under the control of the GS promoter, specifically activated in *Ctnnb1* mutated preneoplastic lesions and tumor cells. The quantitative readout of Tk-1 activity was performed using ¹⁸F-FHBG as a probe in PET. Commencing 12 weeks after tumor initiation, the tumor bearing mice were measured by PET and MRI every 2-4 weeks to pursue tumor development. First tumor lesions could be depicted in MR images starting approximately in week 18 of PB treatment. As illustrated in figure 41, liver tumors in week 22 and 25 of PB treatment could only be detected by MRI (white arrows).

Contrary to the expectations, however, we were unable to obtain specific signals in the PET analysis of tumor-bearing mice using ^{18}F -FHBG and the Tk-1 reporter system after 25 weeks of tumor promotion (figure 41 C). The tracer, however, was functional and accumulated in the intestinal tract and bone marrow.

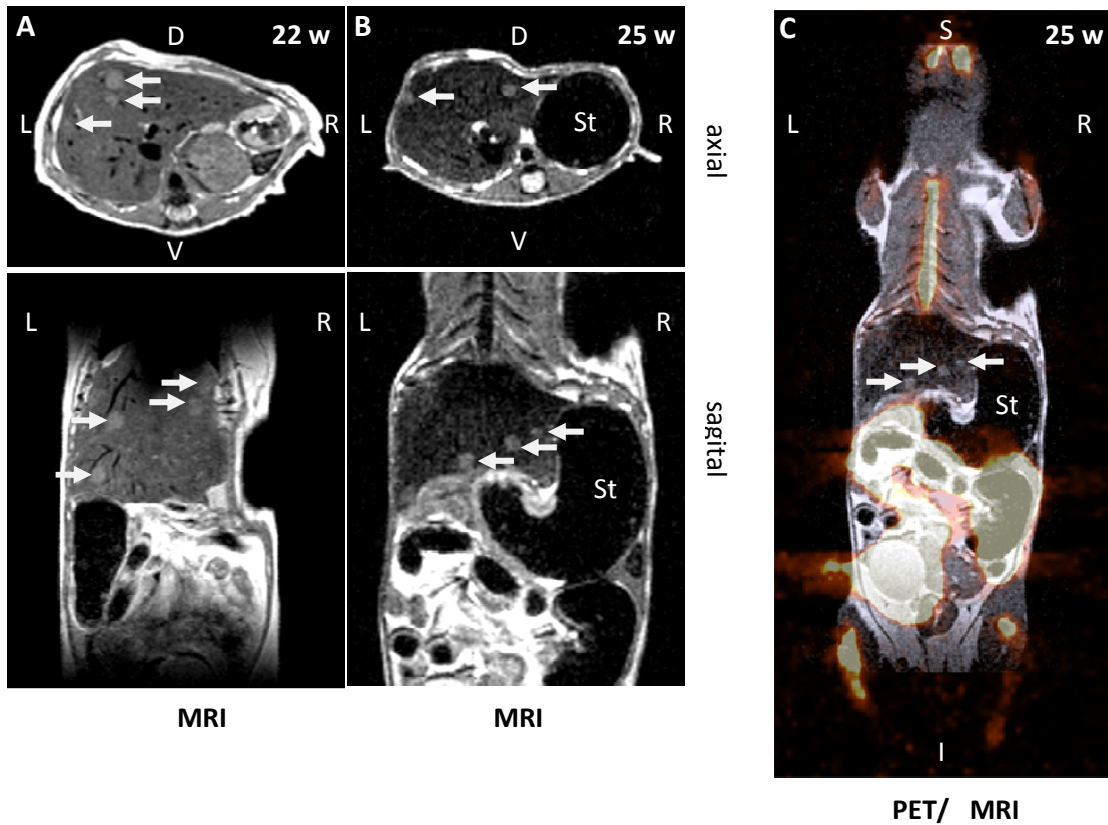


Figure 41: Representative PET and MRI images of one individual GS mouse after initiation with DEN and liver tumor promotion with PB for 25 weeks showing liver tumor growth. Tumors (white arrows) appeared as intensive lesions in the liver with MRI. PET was performed using ^{18}F -FHBG as a tracer, but PET showed no tumors; they were only detectable by MRI. A, MRI after 22 weeks with PB treatment; B, MRI after 25 weeks with PB treatment; C, PET/ MRI fusion after 25 weeks with PB treatment. St, stomach; L, left; R, right; V, ventral; D, dorsal; I, inferior; S, superior. Pictures were taken by A. Schmid.

Figure 42 shows the liver tumor progression over time measured via MRI. The data points represent the total liver tumor volume of one animal, 6 animals were measured at every indicated time point. Tumor growth was very heterogenous. Some mice began to develop liver tumors after 18 weeks of PB treatment, while other mice showed nearly no visible changes even after 22 weeks of PB treatment. At the 22-week time point, only MRI was performed instead of a PET/ MRI measurement. The MRI protocol varied slightly: thus, the detected tumor volumes at week 22 were higher in some animals, due to the sharper and brighter images, as visible in figure 41. After 25 weeks

of PB treatment, all 6 mice had liver tumors; an exact determination of the tumor volume with MRI was only possible, however, in 3 animals.

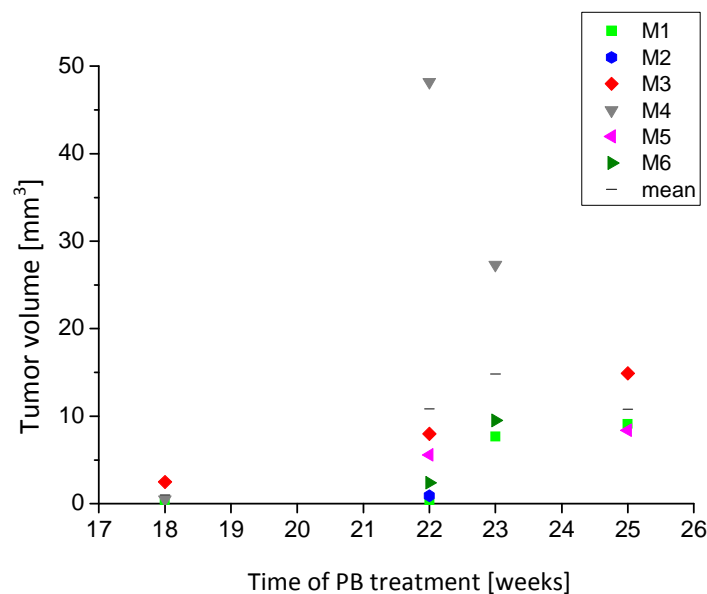


Figure 42: Monitoring of liver tumor burden via MRI in GS mice. Liver tumors were initiated with DEN and promoted with PB for 25 weeks. The liver tumor volume of 6 animals is shown at different time points. Horizontal bars represent the mean tumor volumes. M1 - M6, mouse 1 - mouse 6.

Because liver tumors couldn't be detected with PET, the question is whether these tumors are *Cttnb1* mutated and show the well-known phenotype or not. Only tumors that are mutated in the *Cttnb1* gene can be visualized with PET using a tracer for Tk-1 in this experiment. To substantiate the phenotype of developed liver tumors and to show activity of one other reporter gene, LacZ, two mice were sacrificed after 25 weeks of PB exposure. The livers were cut out and analyzed. One untreated littermate was used as a control. *Cttnb1* mutated liver tumors could be visualized post mortem with X-Gal staining, using the second reporter gene, LacZ, which is under the control of the GS promoter, too. In the X-Gal staining, *Cttnb1* mutated tumors distanced themselves from the surrounding tissue by a blue color. X-Gal positive tumors showed also the expected expression of the GS protein, but not all GS positive tumors displayed the same strong X-Gal staining (figure 43).

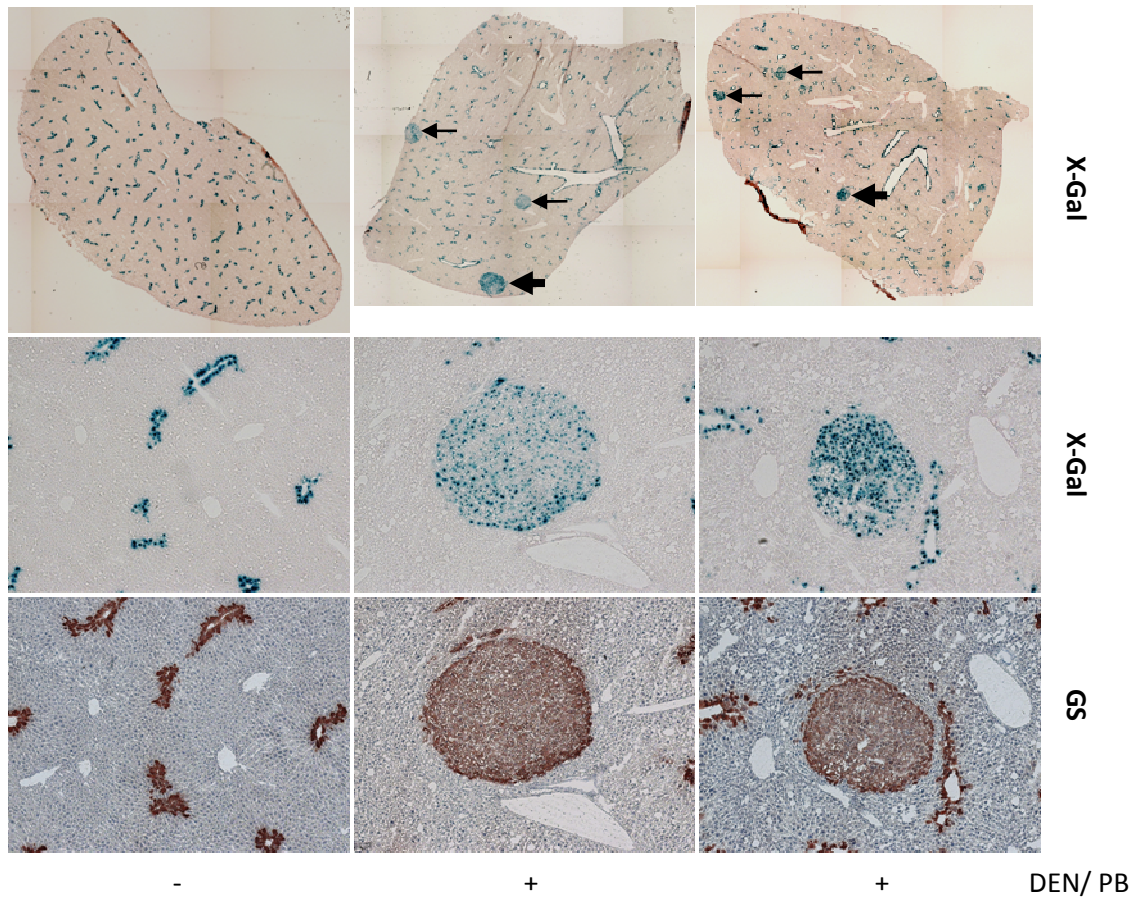


Figure 43: X-Gal and GS staining of liver lobes in GS reporter mice after tumor initiation with DEN and promotion with PB or no treatment. Livers excised after 25 weeks of PB treatment (+) harbored GS positive tumors (positive for X-Gal and GS), while untreated control mice (-) displayed no hepatic changes. Tumors are indicated with black arrows. Pictures were taken with 2.5x and 10x magnification.

Additionally, further immunohistochemical analyses of liver sections from tumor-bearing mice were performed to determine the tumor phenotype. Glucose-6-phosphatase (G6pase) was used as a general tumor marker to visualize liver tumors. GS positive liver tumors were mostly negative for G6pase relative to the surrounding normal tissue. X-Gal and GS positive tumors showed the expected expression of Cyp1a2 and Cyp2c. The mutation analyses of GS positive liver tumors also confirmed the 100 % concordance between GS expression and *Ctnnb1* mutation. 6 out of 6 examined GS positive tumors were mutated in either codon 33 (4 tumors, 67 %) or in codon 32 (2 tumors, 33 %) of the *Ctnnb1* gene. The other GS positive tumors were too small to gain enough tumor DNA for mutation analysis.

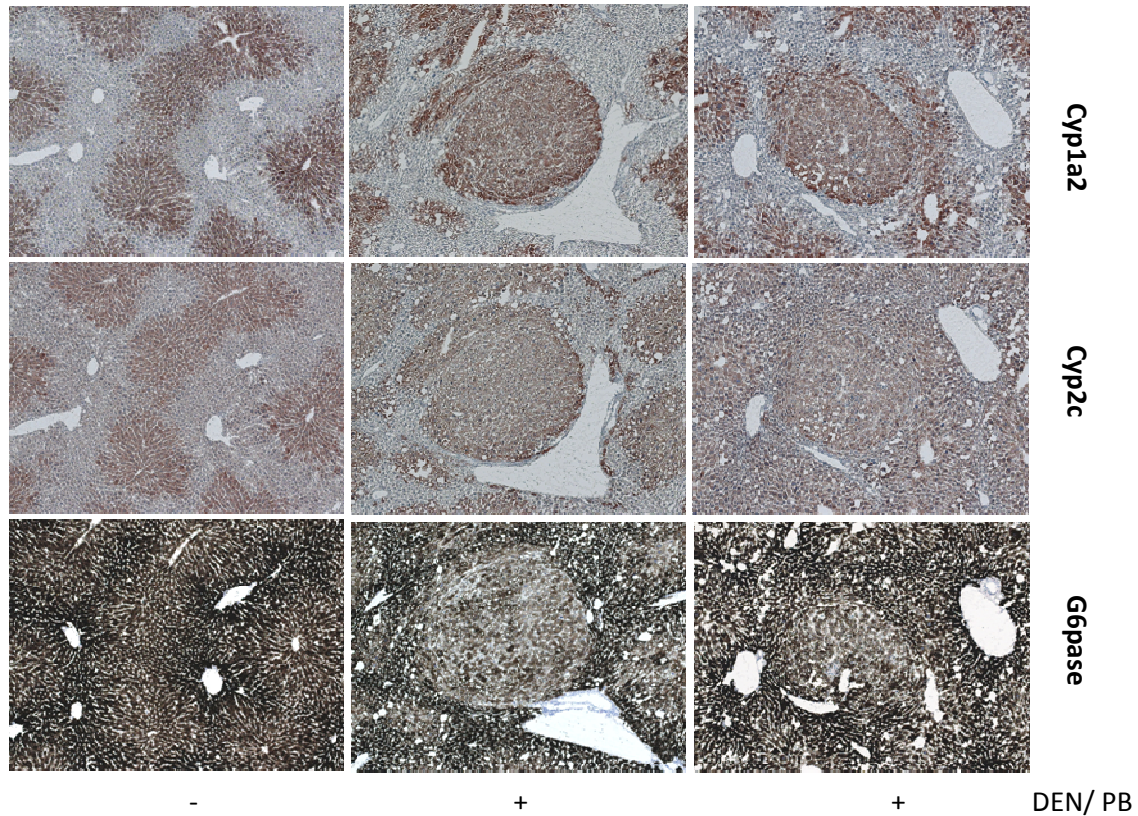


Figure 44: Phenotype of immunostained liver tumors from GS mice. *Ctnnb1* mutated liver tumors with activated β -catenin signaling were positive for Cyp1a2 and Cyp2c. Glucose-6-phosphatase (G6pase) served as a general liver tumor marker. GS positive tumors showed negative G6pase staining relative to the surrounding normal tissue.

To sum up, GS positive and *Ctnnb1* mutated liver tumors could not be visualized with PET using the Tk-1 reporter system in this thesis, although Tk-1 is under the control of the GS promoter and expressed in *Ctnnb1* mutated cells. But life imaging technology via MRI turned out to be a reliable tool to detect and monitor growth characteristics of liver tumors, even at an early stage.

5. Discussion

The present thesis comprises work on two different projects.

Project A dealt with the potential of long non-coding RNA Gtl2 as a biomarker for NGC and tumor suppressor and its characterization. For this purpose, tissue material from animals treated with different NGC and GC compounds was examined. Access to murine, rat and human tissue, normal liver and tumor tissue was available. As cell culture experiments were not satisfactory, switching to animal models was the logical consequence. Due to the lack of an appropriate knockout mouse model, Gtl2 was constitutively overexpressed in murine liver by the use of adenoviral Gtl2.

Project B, in cooperation with the group of Prof. Bernd Pichler, was intended to life image the development of liver tumors in an engineered glutamine synthetase reporter mouse by PET and MRI. For tumor generation, animals were treated with DEN as an initiator followed by chronic PB treatment to promote the development of *Ctnnb1* mutated tumors. Mice were then scanned for tumor development at the Laboratory of Preclinical Imaging and Imaging Technology in Tübingen on a monthly basis. Additionally, this reporter mouse was used to generate a glutamine synthetase gene expression “atlas”, which indirectly predicts in which organs/ cells Wnt signaling is active.

5.1 The Role of the Imprinted Dlk1-Dio3 Cluster in Liver

Emerging evidence suggests that non-coding RNAs play an important physiological role in a variety of biological processes, while aberrant expression can promote cancer (Cheetham *et al.* 2013). Micro RNAs have well ascertained expression patterns by silencing specific target genes. Much less is known about long non-coding RNAs (lncRNAs); their function in cancer remains to be elucidated.

Lempiainen *et al.* 2013 performed a miRNome analysis with liver samples from mice treated with PB, the classic non-genotoxic rodent carcinogen (Whysner *et al.* 1996), to search for an early biomarker for NGC. Noticeable, most PB-induced miRNAs were transcribed from the Dlk1-Dio3 imprinted cluster on chromosome 12. This cluster

encodes for a number of protein coding genes as well as ncRNAs, including long non-coding RNA Gtl2. A connection between Gtl2 and carcinogenesis has been observed in many different tissues and species (Benetatos *et al.* 2011), identifying Gtl2 as a tumor suppressor (Zhou *et al.* 2012), but the findings are to some extent inconsistent. To date, presentation of a mechanism for long non-coding RNA Gtl2 action has failed although Gtl2 is currently the most studied transcript of this region. The aim of this thesis was to identify targets and molecular functions of Gtl2 in hepatocarcinogenesis and to verify its role as a biomarker for NGC and as a tumor suppressor.

Recent studies performed by Novartis in cooperation with our laboratory indicated a dependence of Gtl2 expression on β -catenin and CAR and therefore supported a role in PB-dependent tumor promotion (Lempiainen *et al.* 2013). This was corroborated by the finding of an augmented Gtl2 expression in *Ctnnb1* mutated mouse liver tumors, but not in their *Ras* and *Raf* mutated counterparts, when determined via qPCR. The link between β -Catenin and Gtl2/ MEG3 expression was further strengthened by the observation of an increase in MEG3 expression in *CTNNB1* (encoding human β -Catenin) mutated human hepatoblastoma, a rare liver neoplasm occurring in small infants and children (Darbari *et al.* 2003). Recent analysis demonstrated an 80 % prevalence of mutations in *CTNNB1* (Schmidt *et al.* 2011) in this tumors. Since the tumor cells in the human cancers were never exposed to PB, this evidence suggests that overexpression of Gtl2/ MEG3 in the respective *Ctnnb1*/ *CTNNB1* mutated mouse and human liver tumors is a consequence of constitutive activation of the Wnt/ β -Catenin signaling pathway and not simply caused by PB, even though PB can induce a similar response in normal mouse liver.

Expression of Gtl2 was lower in *Ras*/ *Raf* mutated liver tumors when compared to normal liver. Gtl2 is physiologically expressed in a single layer of hepatocytes surrounding the central veins (see Figure 30 B). Exactly the same hepatocytes do physiologically express the enzyme glutamine synthetase (GS), a marker for the activated Wnt/ β -catenin pathway in these hepatocytes. GS expression is completely shut down when oncogenic Ras signaling is activated in these cells (Braeuning *et al.* 2007). Therefore the reduction in Gtl2 expression in the *Ras* mutated liver tumors is a consequence of activation of the Ras/ MAP kinase pathway.

PB treatment was not able to rescue the physiological expression pattern, since it did not lead to a reexpression of Gtl2 in *Ras* and *Raf* mutated liver tumors. The most likely explanation for this lack of effect of PB is that activation of MAP kinase signaling may override the PB response which is linked to CAR and β -catenin signaling as demonstrated in the paper of Lempiainen *et al.* 2013. In fact there is evidence for a reciprocal inhibitory crosstalk between the MAP kinase and the Wnt/ β -catenin pathways regulating zonation in liver (Hailfinger *et al.* 2006, Braeuning *et al.* 2006, Braeuning *et al.* 2007, Zeller *et al.* 2013), which would also explain the concomitant downregulation of GS and other markers in these tumors. Interestingly, however, was PB not without effect in the *Ras/ Raf* mutated tumors, but it led to a significant reduction of Gtl2 expression in the tumor cells. This inhibitory effect of PB is probably not mediated through CAR, since the nuclear receptor is downregulated in the *Ras/ Raf* mutated liver tumors (Stahl *et al.* 2005, Strathmann *et al.* 2006). It is of note, that PB does not promote the outgrowth of *Ras* mutated mouse liver tumors but rather inhibit their growth (Lee *et al.* 1998, Lee 2000, Moennikes *et al.* 2000) and there may be a possible, but unknown mechanistic link between the two phenomena. PB inhibits Wnt/ β -catenin signaling and cell proliferation in various mouse hepatoma cell lines, when incubated at a concentration between 1 and 3 mM (Braeuning, unpublished). These cells are devoid of CAR expression and do not express Gtl2 (own observation). The PB liver concentration at a diet concentration of 0.05 %, frequently used in tumor promotion experiments, is $\sim 12 \mu\text{g/g}$ liver (Braeuning *et al.* 2014). This is also the diet concentration at which inhibition of *Ras* mutated tumors was observed (Moennikes *et al.* 2000). Roughly estimated, $12 \mu\text{g/g}$ equal 0.05 mM of PB in liver, suggesting that the *Ras* mutated hepatocytes *in vivo* are more responsive to the inhibitory effects of the barbiturate. Not only Gtl2 was decreased in expression in PB treated *Ras/ Raf* mutated tumors, but the whole Dlk1-Dio3 cluster seemed to be affected: maternally imprinted genes Rian and Mirg showed slight downregulation, and the paternal protein coding genes Rtl1 and Dio3 were strongly reduced in their expression. Probably a single enhancer regulates several genes in the cluster, or one gene within the cluster acts in *cis* to transcriptionally silence other genes (Royo and Cavaille 2008). Kota *et al.* identified maternal non-coding RNAs expressed from the intergenic differentially methylated region (IG-DMR) that control Dlk1-Dio3 domain regulation (Kota *et al.*

2014). Apparently, PB, through an unknown but probably CAR unregulated mechanism, modulates the activity of this “master gene” in the *Ras/ Raf* mutated liver tumor cells.

CAR agonists are a group of structurally diverse chemicals that all induce Cyp2b enzymes (Ueda *et al.* 2002), which can therefore serve as a biomarker for CAR activation. It was demonstrated that beside PB, other CAR agonists like PCB 153 were capable of altering the expression of Dlk1-Dio3 cluster genes, especially Gtl2, reaffirming the CAR dependence of Gtl2 expression. PCB 153 behaves like PB and selects for *Ctnnb1* mutated hepatocytes when administered to mice as a tumor promoter (Strathmann *et al.* 2006). The other PCB examined was the planar dioxin-like PCB 126 activating the aryl hydrocarbon receptor (AhR). In this case, Cyp1a1 can be used as a biomarker (Bock and Kohle 2009). PCB 126 was also active in changing the expression of Dlk1-Dio3 cluster genes, especially Gtl2, similar albeit less pronounced when compared to PCB 153. This may suggest that AhR activation may also lead to increased expression of Gtl2. There is some evidence, however, for a crosstalk between AhR and CAR signaling (Petrick and Klaassen 2007), in that the activated AhR transcriptionally regulates CAR.

Two other CAR agonists examined in this study were the fungicides cyproconazole and prochloraz. Many conazoles are known to induce or inhibit hepatic cytochrome P450 isoforms. In mice, Cyp2b and Cyp3a4 have been reported to be induced in the liver, mediated by CAR and PXR nuclear receptors (Maglich *et al.* 2002, Peffer *et al.* 2007, Hester *et al.* 2012). Thus, it was not surprising that Dlk1-Dio3 cluster genes and Cyp2b10 revealed increased expression in conazole treated mice. Prochloraz is known to activate the AhR biomarker Cyp1a1 in rat liver (Vinggaard *et al.* 2005, Vinggaard *et al.* 2006). In the present study with mice, Cyp1a1 and Cyp2b10 expression were both elevated, suggesting an additional effect of prochloraz on CAR activity, which would explain its effect on Gtl2, Rian, Mirg, Rtl1 and Dio3 expression.

PB is a well-documented non-genotoxic hepatocarcinogen in rodents (Lee 2000, Whysner *et al.* 1996), but the relevance of this effect for humans is debated. So called “humanized” mouse models provide a powerful approach for understanding possible species differences. Recently, an initiation-promotion study conducted in our

laboratory with “humanized” CAR/ PXR (hCAR/ hPXR) mice demonstrated that these mice respond to PB treatment with Cyp2b10 induction, like the wildtype mice, and developed liver tumors albeit less than the wildtype mice (Braeuning *et al.* 2014). Luisier *et al.* 2014 demonstrated an augmented Gtl2 level in livers of hCAR/ hPXR mice. These results indicate that the human receptors, when expressed in the mouse genomic environment, respond similarly to PB like the mouse receptors. This toxicologically important statement is underlined by the observation that Gtl2 and other Dlk1-Dio3 cluster genes were also increased in expression in conazole treated hCAR/ hPXR mice, but to a lesser extent, when compared to the respective wildtype controls. Species differences in CAR activation by direct ligands are well-documented and are due to a structural diversity in the ligand binding sites (Nims *et al.* 1993, Auerbach *et al.* 2005). CITCO, for example, is selective for human CAR while TCPOBOP is selective for mouse CAR (Auerbach *et al.* 2005, Nims *et al.* 1993). PB, by contrast, is an indirect CAR activator not directly binding the receptor, and is active in both human and rodent hepatocytes (Kawamoto *et al.* 1999, Yang and Wang 2014). The molecular mechanism by which conazoles activate CAR signaling is not completely understood, but maybe through a signal transmission cascade via the glucocorticoid receptor (Pascussi *et al.* 2003, Duret *et al.* 2006). Given that Gtl2 is a biomarker for PB-type NGC, the results of this study demonstrate that conazoles are also active on the human receptors expressed in the mouse background.

Among the most widespread non-genotoxic carcinogens are peroxisome proliferators (Stanley *et al.* 2006) with clofibrate (CF) as a prominent example. Peroxisomes are small organelles involved in β -oxidation and in the biosynthesis of bile acids and cholesterol (Mannaerts and Van Veldhoven 1993). Chronic administration of peroxisome proliferators to rats and mice results in the formation of hepatocellular carcinoma (Reddy *et al.* 1979). The mechanism of tumor formation is not completely understood, but maybe through oxidative stress resulting in DNA damage or enhanced cell proliferation and decreased apoptosis, respectively (Benigni *et al.* 2013). Chronic administration of CF to rats results in the development of preneoplastic lesions in the liver with an altered gene expression profile, as described by Ittrich *et al.* 2003. The biomarkers for CF and PB, Cyp4a and Cyp2b, respectively, were significantly upregulated in liver, demonstrating that the two NGC, given for 10 weeks, were active

as expected. However, the only very moderate and not statistically significant upregulation of Gtl2 in the treated animals suggests that Gtl2 has limited potential as general NGC biomarker in other species than the mouse. However, it is not clear, whether peroxisome proliferators are able to upregulate Gtl2 in mouse liver. This is presently under investigation in the MARCAR project.

As β -catenin is important for Gtl2 expression in mice, it was investigated to what extent a treatment that leads to the induction of Gtl2 correlates with an effect on the β -catenin signaling pathway. Cyp7a1 was chosen as a suitable readout, since it was described to be transcriptionally upregulated in *Ctnnb1* mutated but downregulated in *Ha-ras* mutated mouse liver tumors (Unterberger *et al.* 2014). As expected, Cyp7a1, which catalyzes the rate limiting step of bile acid synthesis from cholesterol, was increased upon PB and CF treatment in rat liver, suggesting an activation of β -catenin signaling by the two NGCs. However, two other biomarkers, Sds and Gls2, were upregulated in the rat liver study, while their expression is clearly attenuated by active β -catenin in mouse liver (Unterberger *et al.* 2014). A change in β -catenin signaling may therefore not be the cause for the almost complete lack of response in Gtl2 expression in CF and PB exposed rats. In the rat liver bioassay reported by (Ittrich *et al.* 2003) not only NGCs but also two well-known genotoxic carcinogens, namely N-nitrosomorpholine (NNM) and 2-acetylaminofluorene (AAF) were investigated. Liver samples from the treated mice were still available for analysis. The results with respect to Gtl2 expression were not conclusive. NNM did not produce significant effects. AAF, however, clearly enhanced Gtl2 expression in males but reduced its expression in females. This gender differences in response are interesting, since they correlate with another gender difference in response: male rats respond more sensitive to AAF (Ittrich *et al.* 2003). From an overarching perspective, the results obtained with NGC and GC in mice and rats with respect to their effects on Gtl2 expression in the liver are disappointing. Gtl2 may serve as a NGC biomarker in mouse liver but not in the rat and it does not seem to discriminate between NGC and GC when taken the rat data. Data from GC-exposed mice are presently generated within the MARCAR project. The relevance of these results for humans needs to be further investigated.

One of the aims of modern toxicology is to reduce, refine and replace experimental animal use. Moreover, mechanistic investigations are often easier to perform using *in vitro* systems. For this reason, further experiments on Gtl2 were carried out with cultures of freshly isolated hepatocytes of mice. Primary hepatocytes are frequently used *in vitro* models for investigating drug metabolism and signaling pathways. (Klingmuller *et al.* 2006). Cyp2b10 expression, as an indicator for CAR activation, was upregulated after 24 h of treatment of primary mouse hepatocytes but returned to nearly basal level at a later time point of investigation. This was likely due to the well-known difficulty in maintaining a differentiated phenotype over culture time (Guguen-Guillouzo and Guillouzo 2010). Gtl2 mRNA levels were unchanged in the PB exposed primary hepatocytes culture. This could be due to the fact that cells in culture do not respond as in liver. On the other hand, PB-mediated upregulation of Dlk1-Dio3 genes in mouse liver requires weeks of exposure and is not significant before treatment day 7 *in vivo* (Lempiainen *et al.* 2013). Primary hepatocytes have a limited life span, making it very difficult to ensure experiments over a period of several weeks. Thus, primary hepatocytes do not serve as an adequate system for investigating Gtl2 targets and Gtl2 regulation.

Loss of Gtl2 expression has been found in all cancer cell lines derived from bladder, colon, breast, lung and liver described in literature (Braconi *et al.* 2011, Benetatos *et al.* 2011, Zhou *et al.* 2012) and examined in this thesis, except one. Surprisingly, a recently published pediatric human hepatocellular line, named HC-AFW1, derived from a liver neoplasm of a 4 year old boy through culturing of primary tumor specimens showed clear MEG3 expression accompanied by strong β -Catenin expression. This cell line revealed a deletion of 49 bp in exon 3 of CTNNB1 (Armeanu-Ebinger *et al.* 2012). HC-AFW1 is the first pediatric HCC cell line not generated on the background of viral hepatitis or liver cirrhosis like other cell lines (Eicher *et al.* 2011), thus excluding virus- or ethanol-induced side effects. In literature, it was suggested that the ability of Gtl2 to block proliferation might be a reason why Gtl2 expressing cell lines could not be established (Zhang *et al.* 2003, Mitra *et al.* 2012). However, another explanation seems more convincing: HC-AFW1 cells were special as they express the CAR receptor, which is lacking in all other cell lines investigated and is necessary for Dlk1-Dio3 gene cluster expression (Lempiainen *et al.* 2013). The CAR dependence was underpinned by the

identification of an upstream region of one of the three Gtl2 transcript variants which could be determined as directly regulated by CAR expression, given that this reporter vector was the only one with a remarkable and significant inducible luciferase signal in response to CAR.

As it had not been possible to manipulate MEG3 expression in HC-AFW1 via siRNA, another way to alter gene expression has been tested. Gtl2 is an imprinted gene expressed from the maternal allele, which means that the maternal allele is unmethylated while Gtl2 is transcribed. Methylation within the promoter region has been associated with loss of MEG3 expression in human pituitary tumors (Zhao *et al.* 2005). Demethylating the promoter might switch on gene expression. By using the methylation inhibitor 5-azadeoxycytidine (5-Aza-dC), Gtl2 mRNA levels could be raised in hepatoma cells of line 53.2b to a detectable, but still very low level. Reexpression of the unmethylated form during exposure to 5-Aza-dC occurs also in the human HCC cell lines HepG2 and Huh7 (Zhao *et al.* 2005). Because methylation inhibitors have no pathway specificity and the achievable Gtl2 level was very low, another cell system with engineered Gtl2 expressing cells was established. The respective line was termed 70.4 UT K54. Clontech's Tet-On Advanced Inducible Gene Expression System was used, which is a tightly regulated system that produces upon request expression of a gene of interest in target cells, in this case Gtl2, through adding the inducer doxycycline. Additional advantages of the system are its extremely low basal activity and the induction with a prokaryotic antibiotic, not having a known effect on eukaryotes when used at the concentrations required by Clontech (Clontech 2012). Ahler *et al.*, however, criticize potential off-target effects through doxycycline (Ahler *et al.* 2013). For further experiments, the intracellular localization of Gtl2 in 70.4 UT K54 cells based on digitonin cell fractionation was examined. The results demonstrated that the majority of the transcript was located in the nucleus, hence in analogy to the physiological situation in mouse hepatocytes *in vivo*. Cytoplasmic expression of MEG3 in non-neoplastic liver has also been described (Braconi *et al.* 2011), but in general, Gtl2 localization was reported to be nuclear or in both compartments (Schuster-Gossler *et al.* 1998, Kota *et al.* 2014). In the nucleus, it has been found associated with chromatin (Mondal *et al.* 2010). The physiological localization of Gtl2 in 70.4 UT K54 cells primed this cell line to perform Gtl2 target search.

RNA expression patterns in 70.4 UT K54 cells pointed out that forced Gtl2 expression resulted in a significant number of differentially regulated ncRNAs, while protein coding genes were underrepresented in this search. Among the latter were numerous olfactory receptors (Olfr), G protein coupled receptors mainly expressed in olfactory sensory neurons in the olfactory epithelium. All but one were found to be downregulated in the Affymetrix global gene expression analysis after forced Gtl2 expression in 70.4 UT K54 cells. Olfr expression in a liver-derived cell line is at first glance unexpected and may be a microarray artifact, since microarray experiments are widely recognized as being noisy (Bammler *et al.* 2005). However, there is growing evidence that Olfr may be expressed and have additional physiological functions in other tissues (Feldmesser *et al.* 2006), and some Olfr are even overexpressed in tumor cells (Sanz *et al.* 2014). The mouse genome contains approximately 1,200 Olfr genes (Fuss *et al.* 2007). Given this large number, a false-positive response of one or a few Olfr genes is not unlikely. However, the fact that 10 out of 108 protein coding genes were Olfrs, in other words that this group of RNAs was largely overrepresented speaks against the idea of an artefact, even though the changes in the individual Olfr genes could not be validated via qPCR. Strikingly, most of the 10 deregulated Olfrs in 70.4 UT K54 cells were clustered on mainly two chromosomes. Another group of overrepresented genes in the microarray experiment consisted of genes of the immune system. 12 out of 108 protein coding genes belong to this “cluster” and were deregulated. A mechanistic link between the immune and olfactory systems is seen in their monoallelic expression. Monoallelic expression means that only one allele of a gene is actively transcribed, while the other is silent. The expression of a single olfactory or immune system gene is determined by an enhancer element on another chromosome. The enhancer associates with one of many promoters on different chromosomes by folding of the DNA (Keverne 2009). Since polycomb group proteins are linked to monoallelic gene silencing (Alexander *et al.* 2007, Zhang *et al.* 2014), it is possible that Gtl2 acts via the enhancer polycomb repressive complex 2 to regulate the expression of olfactory and immune system genes (figure 46).

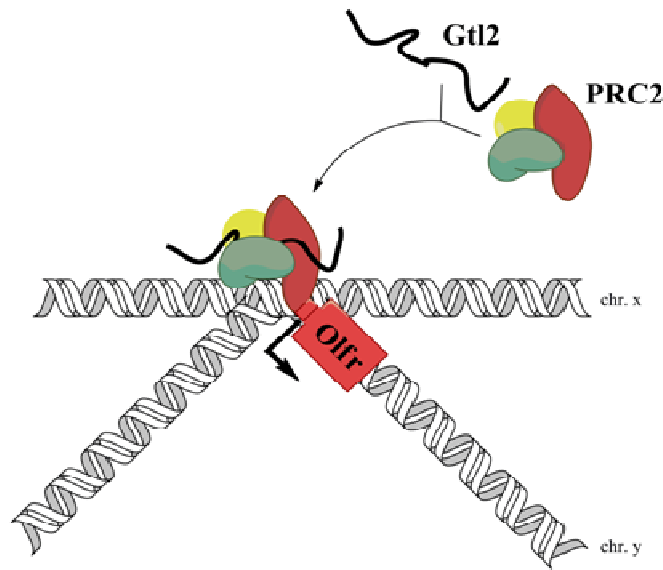


Figure 45: Schematic representation of the interplay between Gtl2, PRC2 and Olfr. The expression of a single olfactory (or immune system) gene is determined by the enhancer PRC2 on another chromosome, which is directed to the Olfr by Gtl2 (adapted from Keverne 2009).

Through Gtl2-protein binding studies, no targets could be identified, except for some “unspecific” binding partners such as ribonuclear and heatshock proteins. Random integration of Gtl2 in the genome may explain this behavior, given that the gene location plays a pivotal role for its function (Ulitsky *et al.* 2011). Presumably, Gtl2 might need components not expressed in cell culture which are required for its physiological action, like CAR, or polycomb repressive complex 2 (PRC2), or other yet unknown molecules. PRC2, for example, is a key epigenetic regulator responsible for histone methylation (Margueron *et al.* 2009). Because none of the PRC2 complex components exhibit a DNA binding domain, Rinn and Chang assume targeting of the complex by chromatin associated long non-coding RNAs (Rinn and Chang 2012). Gtl2 is believed to be one of these RNAs as JARID2 and EZH2, both part of the PRC2 complex, directly bind Gtl2 *in vivo* (Kaneko *et al.* 2014). Although expressed in HeLa cells (Beckedorff *et al.* 2013), it is dubious whether PRC2 complex proteins are transcribed in the murine liver cell lines examined. The results obtained with the cell culture systems were obviously not sufficient for identifying consequences resulting from Gtl2 overexpression in the liver. Mice offer a more realistic system to study physiologic liver functions. Two Gtl2 knockout (KO) mouse models have been reported in literature. Takahashi *et al.* created a Gtl2^{KO} mouse harboring a 10 kb deletion in exons 1 to 5. Mice carrying a maternal deletion have a milder phenotype and are able to survive 4 weeks, whereas mice with

a paternal deletion suffer perinatal lethality, indicating that Gtl2 plays an important role in embryonic development. Due to their short lifetime, these animals are unsuitable for tumor promotion experiments. Only homozygous mutants survive (Takahashi *et al.* 2009). Another mouse model exists with locus specific defects in miRNA expression (Cavaillé, unpublished), but was not made available for our investigations. Hence, a mouse system with altered Gtl2 expression in their hepatocytes was created to study Gtl2 dependent effects *in vivo*. To this end, an adenoviral Gtl2 expressing construct was used. After testing the functionality of the construct *in vitro*, showing a multiplicity of infection (MOI) dependent Gtl2 expression, it was injected into C3H mice via tail vein, while a GFP construct served as a control. Two different time points were chosen, since it was not clear how long Gtl2 needs to transiently integrate and how long expression will take place. As a rough guide to determine end points, verbal information of our project partner was used, who had designed the viral construct. Four and eight days of viral incubation were considered to be sufficient. Taken from the results of the determination of the RNA expression level and from the Gtl2 ISH results, the 4 day time point was the one with a remarkable Gtl2 expression and considered to be relevant for further investigations. Gtl2 was expressed not only around the central vein as it is physiological, but spotted over the whole liver. After 8 days, the return to the normal level was nearly completely performed, implementing a depletion of the viral construct and/ or its RNA.

Since Wnt/ β -catenin and CAR signaling control the perivenous phenotype and therefore also induce a "perivenous" phenotype in *Ctnnb1* mutated tumors in which both pathways are activated, the initial assumption was that Gtl2 is involved in the regulation of perivenous gene expression. Snyder *et al.* identified a transcription factor that modulates β -catenin signaling via direct regulation of the Gtl2 promoter (Snyder *et al.* 2013), suggesting a connection not only between β -catenin signaling and Gtl2 expression but also *vice versa*. Phenotypic changes, however, didn't occur after adenoviral Gtl2 transduction *in vivo*. Pericentral markers remained restricted to their original location. Classic liver zonation with perivenous expression of GS accompanied by Cyp1a2 expression, as previously described by Hailfinger *et al.* 2006 and Braeuning *et al.* 2007, was seen in all groups. Also the initial assumption that Gtl2 may lead to a PB mimetic gene expression could not be confirmed by immunohistochemistry since

the classic PB target Cyp2b was not altered after adenoviral Gtl2 transfer. Conspicuous was an augmentation of inflammatory cells after 8 days of treatment, both in the Gtl2 and GFP group. The viral particles used were deleted in E1 and E3 genes, which render it replication deficient (AgilentTechnologies 2013). But it is known that E1 deficient adenoviral vectors express viral antigens that activate cytotoxic lymphocytes in the liver of mice and destroy transgene expressing hepatocytes (Yang *et al.* 1994), leading to an immune response in the liver which could explain the time-dependent vanishing Gtl2 expression observed. Probably, apoptotic cells should also be increased along with the immune response, since it is known that cytotoxic T-cells eliminate virus infected cells by the induction of apoptosis (Janeway *et al.* 2001). Such an increase was seen after 8 days of treatment, both in the Gtl2 and GFP group. Although Gtl2 exerts a *cis* repressive effect on the adjacent protein coding gene Dlk1 by recruiting PRC2 protein complex (Zhao *et al.* 2010), Dlk1-Dio3 cluster genes remained unaffected after adenoviral Gtl2 transduction. Kaneko *et al.* reported a depletion of EZH2, which is part of the PRC2 complex, upon ectopic expression of lncRNA MEG3. Further more, they speculated that an excess of MEG3, upregulated through lentiviral transduction, mediates this dominant negative effect (Kaneko *et al.* 2014). Such a depletion of the PRC2 complex expression in the present adenoviral system might be a reason for not detecting altered expression of PRC2 regulated genes after adenoviral transduction of Gtl2 *in vivo*. In contrast to normal cells, which only divide a restricted number of times before entering into growth arrest, cancer cells can be kept uninfinitely in culture. The loss of negative cell cycle control can promote tumorigenesis. Given that Gtl2 is a potential tumor marker, it might directly or indirectly affect cell proliferation. Two key classes of regulatory proteins, cyclins (Ccn) and cyclin dependent kinases (Cdk) determine the cell cycle (Nigg 1995) which were measured on mRNA level. All examined cell proliferation associated genes, namely Ccnd1, Cdk2, Cdk4 and PcnA (proliferating cell nuclear antigen) were downregulated in the presence of Gtl2, suggesting retarded cell cycle progression *in vivo*. In line with these findings are data by Ying *et al.*, who showed that downregulation of MEG3 increases cell proliferation of bladder cancer cells (Ying *et al.* 2013). In human glioma and gastric cancer, ectopic MEG3 expression inhibits cell proliferation by upregulating p53 activity (Wang *et al.* 2012, Sun *et al.* 2014). P53 is also believed to inhibit Cdk2, Cdk4 and cyclin D1 activity

through p21 and p27 (Gartel and Tyner 2002). Colony formation was also repressed by MEG3 in a hepatocellular cancer cell line (Braconi *et al.* 2011). Taken together, these observations pointed towards an important role of Gtl2 in cell cycle regulation.

Inhibition of cell cycle progression by Gtl2 points towards a role of the RNA as a tumor suppressor (Zhou *et al.* 2012). This view was supported by Gordon *et al.* who demonstrated that Gtl2 has a role in the control of tumor vascularisation by inhibiting angiogenesis (Gordon *et al.* 2010). On the other hand, as shown in this and a previous study by Lempiainen *et al.* 2013, expression of Gtl2 is upregulated by PB and other tumor promoters and increased in expression in *Ctnnb1* mutated mouse and human liver tumors, suggesting an oncogene-like role of the non-coding RNA. Along these lines, a transcript functioning as a long non-coding RNA, potentially being Gtl2, able to promote HCC, was identified (Lau *et al.* 2014). Gtl2^{KO} animals die early, too early to explore if lack of Gtl2 leads to tumor formation or inhibition. An initiation promotion study in a mouse constitutively overexpressing Gtl2 would help to answer this question.

5.2 The GS Reporter Mouse as a Model to Determine GS Expression

The second part of this work was the activity on a specific reporter mouse, harboring 3 different reporters, namely FLuc (firefly luciferase), LacZ (β -galactosidase) and Tk-1 (thymidine kinase 1) under the control of the glutamine synthetase (GS) promoter. As GS is a commonly known target for β -catenin signaling, (Cadoret *et al.* 2002) its promoter is specifically activated in β -catenin active tissue and *Ctnnb1* mutated tumors. Thus, the GS reporter mouse could be used to generate a glutamine synthetase gene expression “atlas”, which indirectly predicts in which organs and cells Wnt signaling is active. The mouse had been generated commercially within the MARCAR project using a polycistronic 2A sequence from the foot and mouth disease that permitted the production of more than one protein from a single open reading frame (Funston *et al.* 2008). The multi reporter model was composed of GS-2A-LacZ-2A-Tk-1-2A-FLuc, including a nuclear localization signal next to the LacZ open reading frame.

All preliminary testings concerning FLuc, LacZ and Tk-1 reporter gene activities were successful and advised this mouse for further studies. Due to the simple visualization and the simple protocol, LacZ reporter mice are a widespread model to detect spatial patterns of gene expression *in vivo* (Schmidt *et al.* 1998). In principle, cells that function to remove glutamate and ammonia seem to contain high levels of glutamine synthetase, whereas cells that synthesize glutamate contain much lower levels (Lie-Venema *et al.* 1998). In the GS reporter mouse, most GS promoter activity was detected via X-Gal staining of tissue slices in pericentral hepatocytes and in the brain compartments cerebellum, caudate/ putamen and hippocampus, as already noticed by Venkatesh *et al.* 2013 and Liaw *et al.* 1995. They observed that GS is predominantly active in astrocytes of the brain, in kidney and in liver. By taking up ammonia and glutamate to synthesize glutamine, neurons are protected against toxicity (Suarez *et al.* 2002). Blutstein *et al.* showed the upregulation of glutamine synthetase in the hypothalamus and hippocampus both on mRNA and protein level (Blutstein *et al.* 2006), which suggested an important role for cells in the central nervous system to modulate glutaminergic neurotransmission. Most GS promoter activity detected in the digestive tract was located in the stomach, confined to the parietal and chief cells, while some GS was expressed in the squamous epithelium of the esophagus and trachea, in smooth muscle cells of the coecum and less in the basal cells of the tunica mucosa in the medial and distal colon. Parietal cells remove ammonia which is released by bacteria, leading to its detoxification; high glutamine production, on the other hand, may lead to cell swelling (Nakamura and Hagen 2002). The other parts of the digestive tract containing pancreas, spleen, small intestine and the proximal colon showed no remarkable glutamine synthetase activity. James *et al.* determined GS expression in the whole human and rat gastrointestinal tract from esophagus to rectum with almost 90 % of the gastrointestinal tract GS activity in the lower stomach and only little in the colon, as also observed in this thesis. Organs involved in urinary excretion showed different GS expression patterns. The observation from literature that GS is widely expressed throughout the entire proximal tubule, the cortex and the outer medulla in the kidney of mice (van Straaten *et al.* 2006, Verlander *et al.* 2013) was in accordance to our findings. Renal GS, as an important regulatory component of the availability of ammonium comprises an important step through which acid-base

homeostasis is maintained (Conjard *et al.* 2003, Verlander *et al.* 2013). The adrenal gland contained little GS promoter activity in the zona fasciculata of the cortex, while the urinary bladder lacked GS promoter activity. It was high in Leydig cells of the testis as shown in literature (van Straaten *et al.* 2006) and also present in granulosa cells of the ovary. In literature, however, GS was undetected in ovary (van Straaten *et al.* 2006). Xia *et al.* 2003 identified glutamine as a nutrient regulator of gene expression in the heart, which explains why the detected amount of GS in the heart of GS reporter mice was so high. Anatomically located in front of the heart is the thymus. There, GS promoter activity was predominantly seen in adipocytes and not in thymus parenchyma. GS expression in fat was already mentioned to be strongly upregulated during adipocyte differentiation (Bhandari *et al.* 1986). The lung, situated directly beside the thymus, showed less GS expression in the bronchial epithelium, as already seen in preliminary testings and mentioned in literature (van Straaten *et al.* 2006). GS promoter activity was observed in skeletal muscles in the GS reporter mouse. It is known that GS synthesizes glutamine in the muscle (Smith *et al.* 1984). Skeletal muscle constitutes for nearly $\frac{3}{4}$ of the endogenous glutamine synthesis in humans (Biolo *et al.* 1995, Nurjhan *et al.* 1995). During fasting, muscle GS becomes an important glutamine producer for protein synthesis (He *et al.* 2010). In this thesis, GS expression was not observed in the sternum. The sternum is rarely examined concerning its glutamine synthetase expression. Olkku and Mahonen, however, observed GS activity in human osteoblastic cells controlling glutamate concentration in the bone environment (Olkku and Mahonen 2008). A larger study on GS expression was carried out by van Straaten *et al.* They determined GS expression in 18 organs in the mouse (van Straaten *et al.* 2006), as stated in the corresponding sections above. In contrast to our reporter based model with X-Gal staining to detect GS expression, they gained results with immunohistochemical staining for the GS protein. Clear advantages of LacZ reporter models against classic antibody staining are the high sensitivity, simple colorimetric detection and fast production of the reporter signal representing the promoter activity in contrast to the normal GS protein. Van Straaten *et al.* observed GS expression in the cytoplasm, while in our reporter mouse model, LacZ staining, which displayed GS promoter activity, was predominantly seen in the nucleus. The reason for this is that the LacZ reporter gene in the GS mouse encodes a nuclear localization signal. A similar

mouse model as presented here with the LacZ gene under the control of the GS promoter was already mentioned in literature, but extensive β -catenin signaling was generated with the injection of a β -catenin containing adenovirus. β -Galactosidase staining, representing GS activity, was restricted to the perivenous region in the liver, as observed in the present work, but no other organs were examined concerning their GS expression (Cadoret *et al.* 2002).

In summary, the glutamine synthetase reporter mouse is a model ideally suited to examine GS activity, which indirectly predicts in which organs/ cells Wnt signaling is active in the whole mouse body. It can be said that organs with a high amount of GS promoter activity and therefore active Wnt signaling in different cell types of the brain, liver, testis, stomach and kidney function to remove glutamate and ammonia for detoxification and to produce glutamine as an energy source. Organs that produce glutamate harbor lower GS levels, (James *et al.* 1998, James *et al.* 1998), meaning less Wnt signaling. Examples for organs with a low GS expression are the small intestine and pancreas, as already reported by van Straaten *et al.* 2006.

An enzyme based reporter system for PET uses herpes simplex virus thymidine kinase 1 (HSV Tk-1), a reporter gene present in the GS mouse. This viral enzyme phosphorylates its natural substrate thymidine (Hughes *et al.* 1973) but also a broad spectrum of substrates, including acylguanosines. These compounds remain in the cell once they are phosphorylated by Tk-1. Compounds radiolabeled with PET isotopes can be used to identify Tk-1 activity with PET. In the GS reporter mouse, Tk-1 is under the control of the GS promoter and expressed in Wnt/ β -catenin signaling active cells, since GS is a target of β -catenin signaling (Loeppen *et al.* 2002). Thus, the growth of *Cttnb1* mutated tumors, characterized by excessive β -catenin signaling, can be reported with PET. In this doctoral thesis, the commonly known PET tracer ^{18}F -FHBG (9-[4- ^{18}F]fluoro-3-(hydroxymethyl)butyl]guanine) (Gambhir *et al.* 2000, Alauddin and Conti 1998) was used. It is likely that ^{18}F -FHBG entered the cell via nucleotide transporters, as compounds with similar structures do (Mahony *et al.* 1988, Mahony *et al.* 1991, Green *et al.* 2004). Then, ^{18}F -FHBG is trapped in Tk-1 reporter expressing cells once it is phosphorylated by Tk-1. ^{18}F -FHBG is an acylguanosine and incorporates in the DNA (Alauddin *et al.* 2004, Green *et al.* 2004). Mammalian thymidine kinase, not from herpes simplex virus, will only lead to some minimal background phosphorylation

(Green *et al.* 2004). By applying simultaneous PET and MRI imaging, specificity and sensitivity for early tumor detection should be increased. Preliminary tests showed a rapid diffusion of the tracer ^{18}F -FHBG in the mouse body after tail vein injection. A long lasting PET signal was observed in gut and kidney. This was due to the ways of excretion of the tracer ^{18}F -FHBG. Yaghoubi *et al.* 2001 reported the primary clearance of ^{18}F -FHBG through the renal and hepatobiliary way in humans. Although GS was expressed in the brain as seen with X-Gal staining, GS could not be detected in the brain with PET. The reasoning behind this is the inability of the tracer to cross the blood-brain barrier (Yaghoubi *et al.* 2001). In the liver, the PET signal was low. This offered a particularly good basis for detecting pathological changes accompanied by GS promoter activation during hepatocarcinogenesis.

The last part of this work was to life image the development of liver tumors with non-invasive technologies. Thus GS reporter mice were first initiated with DEN and promoted with PB for 25 weeks to generate liver tumors. This treatment scheme (Moennikes *et al.* 2000) produces liver tumors with a prevalence of nearly 80 % mutated in *Cttnb1* (Aydinlik *et al.* 2001), while only few tumors are mutated in *Ras* or *Raf*. *Cttnb1* mutated tumors have enhanced GS expression and could therefore have a selection advantage due to the independence from external glutamine over GS negative tumors (Gebhardt *et al.* 1989). Contrary to the expectations, *Cttnb1* mutated liver tumors could these not be visualized with PET using the Tk-1 reporter system. Tk-1 is under the control of the GS promoter and expressed in *Cttnb1* mutated cells. Therefore, Tk-1 was expected to be active in these tumors. Unfortunately, however, we were unable to obtain specific signals in the PET analysis of tumor-bearing mice, even though the tumors stained post-mortem were positive for GS as demonstrated by immunohistochemistry and LacZ staining and the presence of tumors in the GS reporter mice could be demonstrated by MRI. In the post-mortem analysis, some GS positive liver tumors showed less intensive LacZ staining than others, although all of the examined liver tumors were mutated in the *Cttnb1* gene. The phenotype of the *Cttnb1* mutated was like the one known from previous studies in our laboratory (Loeppen *et al.* 2005): the tumors were GS positive and showed the expected expression of *Cyp1a2* and *Cyp2c*. We have no explanation why PET failed to detect the *Cttnb1* mutated, GS positive liver tumors in this experiment. A tissue dependent

detection limit of PET with ^{18}F -FHBG was reported in literature with a magnitude from 10^6 malignant glioma cells (Su *et al.* 2004) to 10^4 cells in a prostate tumor (Johnson *et al.* 2009). *Cttnb1* mutated liver tumors with a diameter of 1 mm in size contain less than 10^6 cells, as for solid tumors presumed (Pachmann 2012), since PB promotion leads hepatocellular hypertrophie as reported by Holsapple *et al.* 2006 and Elcombe *et al.* 2014 and to loosening-up of the cellular architecture. Thus, fewer cells per tumor are the result. Maybe *Cttnb1* mutated liver tumors contain too low numbers of cells to be detected with PET at week 25 of PB treatment, the latest time point of analysis in this study. Since one voxel in PET has a size of 0.8 mm^3 (Schmid *et al.* 2012), it is potentially difficult to detect bulked and small liver tumors. Maybe, tumors will become detectable a few weeks later once they are larger in size. Another problem might be the tracer injection into the anesthetized animal, since inadequate tracer distribution might result. In general, acylguanosines, to which ^{18}F -FHBG belongs, have two disadvantages compared to pyrimidin nucleosides, the other group of Tk-1 substrates. First, acylguanosines are much less sensitive (Alauddin *et al.* 2004). Second, they are cleared via the hepatobiliary way, resulting in high amounts of radioactivity in the gallbladder and the intestine, as observed in this thesis and by Gambhir *et al.* 1998. The absence of a specific PET signal in our study was not due to a lack of tumor response in the treated animals. Tumor manifestation was clearly visualized by MRI in our study. It can not be discriminated by this technology, however, between *Cttnb1*, *Ha-ras* and *B-raf* mutated liver tumors. All liver tumors appeared in the MRI image as bright areas with a sharp border. However, there are limitations of this *in vivo* imaging technique as the detection limit of mouse liver tumors in MRI is $\sim 1 \text{ mm}$ (Schmid *et al.* 2012). Further experiments to generate larger *Cttnb1* mutated liver tumors are planned and will show if monitoring of these tumors with PET is possible. If PET detection of liver tumors should then work, we would have a tool to categorize the phenotype of liver tumors non-invasively. Furthermore, the reporter mouse model could be used to monitor the therapeutical outcome of tumor treatment regimens. Thus, new types of anti-cancer treatments could be tested non-invasively.

6. Summary (english)

Carcinogenesis is a progressive multistep process comprising various genetic alterations such as mutations in tumor suppressor genes and oncogenes. Non-genotoxic carcinogens (NGC) induce tumor formation by mechanisms other than changes in the underlying DNA sequence. Phenobarbital (PB) is a classic non-genotoxic carcinogen leading to perturbations in gene expression and DNA methylation. In mice, PB selects for *Cttnb1* (encoding β -catenin) mutated liver tumors. Recently, non-coding RNAs from the Dlk1-Dio3 cluster were identified as potential biomarkers for mouse liver tumor promotion caused by PB. One gene within this imprinted region is named Gtl2/ Meg3.

We could show that Gtl2 expression was elevated in mice treated with substances of the PB type like PCB 153 and conazole fungicides. But the transferability of the biomarker potential of Gtl2 to rats was limited. Using a switchable Gtl2 expressing hepatoma cell line, we found out that the expression of several microRNAs, immune system genes and olfactory receptors were altered with enforced Gtl2 expression. A supposable mechanism to regulate olfactory receptor and immune system gene expression could be via the polycomb repressive complex 2. Due to the lack of an appropriate Gtl2 knockout mouse model, Gtl2 was constitutively overexpressed in murine liver by the use of adenoviral Gtl2. There, Gtl2 was found to regulate cell cycle genes. No final decision could be made whether Gtl2 serves as a tumor suppressor as proposed in literature or as a tumor promoter suggested by members of the MARCAR consortium. There were supports for both characteristics. An initiation promotion study in a mouse constitutively overexpressing Gtl2 would help to answer this question.

The second part of this work was to generate a glutamine synthetase (GS) gene expression "atlas" in a GS reporter mouse, which indirectly predicts in which organs/ cells Wnt signaling is active. Most GS promoter activity was found in brain, liver, kidney, testis and heart. In addition, the growth of GS positive liver tumors was pursued non-invasively in the GS reporter mouse by MRI, whereas PET failed to visualize small GS positive liver tumors.

7. Zusammenfassung (deutsch)

Karzinogenese ist ein fortschreitender, mehrstufiger Prozess, der verschiedene genetische Veränderungen wie Mutationen in Tumorsuppressorgenen und Onkogenen umfasst. Nicht-genotoxische Karzinogene (NGC) induzieren die Tumorbildung durch Mechanismen ohne die zugrundeliegende DNA Sequenz zu verändern. Phenobarbital (PB) ist ein klassischer Vertreter der nicht-genotoxischen Karzinogene, das zu Veränderungen in der Genexpression und DNA Methylierung führt. In Mäusen selektiert PB für *Cttnb1* (codiert für β -Catenin) mutierte Lebertumore. Kürzlich wurden nicht-kodierende RNAs aus dem *Dlk1-Dio3* Cluster als potentielle Biomarker für Lebertumore der Maus identifiziert, die durch PB verursacht wurden. Ein Gen innerhalb dieser imprinteten Region ist *Gtl2/ Meg3*.

Wir konnten zeigen, dass die *Gtl2* Expression in Mäusen erhöht war, die mit Substanzen des PB Typs wie PCB 153 und Conazol Fungiziden behandelt wurden. Jedoch war die Übertragbarkeit des Biomarkerpotentials von *Gtl2* auf Ratten begrenzt. Durch Verwendung einer schaltbaren, *Gtl2* exprimierenden Leberkrebs-Zelllinie fanden wir heraus, dass die Expression von mehreren microRNAs, von Genen des Immunsystems und olfaktorischen Rezeptoren durch verstärkte *Gtl2* Expression verändert war. Ein denkbarer Mechanismus für die Regulation der Expression von olfaktorischen Rezeptoren und Genen des Immunsystems könnte über den polycomb repressive complex 2 ablaufen. Aufgrund des Mangels an einem geeigneten *Gtl2* knockout Mausmodell wurde *Gtl2* durch adenovirales *Gtl2* in der Mausleber konstitutiv überexprimiert. Dabei wurde *Gtl2* als Regulator der Gene des Zellzyklus identifiziert. Es konnte aber keine abschließende Entscheidung getroffen werden, ob *Gtl2* als Tumorsuppressor fungiert, wie in der Literatur vorgeschlagen, oder aber als Tumorpromoter, wie Mitglieder des MARCAR Konsortiums annehmen. Es gab Hinweise für beide Möglichkeiten. Ein Initiations-Promotions-Experiment in Mäusen, die *Gtl2* konstitutiv überexprimieren, würde helfen, diese Frage zu beantworten.

Der zweite Teil dieser Arbeit befasste sich mit dem Anlegen eines Glutaminsynthetase (GS) Expressions-Atlases in einer GS Reportermaus, wodurch indirekt vorausgesagt werden kann, in welchen Organen/ Zellen der Wnt Signalweg aktiv ist. Am meisten GS Promoteraktivität wurde in Gehirn, Leber, Niere, Hoden und Herz gefunden. Zusätzlich wurde das Wachstum GS positiver Lebertumore in der GS Reportermaus durch MRT nicht-invasiv verfolgt, wohingegen es misslang, kleine GS positive Lebertumore mit PET sichtbar zu machen.

8. Curriculum vitae

PERSONAL DATA

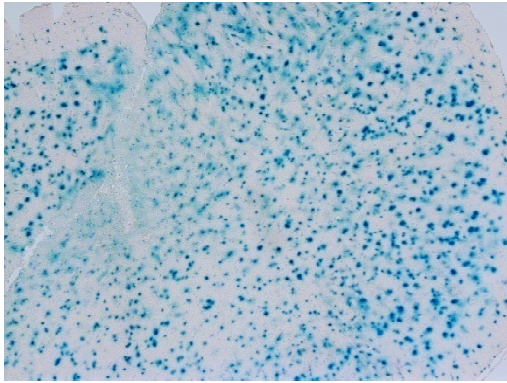
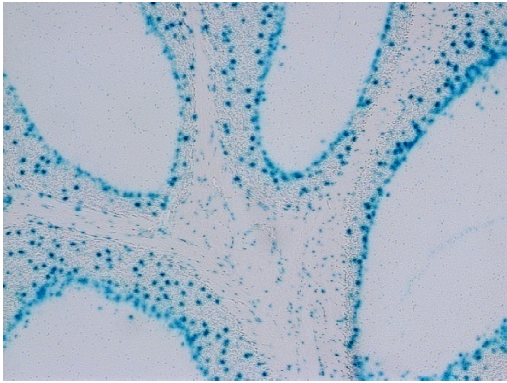
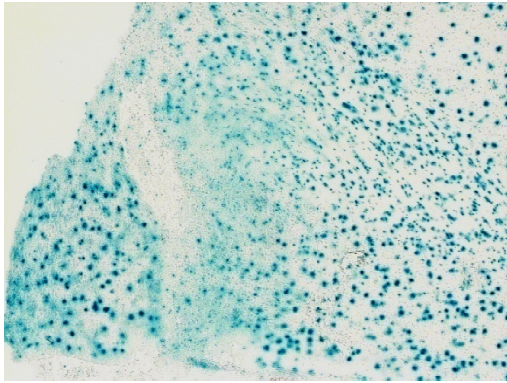
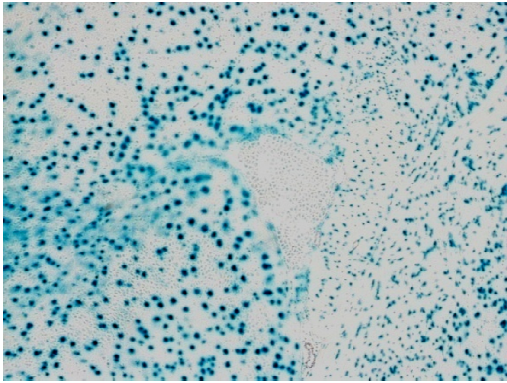
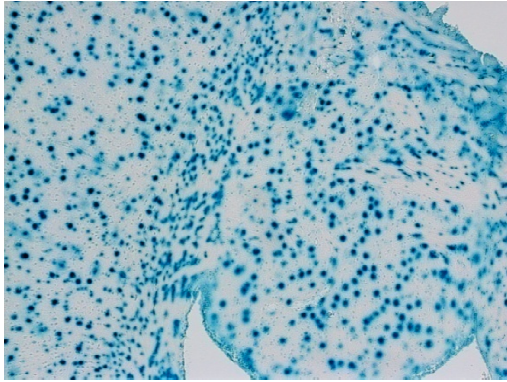
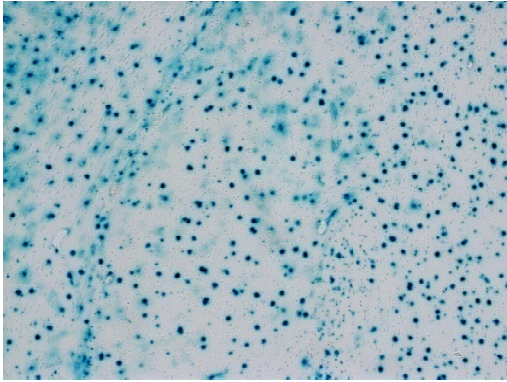
Name: Eva Christina Zeller
Born: March 09 1986, Göppingen
Nationality: German
Parents: Max Zeller and Gabriele Berlinger-Zeller

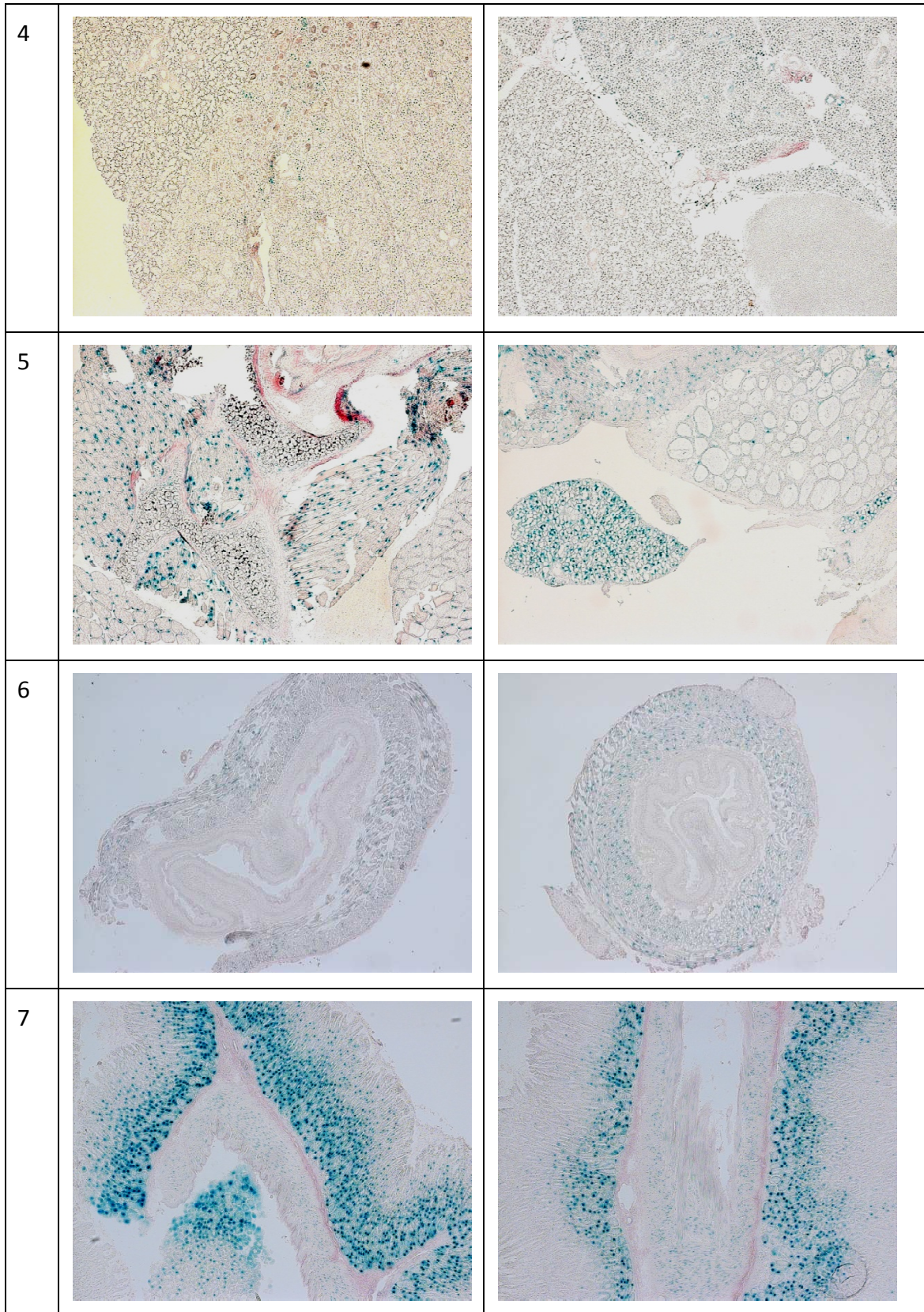
EDUCATION

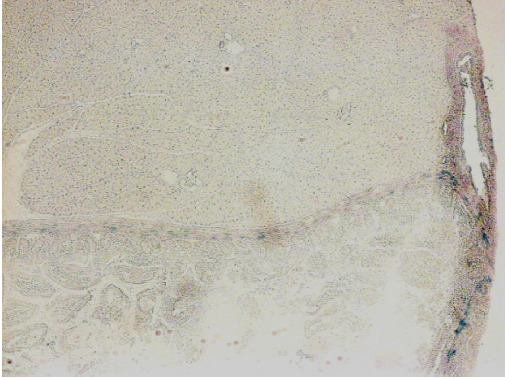
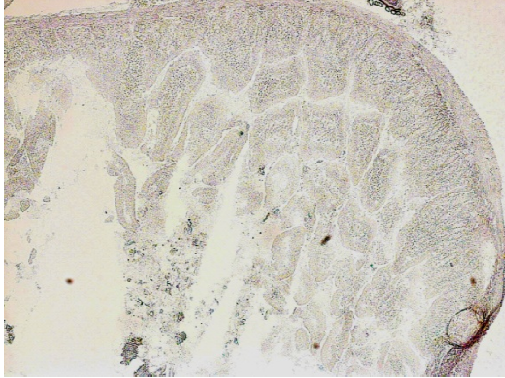
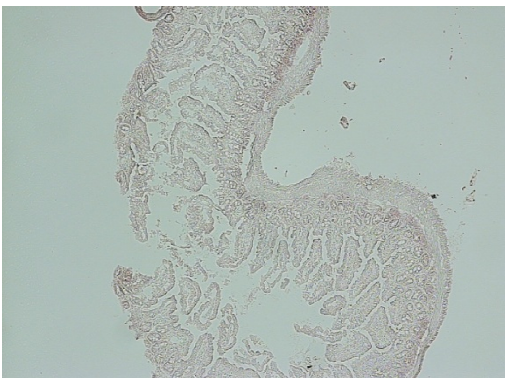
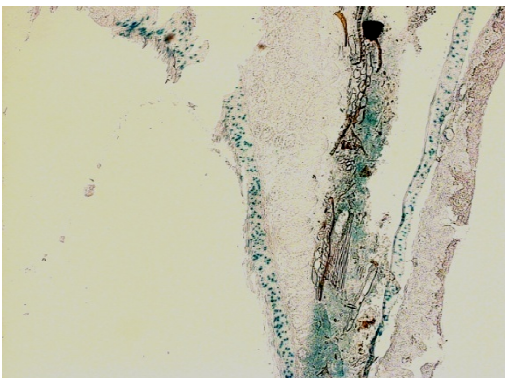
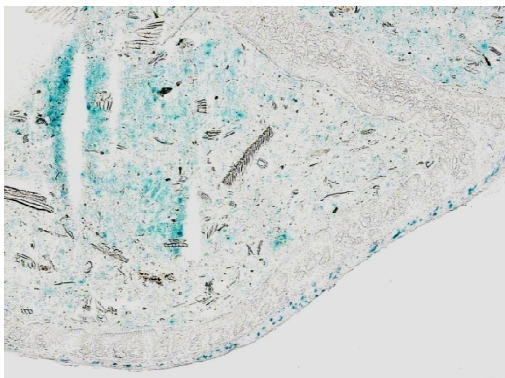
1996-2005 Hohenstaufen-Gymnasium Göppingen
2005 General qualification for university entrance
2005-2007 Basic study biochemistry, Eberhard Karls Universität Tübingen
2007-2010 Main study biochemistry, Eberhard Karls Universität Tübingen
08/2010-03/2011 Diploma thesis: "Die Regulation von Dusp6 und Dusp14 durch β -Catenin"
06/2011-12/2014 Dissertation: "The Role of Gtl2 in Hepatocarcinogenesis"

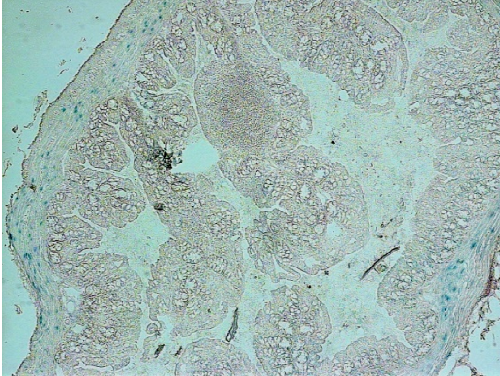
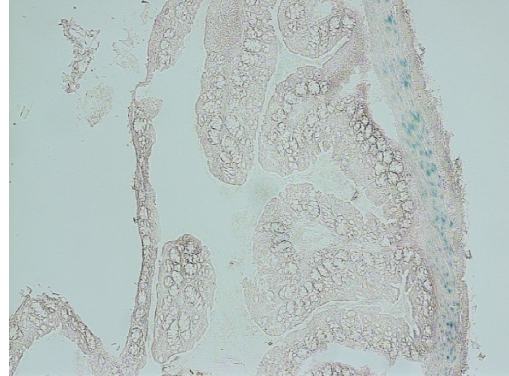
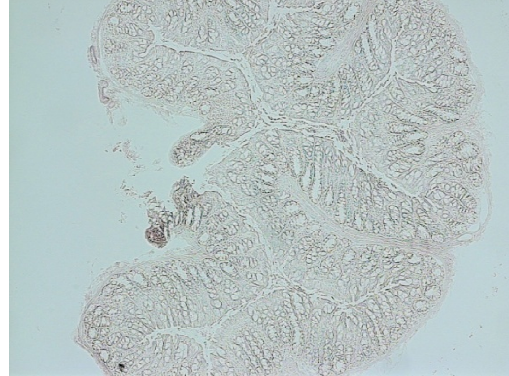
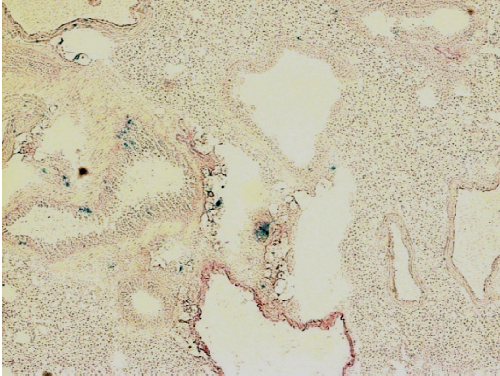
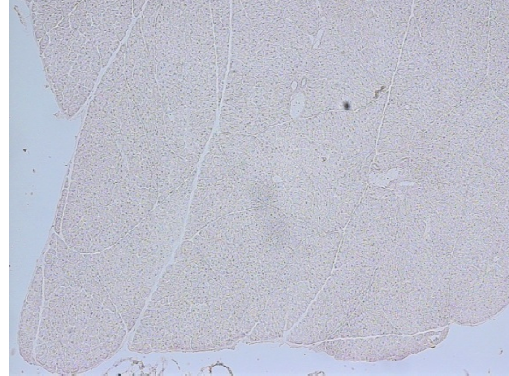
9. Supplementary data

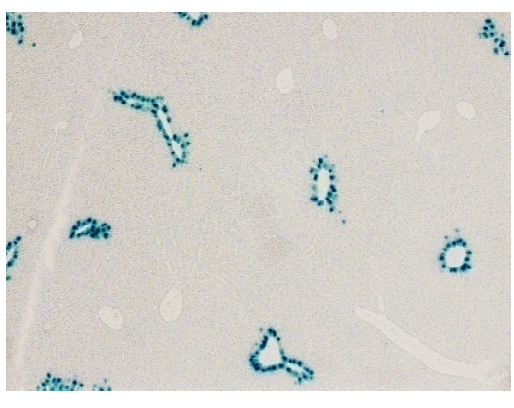
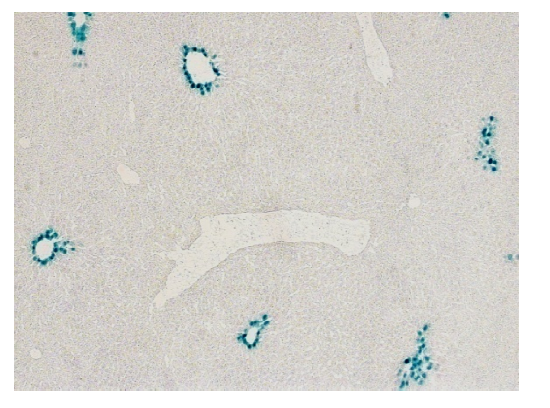
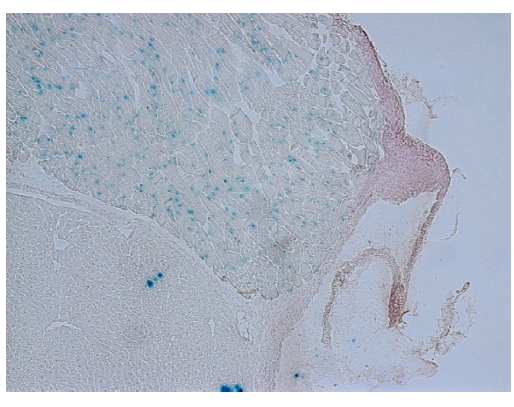
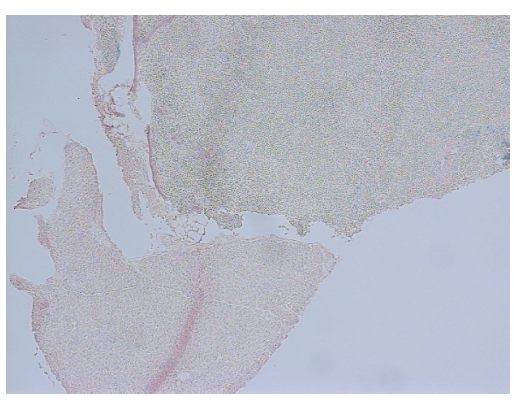
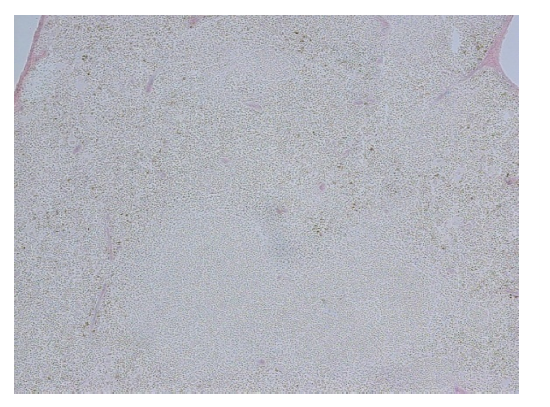
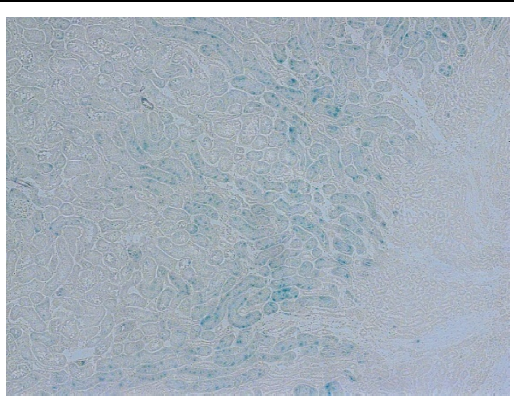
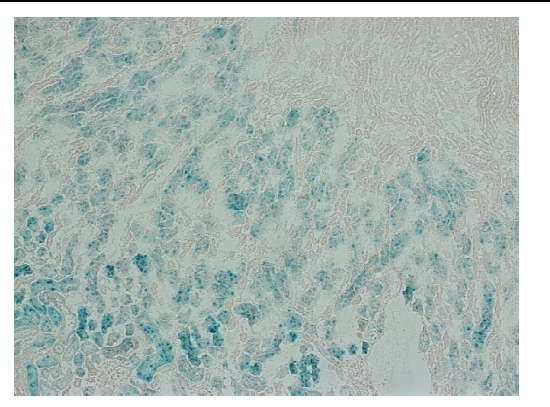
Figure 46: Organ slices of male (left) and female (right) GS mice stained with β -galactosidase, reflecting GS promoter activity. (1) cerebellum, (2) hippocampus, (3) caudate/ putamen, (4) salivary gland, (5) thyroid gland, (6) esophagus & trachea, (7) stomach, (8) duodenum, (9) jejunum, (10) ileum, (11) coecum, (12) colon proximal, (13) colon medial, (14) colon distal, (15) pancreas, (16) liver, (17) gall bladder, (18) spleen, (19) kidney, (20) adrenal gland, (21) urinary bladder, (22) ovary, (23) uterus, (24) cervix, (25) testis, (26) heart, (27) thymus, (28) lung, (29) muscle, (30) sternum. For localization of β -galactosidase positive cells, please see table 21.

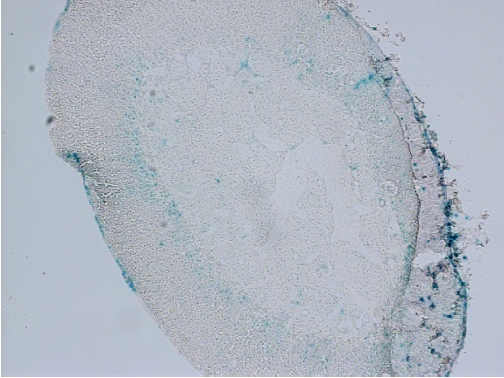
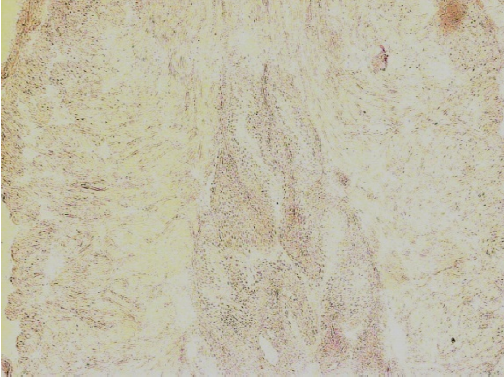
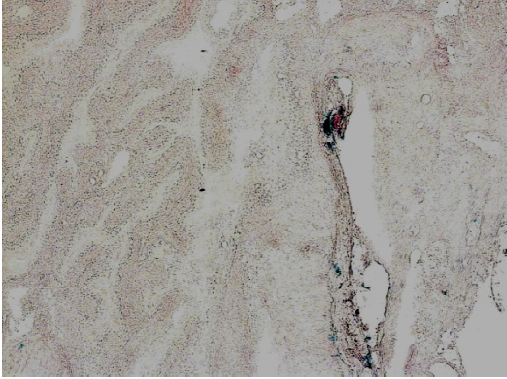
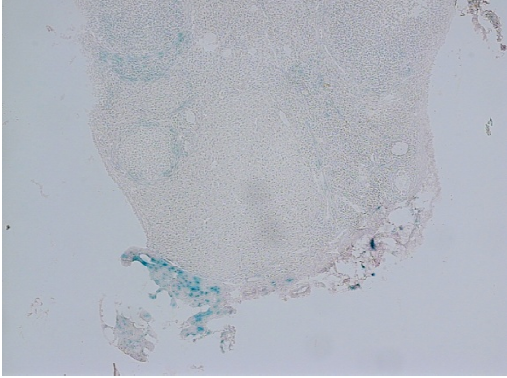
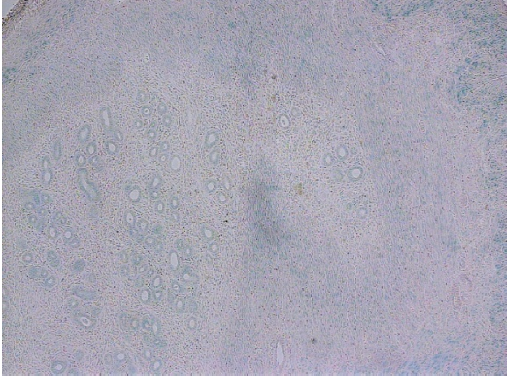
#	Male GS mouse	Female GS mouse
1		
2		
3		

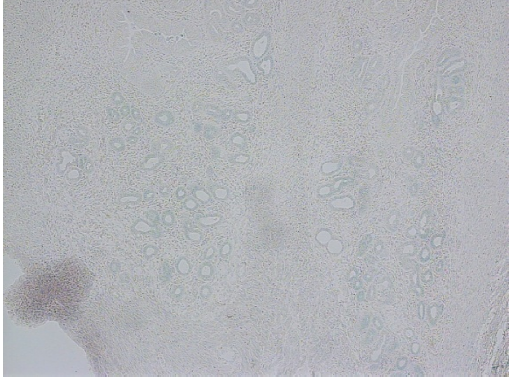
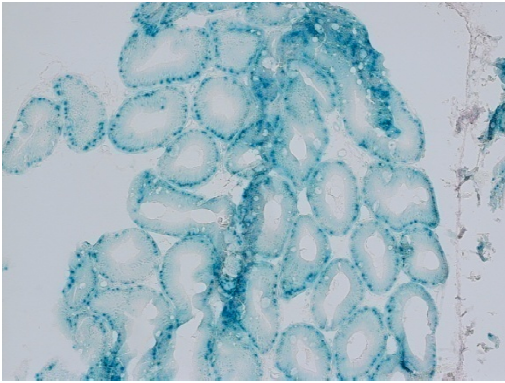
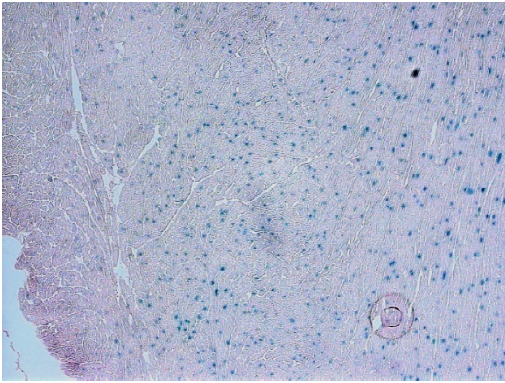
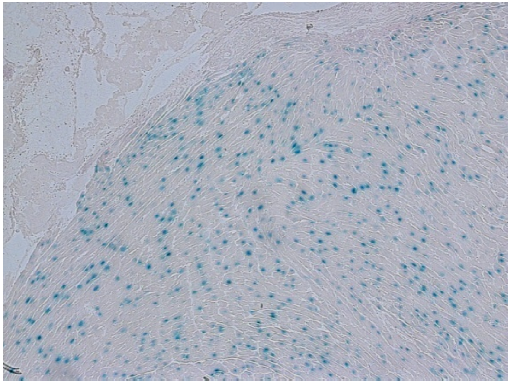
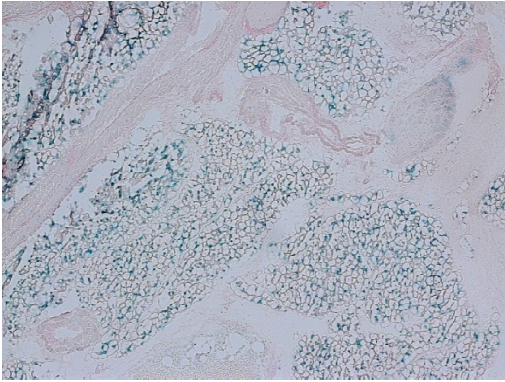
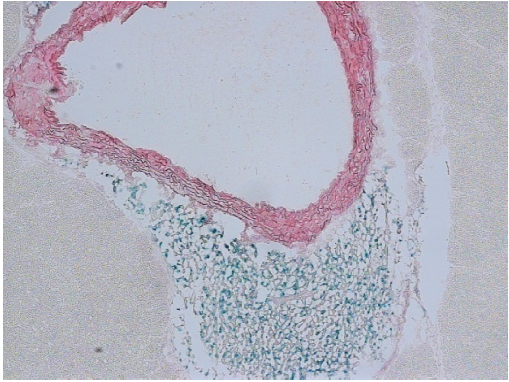


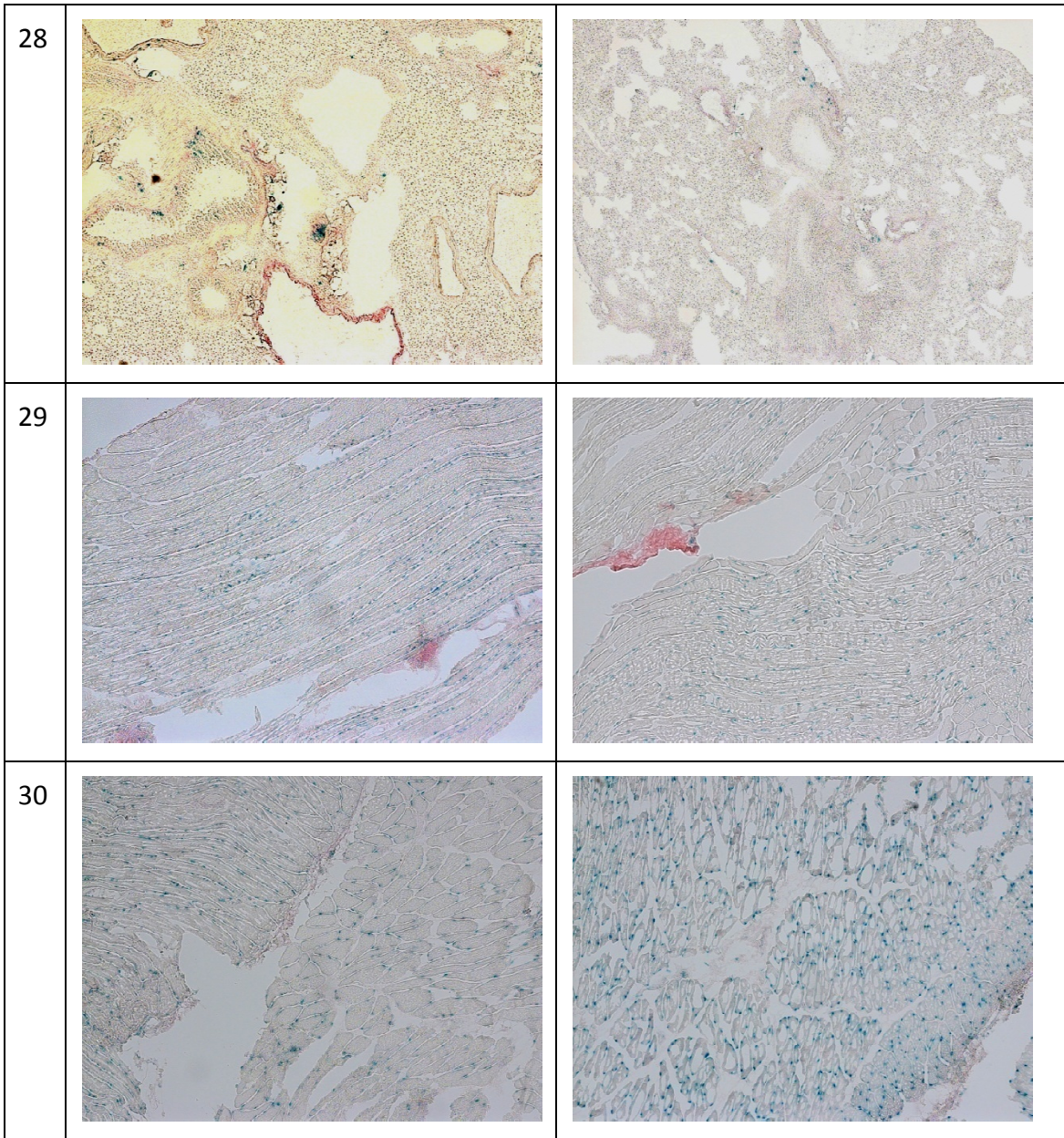
8		
9		
10		
11		

12		
13		
14		
15		

16		
17		not isolated
18		
19		

20		not isolated
21		
22	-	
23	-	

24	-	
25		-
26		
27		



10. Literature

- AgilentTechnologies (2013). "AdEasy Adenoviral Vector System - Instruction Manual." AgilentTechnologies Revision C.01(12): 43.
- Ahler, E., W. J. Sullivan, A. Cass, D. Braas, A. G. York, S. J. Bensinger, T. G. Graeber and H. R. Christofk (2013). "Doxycycline Alters Metabolism and Proliferation of Human Cell Lines." PLoS One **8**(5).
- Aktories, K., U. Förstermann, F. B. Hofmann and K. Starke (2013). Allgemeine und spezielle Pharmakologie und Toxikologie. München, Elsevier GmbH.
- Alauddin, M. M. and P. S. Conti (1998). "Synthesis and preliminary evaluation of 9-(4-[18F]-fluoro-3-hydroxymethylbutyl)guanine ([18F]FHBG): a new potential imaging agent for viral infection and gene therapy using PET." Nucl Med Biol **25**(3): 175-80.
- Alauddin, M. M., A. Shahinian, E. M. Gordon and P. S. Conti (2004). "Direct comparison of radiolabeled probes FMAU, FHBG, and FHPG as PET imaging agents for HSV1-tk expression in a human breast cancer model." Mol Imaging **3**(2): 76-84.
- Alexander, M. K., S. Mlynarczyk-Evans, M. Royce-Tolland, A. Plocik, S. Kalantry, T. Magnuson and B. Panning (2007). "Differences between homologous alleles of olfactory receptor genes require the Polycomb Group protein Eed." J Cell Biol **179**(2): 269-76.
- Armeanu-Ebinger, S., J. Wenz, G. Seitz, I. Leuschner, R. Handgretinger, U. A. Mau-Holzmann, M. Bonin, B. Sipos, J. Fuchs and S. W. Warmann (2012). "Characterisation of the Cell Line HC-AFW1 Derived from a Pediatric Hepatocellular Carcinoma." PLoS One **7**(5).
- Assie, G., E. Letouze, M. Fassnacht, A. Jouinot, W. Luscap, O. Barreau, H. Omeiri, S. Rodriguez, K. Perlemoine, F. Rene-Corail, N. Elarouci, S. Sbiera, M. Kroiss, B. Allolio, J. Waldmann, M. Quinkler, M. Mannelli, F. Mantero, T. Papatomas, R. De Krijger, A. Tabarin, V. Kerlan, E. Baudin, F. Tissier, B. Dousset, L. Groussin, L. Amar, E. Clauser, X. Bertagna, B. Ragazzon, F. Beuschlein, R. Libe, A. de Reynies and J. Bertherat (2014). "Integrated genomic characterization of adrenocortical carcinoma." Nature Genetics **46**(6): 607-612.
- Astuti, D., F. Latif, K. Wagner, D. Gentle, W. N. Cooper, D. Catchpoole, R. Grundy, A. C. Ferguson-Smith and E. R. Maher (2005). "Epigenetic alteration at the DLK1-GTL2 imprinted domain in human neoplasia: analysis of neuroblastoma, pheochromocytoma and Wilms' tumour." Br J Cancer **92**(8): 1574-80.
- Auerbach, S. S., M. A. Stoner, S. Su and C. J. Omiecinski (2005). "Retinoid X receptor-alpha-dependent transactivation by a naturally occurring structural variant of human constitutive androstane receptor (NR1I3)." Mol Pharmacol **68**(5): 1239-53.
- AWMFOonline (2010). "Leitlinie der Gesellschaft für Pädiatrische Onkologie und Hämatologie - Hepatoblastom." http://www.awmf.org/uploads/tx_szleitlinien/025-011l_S1_Hepatoblastom.pdf.
- Aydinlik, H., T. D. Nguyen, O. Moennikes, A. Buchmann and M. Schwarz (2001). "Selective pressure during tumor promotion by phenobarbital leads to clonal outgrowth of beta-catenin-mutated mouse liver tumors." Oncogene **20**(53): 7812-6.

- Bammler, T., R. P. Beyer, S. Bhattacharya, G. A. Boorman, A. Boyles, B. U. Bradford, R. E. Bumgarner, P. R. Bushel, K. Chaturvedi, D. Choi, M. L. Cunningham, S. Dengs, H. K. Dressman, R. D. Fannin, F. M. Farun, J. H. Freedman, R. C. Fry, A. Harper, M. C. Humble, P. Hurban, T. J. Kavanagh, W. K. Kaufmann, K. F. Kerr, L. Jing, J. A. Lapidus, M. R. Lasarev, J. Li, Y. J. Li, E. K. Lobenhofer, X. Lu, R. L. Malek, S. Milton, S. R. Nagalla, J. P. O'Malley, V. S. Palmer, P. Pattee, R. S. Paules, C. M. Perou, K. Phillips, L. X. Qin, Y. Qiu, S. D. Quigley, M. Rodland, I. Rusyn, L. D. Samson, D. A. Schwartz, Y. Shi, J. L. Shin, S. O. Sieber, S. Slifer, M. C. Speer, P. S. Spencer, D. I. Sproles, J. A. Swenberg, W. A. Suk, R. C. Sullivan, R. Tian, R. W. Tennant, S. A. Todd, C. J. Tucker, B. Van Houten, B. K. Weis, S. Xuan, H. Zarbl and T. R. Consortium (2005). "Standardizing global gene expression analysis between laboratories and across platforms." *Nature Methods* **2**(5): 351-356.
- Beckedorff, F. C., A. C. Ayupe, R. Crocci-Souza, M. S. Amaral, H. I. Nakaya, D. T. Soltys, C. F. M. Menck, E. M. Reis and S. Verjovski-Almeida (2013). "The Intronic Long Noncoding RNA ANRASSF1 Recruits PRC2 to the RASSF1A Promoter, Reducing the Expression of RASSF1A and Increasing Cell Proliferation." *Plos Genetics* **9**(8).
- Becker, N. and S. Holzmeier. (2014, 3.6.2014). "Krebsatlas - Krebsmortalität im Überblick - Die häufigsten Todesursachengruppen in Deutschland 2012." from http://www.dkfz.de/de/krebsatlas/gesamt/mort_2.html.
- Benetatos, L., G. Vartholomatos and E. Hatzimichael (2011). "MEG3 imprinted gene contribution in tumorigenesis." *International Journal of Cancer* **129**(4): 773-779.
- Benigni, R., C. Bossa and O. Tcheremenskaia (2013). "Nongenotoxic Carcinogenicity of Chemicals: Mechanisms of Action and Early Recognition through a New Set of Structural Alerts." *Chemical Reviews* **113**(5): 2940-2957.
- Bernhard, H. P., G. J. Darlington and F. H. Ruddle (1973). "Expression of liver phenotypes in cultured mouse hepatoma cells: synthesis and secretion of serum albumin." *Dev Biol* **35**(1): 83-96.
- Bhandari, B., D. M. Burns, R. C. Hoffman and R. E. Miller (1986). "Glutamine synthetase mRNA in cultured 3T3-L1 adipocytes. Complexity, content and hormonal regulation." *Mol Cell Endocrinol* **47**(1-2): 49-57.
- Bilger, A., L. M. Bennett, R. A. Carabeo, T. A. Chiaverotti, C. Dvorak, K. M. Liss, S. A. Schadewald, H. C. Pitot and N. R. Drinkwater (2004). "A potent modifier of liver cancer risk on distal mouse chromosome 1: linkage analysis and characterization of congenic lines." *Genetics* **167**(2): 859-66.
- Biolo, G., R. Y. Fleming, S. P. Maggi and R. R. Wolfe (1995). "Transmembrane transport and intracellular kinetics of amino acids in human skeletal muscle." *Am J Physiol* **268**(1 Pt 1): E75-84.
- Blutstein, T., N. Devidze, E. Choleris, A. M. Jasnow, D. W. Pfaff and J. A. Mong (2006). "Oestradiol up-regulates glutamine synthetase mRNA and protein expression in the hypothalamus and hippocampus: Implications for a role of hormonally responsive glia in amino acid neurotransmission." *Journal of Neuroendocrinology* **18**(9): 692-702.
- Bock, K. W. and C. Kohle (2009). "The mammalian aryl hydrocarbon (Ah) receptor: from mediator of dioxin toxicity toward physiological functions in skin and liver." *Biological Chemistry* **390**(12): 1225-1235.
- Braconi, C., T. Kogure, N. Valeri, N. Huang, G. Nuovo, S. Costinean, M. Negrini, E. Miotto, C. M. Croce and T. Patel (2011). "microRNA-29 can regulate expression of the long non-coding RNA gene MEG3 in hepatocellular cancer." *Oncogene* **30**(47): 4750-4756.

- Braeuning, A., A. Gavrilov, S. Brown, C. R. Wolf, C. J. Henderson and M. Schwarz (2014). "Phenobarbital-Mediated Tumor Promotion in Transgenic Mice with Humanized CAR and PXR." Toxicological Sciences **140**(2): 259-270.
- Braeuning, A., C. Ittrich, C. Kohle, A. Buchmann and M. Schwarz (2007). "Zonal gene expression in mouse liver resembles expression patterns of Ha-ras and beta-catenin mutated hepatomas." Drug Metab Dispos **35**(4): 503-7.
- Braeuning, A., C. Ittrich, C. Kohle, S. Hailfinger, M. Bonin, A. Buchmann and M. Schwarz (2006). "Differential gene expression in periportal and perivenous mouse hepatocytes." FEBS J **273**(22): 5051-61.
- Braeuning, A., C. Ittrich, C. Kohle, S. Hailfinger, M. Bonin, A. Buchmann and M. Schwarz (2006). "Differential gene expression in periportal and perivenous mouse hepatocytes." Febs Journal **273**(22): 5051-5061.
- Braeuning, A., M. Menzel, E. M. Kleinschnitz, N. Harada, Y. Tamai, C. Kohle, A. Buchmann and M. Schwarz (2007). "Serum components and activated Ha-ras antagonize expression of perivenous marker genes stimulated by beta-catenin signaling in mouse hepatocytes." FEBS J **274**(18): 4766-77.
- Buchmann, A., R. Bauer-Hofmann, J. Mahr, N. R. Drinkwater, A. Luz and M. Schwarz (1991). "Mutational activation of the c-Ha-ras gene in liver tumors of different rodent strains: correlation with susceptibility to hepatocarcinogenesis." Proc Natl Acad Sci U S A **88**(3): 911-5.
- Butterworth, B. E., J. A. Popp, R. B. Conolly and T. L. Goldsworthy (1992). "Chemically induced cell proliferation in carcinogenesis." IARC Sci Publ(116): 279-305.
- Cadore, A., C. Ovejero, S. Saadi-Kheddouci, E. Souil, M. Fabre, B. Romagnolo, A. Kahn and C. Perret (2001). "Hepatomegaly in transgenic mice expressing an oncogenic form of beta-catenin." Cancer Res **61**(8): 3245-9.
- Cadore, A., C. Ovejero, B. Terris, E. Souil, L. Levy, W. H. Lamers, J. Kitajewski, A. Kahn and C. Perret (2002). "New targets of beta-catenin signaling in the liver are involved in the glutamine metabolism." Oncogene **21**(54): 8293-301.
- Cheetham, S. W., F. Gruhl, J. S. Mattick and M. E. Dinger (2013). "Long noncoding RNAs and the genetics of cancer." British Journal of Cancer **108**(12): 2419-2425.
- Clontech (2012). "Tet-On Advanced Inducible Gene Expression System User Manual." **Version 102312**: 19.
- Conjard, A., O. Komaty, H. Delage, M. Boghossian, M. Martin, B. Ferrier and G. Baverel (2003). "Inhibition of glutamine synthetase in the mouse kidney: a novel mechanism of adaptation to metabolic acidosis." J Biol Chem **278**(40): 38159-66.
- Croce, C. M. (2008). "Oncogenes and cancer." N Engl J Med **358**(5): 502-11.
- da Rocha, S. T., C. A. Edwards, M. Ito, T. Ogata and A. C. Ferguson-Smith (2008). "Genomic imprinting at the mammalian Dlk1-Dio3 domain." Trends Genet **24**(6): 306-16.
- Darbari, A., K. M. Sabin, C. N. Shapiro and K. B. Schwarz (2003). "Epidemiology of primary hepatic malignancies in U.S. children." Hepatology **38**(3): 560-6.
- de La Coste, A., B. Romagnolo, P. Billuart, C. A. Renard, M. A. Buendia, O. Soubrane, M. Fabre, J. Chelly, C. Beldjord, A. Kahn and C. Perret (1998). "Somatic mutations of the beta-catenin gene are frequent in mouse and human hepatocellular carcinomas." Proc Natl Acad Sci U S A **95**(15): 8847-51.

- Duret, C., M. Daujat-Chavanieu, J. M. Pascussi, L. Pichard-Garcia, P. Balaguer, J. M. Fabre, M. J. Vilarem, P. Maurel and S. Gerbal-Chaloin (2006). "Ketoconazole and miconazole are antagonists of the human glucocorticoid receptor: consequences on the expression and function of the constitutive androstane receptor and the pregnane X receptor." Mol Pharmacol **70**(1): 329-39.
- Eicher, C., A. Dewerth, B. Kirchner, S. W. Warmann, J. Fuchs and S. Armeanu-Ebinger (2011). "Development of a drug resistance model for hepatoblastoma." International Journal of Oncology **38**(2): 447-454.
- Elcombe, C. R., R. C. Pepper, D. C. Wolf, J. Bailey, R. Bars, D. Bell, R. C. Cattley, S. S. Ferguson, D. Geter, A. Goetz, J. I. Goodman, S. Hester, A. Jacobs, C. J. Omiecinski, R. Schoeny, W. Xie and B. G. Lake (2014). "Mode of action and human relevance analysis for nuclear receptor-mediated liver toxicity: A case study with phenobarbital as a model constitutive androstane receptor (CAR) activator." Crit Rev Toxicol **44**(1): 64-82.
- Farazi, P. A. and R. A. DePinho (2006). "Hepatocellular carcinoma pathogenesis: from genes to environment." Nat Rev Cancer **6**(9): 674-87.
- Fearon, E. R. and B. Vogelstein (1990). "A genetic model for colorectal tumorigenesis." Cell **61**(5): 759-67.
- Feldmesser, E., T. Olender, M. Khen, I. Yanai, R. Ophir and D. Lancet (2006). "Widespread ectopic expression of olfactory receptor genes." Bmc Genomics **7**.
- Funston, G. M., S. E. Kallioinen, P. de Felipe, M. D. Ryan and R. D. Iggo (2008). "Expression of heterologous genes in oncolytic adenoviruses using picornaviral 2A sequences that trigger ribosome skipping." Journal of General Virology **89**: 389-396.
- Fuss, S., A. Celik and C. Desplan (2007). "Olfactory identity kicked up a NOTCH." Nat Neurosci **10**(2): 138-40.
- Gambhir, S. S., J. R. Barrio, L. Wu, M. Iyer, M. Namavari, N. Satyamurthy, E. Bauer, C. Parrish, D. C. MacLaren, A. R. Borghei, L. A. Green, S. Sharfstein, A. J. Berk, S. R. Cherry, M. E. Phelps and H. R. Herschman (1998). "Imaging of adenoviral-directed herpes simplex virus type 1 thymidine kinase reporter gene expression in mice with radiolabeled ganciclovir." J Nucl Med **39**(11): 2003-11.
- Gambhir, S. S., H. R. Herschman, S. R. Cherry, J. R. Barrio, N. Satyamurthy, T. Toyokuni, M. E. Phelps, S. M. Larson, J. Balatoni, R. Finn, M. Sadelain, J. Tjuvajev and R. Blasberg (2000). "Imaging transgene expression with radionuclide imaging technologies." Neoplasia **2**(1-2): 118-38.
- Gartel, A. L. and A. L. Tyner (2002). "The role of the cyclin-dependent kinase inhibitor p21 in apoptosis." Molecular Cancer Therapeutics **1**(8): 639-649.
- Gebhardt, R. (1992). "Metabolic zonation of the liver: regulation and implications for liver function." Pharmacol Ther **53**(3): 275-354.
- Gebhardt, R., T. Tanaka and G. M. Williams (1989). "Glutamine-Synthetase Heterogeneous Expression as a Marker for the Cellular Lineage of Preneoplastic and Neoplastic Liver Populations." Carcinogenesis **10**(10): 1917-1923.
- Ghafoory, S., K. Breitkopf-Heinlein, Q. Li, C. Scholl, S. Dooley and S. Wolf (2013). "Zonation of Nitrogen and Glucose Metabolism Gene Expression upon Acute Liver Damage in Mouse." PLoS One **8**(10).
- Giles, R. H., J. H. van Es and H. Clevers (2003). "Caught up in a Wnt storm: Wnt signaling in cancer." Biochim Biophys Acta **1653**(1): 1-24.

- Gordon, F. E., C. L. Nutt, P. Cheunsuchon, Y. Nakayama, K. A. Provencher, K. A. Rice, Y. L. Zhou, X. Zhang and A. Klibanski (2010). "Increased Expression of Angiogenic Genes in the Brains of Mouse Meg3-Null Embryos." Endocrinology **151**(6): 2443-2452.
- Green, L. A., K. Nguyen, B. Berenji, M. Iyer, E. Bauer, J. R. Barrio, M. Namavari, N. Satyamurthy and S. S. Gambhir (2004). "A tracer kinetic model for F-18-FHBG for quantitating herpes simplex virus type 1 thymidine kinase reporter gene expression in living animals using PET." Journal of Nuclear Medicine **45**(9): 1560-1570.
- Guguen-Guillouzo, C. and A. Guillouzo (2010). "General review on in vitro hepatocyte models and their applications." Methods Mol Biol **640**: 1-40.
- Hailfinger, S., M. Jaworski, A. Braeuning, A. Buchmann and M. Schwarz (2006). "Zonal gene expression in murine liver: lessons from tumors." Hepatology **43**(3): 407-14.
- He, Y. J., T. B. M. Hakvoort, S. E. Kohler, J. L. M. Vermeulen, D. R. de Waart, C. de Theije, G. A. M. ten Have, H. M. H. van Eijk, C. Kunne, W. T. Labruyere, S. M. Houten, M. Sokolovic, J. M. Ruijter, N. E. P. Deutz and W. H. Lamers (2010). "Glutamine Synthetase in Muscle Is Required for Glutamine Production during Fasting and Extrahepatic Ammonia Detoxification." Journal of Biological Chemistry **285**(13): 9516-9524.
- Hester, S., T. Moore, W. T. Padgett, L. Murphy, C. E. Wood and S. Nesnow (2012). "The Hepatocarcinogenic Conazoles: Cyproconazole, Epoxiconazole, and Propiconazole Induce a Common Set of Toxicological and Transcriptional Responses." Toxicological Sciences **127**(1): 54-65.
- Holden, P. and W. A. Horton (2009). "Crude subcellular fractionation of cultured mammalian cell lines." BMC Res Notes **2**: 243.
- Holsapple, M. P., H. C. Pitot, S. M. Cohen, A. R. Boobis, J. E. Klaunig, T. Pastoor, V. L. Dellarco and Y. P. Dragan (2006). "Mode of action in relevance of rodent liver tumors to human cancer risk." Toxicol Sci **89**(1): 51-6.
- Honkakoski, P., I. Zelko, T. Sueyoshi and M. Negishi (1998). "The nuclear orphan receptor CAR-retinoid X receptor heterodimer activates the phenobarbital-responsive enhancer module of the CYP2B gene." Mol Cell Biol **18**(10): 5652-8.
- Hore, T. A., R. W. Rapkins and J. A. Graves (2007). "Construction and evolution of imprinted loci in mammals." Trends Genet **23**(9): 440-8.
- Hu, Y. C., Z. H. Yang, K. J. Zhong, L. J. Niu, X. J. Pan, D. C. Wu, X. J. Sun, P. K. Zhou, M. X. Zhu and Y. Y. Huo (2009). "Alteration of transcriptional profile in human bronchial epithelial cells induced by cigarette smoke condensate." Toxicol Lett **190**(1): 23-31.
- Hughes, W. L., M. Christine and D. Stollar (1973). "A radioimmunoassay for measurement of serum thymidine." Anal Biochem **55**(2): 468-78.
- Ittrich, C., E. Deml, D. Oesterle, K. Kuttler, W. Mellert, S. Brendler-Schwaab, H. Enzmann, L. Schladt, P. Bannasch, T. Haertel, O. Monnikes, M. Schwarz and A. Kopp-Schneider (2003). "Prevalidation of a rat liver foci bioassay (RLFB) based on results from 1600 rats: A study report." Toxicologic Pathology **31**(1): 60-79.
- James, L. A., P. G. Lunn and M. Elia (1998). "Glutamine metabolism in the gastrointestinal tract of the rat assess by the relative activities of glutaminase (EC 3.5.1.2) and glutamine synthetase (EC 6.3.1.2)." Br J Nutr **79**(4): 365-72.
- James, L. A., P. G. Lunn, S. Middleton and M. Elia (1998). "Distribution of glutaminase and glutamine synthetase activities in the human gastrointestinal tract." Clinical Science **94**(3): 313-319.

- Janeway, C. J., P. Travers and M. Walport (2001). Immunobiology: The Immune System in Health and Disease. 5th edition. New York, Garland Science.
- Jaworski, M., A. Buchmann, P. Bauer, O. Riess and M. Schwarz (2005). "B-raf and Ha-ras mutations in chemically induced mouse liver tumors." Oncogene **24**(7): 1290-5.
- Jaworski, M., A. Buchmann, P. Bauer, O. Riess and M. Schwarz (2005). "B-Raf and Ha-ras mutations in chemically induced mouse liver tumors." Oncogene **24**(7): 1290-1295.
- Johnson, M., B. D. Karanikolas, S. J. Priceman, R. Powell, M. E. Black, H. M. Wu, J. Czernin, S. C. Huang and L. Wu (2009). "Titration of variant HSV1-tk gene expression to determine the sensitivity of 18F-FHBG PET imaging in a prostate tumor." J Nucl Med **50**(5): 757-64.
- Jones, P. A. and S. M. Taylor (1980). "Cellular-Differentiation, Cytidine Analogs and DNA Methylation." Cell **20**(1): 85-93.
- Jungermann, K. (1995). "Zonation of metabolism and gene expression in liver." Histochem Cell Biol **103**(2): 81-91.
- Kakizaki, S., D. Takizawa, H. Tojima, N. Horiguchi, Y. Yamazaki and M. Mori (2011). "Nuclear Receptors CAR and PXR; therapeutic targets for cholestatic liver disease." Frontiers in Bioscience-Landmark **16**: 2988-+.
- Kaneko, S., R. Bonasio, R. Saldana-Meyer, T. Yoshida, J. Son, K. Nishino, A. Umezawa and D. Reinberg (2014). "Interactions between JARID2 and Noncoding RNAs Regulate PRC2 Recruitment to Chromatin." Molecular Cell **53**(2): 290-300.
- Kawamoto, T., T. Sueyoshi, I. Zelko, R. Moore, K. Washburn and M. Negishi (1999). "Phenobarbital-responsive nuclear translocation of the receptor CAR in induction of the CYP2B gene." Mol Cell Biol **19**(9): 6318-22.
- Keverne, B. (2009). "Monoallelic gene expression and mammalian evolution." Bioessays **31**(12): 1318-26.
- Klaunig, J. E., L. M. Kamendulis and Y. Xu (2000). "Epigenetic mechanisms of chemical carcinogenesis." Hum Exp Toxicol **19**(10): 543-55.
- Klingmuller, U., A. Bauer, S. Bohl, P. J. Nickel, K. Breitkopf, S. Dooley, S. Zellmer, C. Kern, I. Merfort, T. Sparna, J. Donauer, G. Walz, M. Geyer, C. Kreutz, M. Hermes, F. Gotschel, A. Hecht, D. Walter, L. Egger, K. Neubert, C. Borner, M. Brulport, W. Schormann, C. Sauer, F. Baumann, R. Preiss, S. MacNelly, P. Godoy, E. Wiercinska, L. Ciucan, J. Edelmann, K. Zeilinger, M. Heinrich, U. M. Zanger, R. Gebhardt, T. Maiwald, R. Heinrich, J. Timmer, F. von Weizsacker and J. G. Hengstler (2006). "Primary mouse hepatocytes for systems biology approaches: a standardized in vitro system for modelling of signal transduction pathways." Proc Natl Acad Sci U S A **103**(6): 433-447.
- Köber, U. (2013). "Characterization of a Stably Transfected Mouse Hepatoma Cell Line with Inducible Expression of the Large Noncoding RNA Gtl2 " bachelor thesis.
- Koch, A., N. Weber, A. Waha, W. Hartmann, D. Denkhäus, J. Behrens, W. Birchmeier, D. von Schweinitz and T. Pietsch (2004). "Mutations and elevated transcriptional activity of conductin (AXIN2) in hepatoblastomas." J Pathol **204**(5): 546-54.
- Kodama, S. and M. Negishi (2006). "Phenobarbital confers its diverse effects by activating the orphan nuclear receptor car." Drug Metab Rev **38**(1-2): 75-87.
- Kota, S. K., D. Lleres, T. Bouschet, R. Hirasawa, A. Marchand, C. Begon-Pescia, I. Sanli, P. Arnaud, L. Journot, M. Girardot and R. Feil (2014). "ICR Noncoding RNA Expression Controls Imprinting and DNA Replication at the Dlk1-Dio3 Domain." Dev Cell.

- Kress, S., J. Konig, J. Schweizer, H. Lohrke, R. Bauer-Hofmann and M. Schwarz (1992). "p53 mutations are absent from carcinogen-induced mouse liver tumors but occur in cell lines established from these tumors." Mol Carcinog **6**(2): 148-58.
- Lamminpaa, A., E. Pukkala, L. Teppo and P. J. Neuvonen (2002). "Cancer incidence among patients using antiepileptic drugs: a long-term follow-up of 28,000 patients." Eur J Clin Pharmacol **58**(2): 137-41.
- Laskin, D. L., F. M. Robertson, A. M. Pilaro and J. D. Laskin (1988). "Activation of liver macrophages following phenobarbital treatment of rats." Hepatology **8**(5): 1051-5.
- Lau, C. C., T. T. Sun, A. K. K. Ching, M. He, J. W. Li, A. M. Wong, N. N. Co, A. W. H. Chan, P. S. Li, R. W. M. Lung, J. H. M. Tong, P. B. S. Lai, H. L. Y. Chan, K. F. To, T. F. Chan and N. Wong (2014). "Viral-Human Chimeric Transcript Predisposes Risk to Liver Cancer Development and Progression." Cancer Cell **25**(3): 335-349.
- Lee, G. H. (2000). "Paradoxical effects of phenobarbital on mouse hepatocarcinogenesis." Toxicologic Pathology **28**(2): 215-225.
- Lee, G. H., T. Ooasa and M. Osanai (1998). "Mechanism of the paradoxical, inhibitory effect of phenobarbital on hepatocarcinogenesis initiated in infant B6C3F(1) mice with diethylnitrosamine." Cancer Research **58**(8): 1665-1669.
- Lempiainen, H., P. Couttet, F. Bolognani, A. Muller, V. Dubost, R. Luisier, A. D. R. Espinola, V. Vitry, E. B. Unterberger, J. P. Thomson, F. Treindl, U. Metzger, C. Wrzodek, F. Hahne, T. Zollinger, S. Brasa, M. Kalteis, M. Marcellin, F. Giudicelli, A. Braeuning, L. Morawiec, N. Zamurovic, U. Langle, N. Scheer, D. Schubeler, J. Goodman, S. D. Chibout, J. Marlowe, D. Theil, D. J. Heard, O. Grenet, A. Zell, M. F. Templin, R. R. Meehan, R. C. Wolf, C. R. Elcombe, M. Schwarz, P. Moulin, R. Terranova and J. G. Moggs (2013). "Identification of Dlk1-Dio3 Imprinted Gene Cluster Noncoding RNAs as Novel Candidate Biomarkers for Liver Tumor Promotion." Toxicological Sciences **131**(2): 375-386.
- Liaw, S. H., I. C. Kuo and D. Eisenberg (1995). "Discovery of the Ammonium Substrate Site on Glutamine-Synthetase, a 3rd Cation-Binding Site." Protein Science **4**(11): 2358-2365.
- Lie-Venema, H., T. B. Hakvoort, F. J. van Hemert, A. F. Moorman and W. H. Lamers (1998). "Regulation of the spatiotemporal pattern of expression of the glutamine synthetase gene." Prog Nucleic Acid Res Mol Biol **61**: 243-308.
- Loeppen, S., C. Koehle, A. Buchmann and M. Schwarz (2005). "A beta-catenin-dependent pathway regulates expression of cytochrome P450 isoforms in mouse liver tumors." Carcinogenesis **26**(1): 239-48.
- Loeppen, S., C. Koehle, A. Buchmann and M. Schwarz (2005). "A beta-catenin-dependent pathway regulates expression of cytochrome P450 isoforms in mouse liver tumors." Carcinogenesis **26**(1): 239-248.
- Loeppen, S., D. Schneider, F. Gaunitz, R. Gebhardt, R. Kurek, A. Buchmann and M. Schwarz (2002). "Overexpression of glutamine synthetase is associated with beta-catenin-mutations in mouse liver tumors during promotion of hepatocarcinogenesis by phenobarbital." Cancer Res **62**(20): 5685-8.
- Logan, C. Y. and R. Nusse (2004). "The Wnt signaling pathway in development and disease." Annu Rev Cell Dev Biol **20**: 781-810.

- Luisier, R., H. Lempiainen, N. Scherbichler, A. Braeuning, M. Geissler, V. Dubost, A. Muller, N. Scheer, S. D. Chibout, H. Hara, F. Picard, D. Theil, P. Couttet, A. Vitobello, O. Grenet, B. Grasl-Kraupp, H. Ellinger-Ziegelbauer, J. P. Thomson, R. R. Meehan, C. R. Elcombe, C. J. Henderson, C. R. Wolf, M. Schwarz, P. Moulin, R. Terranova and J. G. Moggs (2014). "Phenobarbital Induces Cell Cycle Transcriptional Responses in Mouse Liver Humanized for Constitutive Androstane and Pregnane X Receptors." Toxicological Sciences **139**(2): 501-511.
- Maglich, J. M., C. M. Stoltz, B. Goodwin, D. Hawkins-Brown, J. T. Moore and S. A. Kliewer (2002). "Nuclear pregnane X receptor and constitutive androstane receptor regulate overlapping but distinct sets of genes involved in xenobiotic detoxification." Molecular Pharmacology **62**(3): 638-646.
- Mahony, W. B., B. A. Domin, R. T. McConnell and T. P. Zimmerman (1988). "Acyclovir Transport into Human-Erythrocytes." Journal of Biological Chemistry **263**(19): 9285-9291.
- Mahony, W. B., B. A. Domin and T. P. Zimmerman (1991). "Ganciclovir Permeation of the Human Erythrocyte-Membrane." Biochemical Pharmacology **41**(2): 263-271.
- Malumbres, M. and M. Barbacid (2003). "RAS oncogenes: the first 30 years." Nat Rev Cancer **3**(6): 459-65.
- Mannaerts, G. P. and P. P. Van Veldhoven (1993). "Metabolic pathways in mammalian peroxisomes." Biochimie **75**(3-4): 147-58.
- MARCAR (2010). "MARCAR - The project." <http://www.imi-marcar.eu/>.
- Margueron, R., N. Justin, K. Ohno, M. L. Sharpe, J. Son, W. J. Drury, P. Voigt, S. R. Martin, W. R. Taylor, V. De Marco, V. Pirrotta, D. Reinberg and S. J. Gamblin (2009). "Role of the polycomb protein EED in the propagation of repressive histone marks." Nature **461**(7265): 762-U11.
- Mitra, S. A., A. P. Mitra and T. J. Triche (2012). "A central role for long non-coding RNA in cancer." Front Genet **3**: 17.
- Miyoshi, N., H. Wagatsuma, S. Wakana, T. Shiroishi, M. Nomura, K. Aisaka, T. Kohda, M. A. Surani, T. Kaneko-Ishino and F. Ishino (2000). "Identification of an imprinted gene, Meg3/Gtl2 and its human homologue MEG3, first mapped on mouse distal chromosome 12 and human chromosome 14q." Genes Cells **5**(3): 211-20.
- Miyoshi, Y., K. Iwao, Y. Nagasawa, T. Aihara, Y. Sasaki, S. Imaoka, M. Murata, T. Shimano and Y. Nakamura (1998). "Activation of the beta-catenin gene in primary hepatocellular carcinomas by somatic alterations involving exon 3." Cancer Res **58**(12): 2524-7.
- Moennikes, O., A. Buchmann, A. Romualdi, T. Ott, J. Werringloer, K. Willecke and M. Schwarz (2000). "Lack of phenobarbital-mediated promotion of hepatocarcinogenesis in connexin32-null mice." Cancer Res **60**(18): 5087-91.
- Mondal, T., M. Rasmussen, G. K. Pandey, A. Isaksson and C. Kanduri (2010). "Characterization of the RNA content of chromatin." Genome Research **20**(7): 899-907.
- Morin, P. J. (1999). "beta-catenin signaling and cancer." Bioessays **21**(12): 1021-30.
- Nakamura, E. and S. J. Hagen (2002). "Role of glutamine and arginase in protection against ammonia-induced cell death in gastric epithelial cells." Am J Physiol Gastrointest Liver Physiol **283**(6): G1264-75.
- Nigg, E. A. (1995). "Cyclin-dependent protein kinases: key regulators of the eukaryotic cell cycle." Bioessays **17**(6): 471-80.

- Nims, R. W., P. R. Sinclair, J. F. Sinclair, K. H. Dragnev, C. R. Jones, D. W. Mellini, P. E. Thomas and R. A. Lubet (1993). "Dose-response relationships for the induction of P450 2B by 1,4-bis[2-(3,5-dichloropyridyloxy)]benzene (TCPOBOP) in rat and cultured rat hepatocytes." *Xenobiotica* **23**(12): 1411-26.
- Nurjhan, N., A. Bucci, G. Perriello, M. Stumvoll, G. Dailey, D. M. Bier, I. Toft, T. G. Jenssen and J. E. Gerich (1995). "Glutamine: a major gluconeogenic precursor and vehicle for interorgan carbon transport in man." *J Clin Invest* **95**(1): 272-7.
- Nusse, R. and H. E. Varmus (1982). "Many tumors induced by the mouse mammary tumor virus contain a provirus integrated in the same region of the host genome." *Cell* **31**(1): 99-109.
- Oda, H., Y. Imai, Y. Nakatsuru, J. Hata and T. Ishikawa (1996). "Somatic mutations of the APC gene in sporadic hepatoblastomas." *Cancer Res* **56**(14): 3320-3.
- Oliveira, P. A., A. Colaco, R. Chaves, H. Guedes-Pinto, P. L. De-La-Cruz and C. Lopes (2007). "Chemical carcinogenesis." *An Acad Bras Cienc* **79**(4): 593-616.
- Olkku, A. and A. Mahonen (2008). "Wnt and steroid pathways control glutamate signalling by regulating glutamine synthetase activity in osteoblastic cells." *Bone* **43**(3): 483-93.
- Pachmann, K. (2012). "Die Bedeutung der im Blut zirkulierenden Tumorzellen in der Metastasierungskaskade." *Deutsche Zeitschrift für Onkologie* **42**: 11-16.
- Parzefall, W., E. Erber, R. Sedivy and R. Schulte-Hermann (1991). "Testing for induction of DNA synthesis in human hepatocyte primary cultures by rat liver tumor promoters." *Cancer Res* **51**(4): 1143-7.
- Pascussi, J. M., M. Busson-Le Coniat, P. Maurel and M. J. Vilarem (2003). "Transcriptional analysis of the orphan nuclear receptor constitutive androstane receptor (NR1I3) gene promoter: identification of a distal glucocorticoid response element." *Mol Endocrinol* **17**(1): 42-55.
- Peffer, R. C., J. G. Moggs, T. Pastoor, R. A. Currie, J. Wright, G. Milburn, F. Waechter and I. Rusyn (2007). "Mouse liver effects of cyproconazole, a triazole fungicide: role of the constitutive androstane receptor." *Toxicol Sci* **99**(1): 315-25.
- Peraino, C., R. J. Fry and E. Staffeldt (1971). "Reduction and enhancement by phenobarbital of hepatocarcinogenesis induced in the rat by 2-acetylaminofluorene." *Cancer Res* **31**(10): 1506-12.
- Petrick, J. S. and C. D. Klaassen (2007). "Importance of hepatic induction of constitutive androstane receptor and other transcription factors that regulate xenobiotic metabolism and transport." *Drug Metabolism and Disposition* **35**(10): 1806-1815.
- Phillips, J. M., L. D. Burgoon and J. I. Goodman (2009). "The Constitutive Active/Androstane Receptor Facilitates Unique Phenobarbital-Induced Expression Changes of Genes Involved in Key Pathways in Precancerous Liver and Liver Tumors." *Toxicological Sciences* **110**(2): 319-333.
- Polakis, P. (2000). "Wnt signaling and cancer." *Genes Dev* **14**(15): 1837-51.
- Qu, C. S., T. Jiang, Y. Li, X. W. Wang, H. T. Cao, H. P. Xu, J. Qu and J. G. Chen (2013). "Gene expression and IG-DMR hypomethylation of maternally expressed gene 3 in developing corticospinal neurons." *Gene Expression Patterns* **13**(1-2): 51-56.
- Reddy, J. K., S. Sell, D. L. Azarnoff and M. S. Rao (1979). "Mitogenic and Carcinogenic Effects of a Hypolipidemic Peroxisome Proliferator, [4-Chloro-6-(2,3-Xylidino)-2-Pyrimidinylthio]Acetic Acid (Wy-14,643), in Rat and Mouse-Liver." *Cancer Research* **39**(1): 152-161.

- Remmer, H. and H. J. Merker (1963). "Drug-Induced Changes in the Liver Endoplasmic Reticulum: Association with Drug-Metabolizing Enzymes." Science **142**(3600): 1657-8.
- Reya, T. and H. Clevers (2005). "Wnt signalling in stem cells and cancer." Nature **434**(7035): 843-50.
- Rignall, B., K. Grote, A. Gavrillov, M. Weimer, A. Kopp-Schneider, E. Krause, K. E. Appel, A. Buchmann, L. W. Robertson, H. J. Lehmler, I. Kania-Korwel, I. Chahoud and M. Schwarz (2013). "Biological and Tumor-Promoting Effects of Dioxin-like and Non-Dioxin-like Polychlorinated Biphenyls in Mouse Liver After Single or Combined Treatment." Toxicological Sciences **133**(1): 29-41.
- Rijsewijk, F., M. Schuermann, E. Wagenaar, P. Parren, D. Weigel and R. Nusse (1987). "The Drosophila homolog of the mouse mammary oncogene int-1 is identical to the segment polarity gene wingless." Cell **50**(4): 649-57.
- Rinn, J. L. and H. Y. Chang (2012). "Genome Regulation by Long Noncoding RNAs." Annual Review of Biochemistry, Vol **81** **81**: 145-166.
- Royo, H. and J. Cavaille (2008). "Non-coding RNAs in imprinted gene clusters." Biology of the Cell **100**(3): 149-166.
- Sansom, O. J., K. R. Reed, M. van de Wetering, V. Muncan, D. J. Winton, H. Clevers and A. R. Clarke (2005). "Cyclin D1 is not an immediate target of beta-catenin following Apc loss in the intestine." J Biol Chem **280**(31): 28463-7.
- Sanz, G., I. Leray, A. Dewaele, J. Sobilo, S. Lerondel, S. Bouet, D. Grebert, R. Monnerie, E. Pajot-Augy and L. M. Mir (2014). "Promotion of Cancer Cell Invasiveness and Metastasis Emergence Caused by Olfactory Receptor Stimulation." PLoS One **9**(1).
- Schmid, A., H. Braumuller, H. F. Wehrl, M. Rocken and B. J. Pichler (2013). "Non-invasive Monitoring of Pancreatic Tumor Progression in the RIP1-Tag2 Mouse by Magnetic Resonance Imaging." Molecular Imaging and Biology **15**(2): 186-193.
- Schmid, A., B. Rignall, B. J. Pichler and M. Schwarz (2012). "Quantitative analysis of the growth kinetics of chemically induced mouse liver tumors by magnetic resonance imaging." Toxicol Sci **126**(1): 52-9.
- Schmid, A., J. Schmitz, J. G. Mannheim, F. C. Maier, K. Fuchs, H. F. Wehrl and B. J. Pichler (2012). "Feasibility of sequential PET/MRI using a state-of-the-art small animal PET and a 1 T benchtop MRI." Mol Imaging Biol **15**(2): 155-65.
- Schmidt, A., A. Braeuning, P. Ruck, G. Seitz, S. Armeanu-Ebinger, J. Fuchs, S. W. Warmann and M. Schwarz (2011). "Differential expression of glutamine synthetase and cytochrome P450 isoforms in human hepatoblastoma." Toxicology **281**(1-3): 7-14.
- Schmidt, A., K. Tief, A. Foletti, A. Hunziker, D. Penna, E. Hummler and F. Beermann (1998). "lacZ Transgenic mice to monitor gene expression in embryo and adult." Brain Research Protocols **3**(1): 54-60.
- Schuster-Gossler, K., P. Bilinski, T. Sado, A. Ferguson-Smith and A. Gossler (1998). "The mouse Gtl2 gene is differentially expressed during embryonic development, encodes multiple alternatively spliced transcripts, and may act as an RNA." Developmental Dynamics **212**(2): 214-228.
- Smith, R. J., S. Larson, S. E. Stred and R. P. Durschlag (1984). "Regulation of glutamine synthetase and glutaminase activities in cultured skeletal muscle cells." J Cell Physiol **120**(2): 197-203.

- Snyder, C. M., A. L. Rice, N. L. Estrella, A. Held, S. C. Kandarian and F. J. Naya (2013). "MEF2A regulates the Gtl2-Dio3 microRNA mega-cluster to modulate WNT signaling in skeletal muscle regeneration." Development **140**(1): 31-42.
- Stahl, S., C. Ittrich, P. Marx-Stoelting, C. Kohle, O. Altug-Teber, O. Riess, M. Bonin, J. Jobst, S. Kaiser, A. Buchmann and M. Schwarz (2005). "Genotype-phenotype relationships in hepatocellular tumors from mice and man." Hepatology **42**(2): 353-61.
- Stanley, L. A., B. C. Horsburgh, J. Ross, N. Scheer and C. R. Wolf (2006). "PXR and CAR: Nuclear receptors which play a pivotal role in drug disposition and chemical toxicity." Drug Metabolism Reviews **38**(3): 515-597.
- Stiegler, N. (2009). "The Influence of β -Catenin and GSK3 β on Apoptosis Induced by Anti-Cancer Drugs in Mouse Hepatoma Cells." diploma thesis.
- Strathmann, J., M. Schwarz, J. C. Tharappel, H. P. Glauert, B. T. Spear, L. W. Robertson, K. E. Appel and A. Buchmann (2006). "PCB 153, a non-dioxin-like tumor promoter, selects for beta-catenin (Catnb)-mutated mouse liver tumors." Toxicol Sci **93**(1): 34-40.
- Su, H., A. Forbes, S. S. Gambhir and J. Braun (2004). "Quantitation of cell number by a positron emission tomography reporter gene strategy." Mol Imaging Biol **6**(3): 139-48.
- Suarez, I., G. Bodega and B. Fernandez (2002). "Glutamine synthetase in brain: effect of ammonia." Neurochemistry International **41**(2-3): 123-142.
- Sun, M., R. Xia, F. Y. Jin, T. P. Xu, Z. J. Liu, W. De and X. H. Liu (2014). "Downregulated long noncoding RNA MEG3 is associated with poor prognosis and promotes cell proliferation in gastric cancer." Tumor Biology **35**(2): 1065-1073.
- TaconicArtemis (2012). "TUE001 project goal: Constitutive Knock-In of LacZ with optional conditional Knock-In of FLuc and/or Tk-1 in the Glul gene - targeting strategy." **1**: 6.
- Takada, S., M. Paulsen, M. Tevendale, C. E. Tsai, G. Kelsey, B. M. Cattanch and A. C. Ferguson-Smith (2002). "Epigenetic analysis of the Dlk1-Gtl2 imprinted domain on mouse chromosome 12: implications for imprinting control from comparison with Igf2-H19." Hum Mol Genet **11**(1): 77-86.
- Takahashi, N., A. Okamoto, R. Kobayashi, M. Shirai, Y. Obata, H. Ogawa, Y. Sotomaru and T. Kono (2009). "Deletion of Gtl2, imprinted non-coding RNA, with its differentially methylated region induces lethal parent-origin-dependent defects in mice." Hum Mol Genet **18**(10): 1879-88.
- Trosko, J. E. (2001). "Commentary: is the concept of "tumor promotion" a useful paradigm?" Mol Carcinog **30**(3): 131-7.
- Ueda, A., H. K. Hamadeh, H. K. Webb, Y. Yamamoto, T. Sueyoshi, C. A. Afshari, J. M. Lehmann and M. Negishi (2002). "Diverse roles of the nuclear orphan receptor CAR in regulating hepatic genes in response to phenobarbital." Molecular Pharmacology **61**(1): 1-6.
- Ulitsky, I., A. Shkumatava, C. H. Jan, H. Sive and D. P. Bartel (2011). "Conserved Function of lincRNAs in Vertebrate Embryonic Development despite Rapid Sequence Evolution." Cell **147**(7): 1537-1550.
- Unterberger, E. B., J. Eichner, C. Wrzodek, H. Lempiainen, R. Luisier, R. Terranova, U. Metzger, S. Plummer, T. Knorpp, A. Braeuning, J. Moggs, M. F. Templin, V. Honndorf, M. Piotto, A. Zell and M. Schwarz (2014). "Ha-ras and beta-catenin oncoproteins orchestrate metabolic programs in mouse liver tumors." International Journal of Cancer **135**(7): 1574-1585.

- van Straaten, H. W., Y. He, M. M. van Duist, W. T. Labruyere, J. L. Vermeulen, P. J. van Dijk, J. M. Ruijter, W. H. Lamers and T. B. Hakvoort (2006). "Cellular concentrations of glutamine synthetase in murine organs." Biochem Cell Biol **84**(2): 215-31.
- Venkatesh, K., L. Srikanth, B. Vengamma, C. Chandrasekhar, A. Sanjeevkumar, B. C. M. Prasad and P. V. G. K. Sarma (2013). "In vitro differentiation of cultured human CD34+cells into astrocytes." Neurology India **61**(4): 383-388.
- Verlander, J. W., D. Chu, H. W. Lee, M. E. Handlogten and I. D. Weiner (2013). "Expression of glutamine synthetase in the mouse kidney: localization in multiple epithelial cell types and differential regulation by hypokalemia." Am J Physiol Renal Physiol **305**(5): F701-13.
- Vestweber, D. and R. Kemler (1984). "Some Structural and Functional-Aspects of the Cell-Adhesion Molecule Uvomorulin." Cell Differentiation **15**(2-4): 269-273.
- Vinggaard, A. M., S. Christiansen, P. Laier, M. E. Poulsen, V. Breinholt, K. Jarfelt, H. Jacobsen, M. Dalgaard, C. Nellemann and U. Hass (2005). "Perinatal exposure to the fungicide prochloraz feminizes the male rat offspring." Toxicol Sci **85**(2): 886-97.
- Vinggaard, A. M., U. Hass, M. Dalgaard, H. R. Andersen, E. Bonefeld-Jorgensen, S. Christiansen, P. Laier and M. E. Poulsen (2006). "Prochloraz: an imidazole fungicide with multiple mechanisms of action." Int J Androl **29**(1): 186-92.
- Wang, P. J., Z. Q. Ren and P. Y. Sun (2012). "Overexpression of the long non-coding RNA MEG3 impairs in vitro glioma cell proliferation." Journal of Cellular Biochemistry **113**(6): 1868-1874.
- Wang, X. Q., H. Li, V. Van Putten, R. A. Winn, L. E. Heasley and R. A. Nemenoff (2009). "Oncogenic K-Ras regulates proliferation and cell junctions in lung epithelial cells through induction of cyclooxygenase-2 and activation of metalloproteinase-9." Mol Biol Cell **20**(3): 791-800.
- Weinberg, R. A. (1991). "Tumor suppressor genes." Science **254**(5035): 1138-46.
- Whysner, J., P. M. Ross and G. M. Williams (1996). "Phenobarbital mechanistic data and risk assessment: Enzyme induction, enhanced cell proliferation, and tumor promotion." Pharmacology & Therapeutics **71**(1-2): 153-191.
- Wong, C. M., S. T. Fan and I. O. Ng (2001). "beta-Catenin mutation and overexpression in hepatocellular carcinoma: clinicopathologic and prognostic significance." Cancer **92**(1): 136-45.
- Xia, Y., H. Y. Wen, M. E. Young, P. H. Guthrie, H. Taegtmeier and R. E. Kellems (2003). "Mammalian target of rapamycin and protein kinase A signaling mediate the cardiac transcriptional response to glutamine." Journal of Biological Chemistry **278**(15): 13143-13150.
- Yaghoubi, S., J. R. Barrio, M. Dahlbom, M. Iyer, M. Namavari, R. Goldman, H. R. Herschman, M. E. Phelps and S. S. Gambhir (2001). "Human pharmacokinetic and dosimetry studies of [F-18]FHBG: A reporter probe for imaging herpes simplex virus type-1 thymidine kinase reporter gene expression." Journal of Nuclear Medicine **42**(8): 1225-1234.
- Yamamoto, Y., T. Kawamoto and M. Negishi (2003). "The role of the nuclear receptor CAR as a coordinate regulator of hepatic gene expression in defense against chemical toxicity." Arch Biochem Biophys **409**(1): 207-11.
- Yang, H. and H. Wang (2014). "Signaling control of the constitutive androstane receptor (CAR)." Protein Cell **5**(2): 113-23.

- Yang, Y., H. C. Ertl and J. M. Wilson (1994). "MHC class I-restricted cytotoxic T lymphocytes to viral antigens destroy hepatocytes in mice infected with E1-deleted recombinant adenoviruses." Immunity **1**(5): 433-42.
- Ying, L., Y. R. Huang, H. G. Chen, Y. W. Wang, L. Xia, Y. H. Chen, Y. D. Liu and F. Qiu (2013). "Downregulated MEG3 activates autophagy and increases cell proliferation in bladder cancer." Molecular Biosystems **9**(3): 407-411.
- Zeller, E., K. Hammer, M. Kirschnick and A. Braeuning (2013). "Mechanisms of RAS/beta-catenin interactions." Archives of Toxicology **87**(4): 611-632.
- Zhang, H., M. J. Zeitz, H. Wang, B. Niu, S. Ge, W. Li, J. Cui, G. Wang, G. Qian, M. J. Higgins, X. Fan, A. R. Hoffman and J. F. Hu (2014). "Long noncoding RNA-mediated intrachromosomal interactions promote imprinting at the Kcnq1 locus." J Cell Biol **204**(1): 61-75.
- Zhang, X., K. Rice, Y. Y. Wang, W. D. Chen, Y. Zhong, Y. Nakayama, Y. L. Zhou and A. Klibanski (2010). "Maternally Expressed Gene 3 (MEG3) Noncoding Ribonucleic Acid: Isoform Structure, Expression, and Functions." Endocrinology **151**(3): 939-947.
- Zhang, X., Y. L. Zhou and A. Klibanski (2010). "Isolation and characterization of novel pituitary tumor related genes: A cDNA representational difference approach." Molecular and Cellular Endocrinology **326**(1-2): 40-47.
- Zhang, X., Y. L. Zhou, K. R. Mehta, D. C. Danila, S. Scolavino, S. R. Johnson and A. Klibanski (2003). "A pituitary-derived MEG3 isoform functions as a growth suppressor in tumor cells." Journal of Clinical Endocrinology & Metabolism **88**(11): 5119-5126.
- Zhao, J., D. Dahle, Y. Zhou, X. Zhang and A. Klibanski (2005). "Hypermethylation of the promoter region is associated with the loss of MEG3 gene expression in human pituitary tumors." J Clin Endocrinol Metab **90**(4): 2179-86.
- Zhao, J., T. K. Ohsumi, J. T. Kung, Y. Ogawa, D. J. Grau, K. Sarma, J. J. Song, R. E. Kingston, M. Borowsky and J. T. Lee (2010). "Genome-wide Identification of Polycomb-Associated RNAs by RIP-seq." Molecular Cell **40**(6): 939-953.
- Zhou, Y., Y. Zhong, Y. Wang, X. Zhang, D. L. Batista, R. Gejman, P. J. Ansell, J. Zhao, C. Weng and A. Klibanski (2007). "Activation of p53 by MEG3 non-coding RNA." J Biol Chem **282**(34): 24731-42.
- Zhou, Y. L., X. Zhang and A. Klibanski (2012). "MEG3 noncoding RNA: a tumor suppressor." Journal of Molecular Endocrinology **48**(3): R45-R53.